The Dissertation Committee for René Ravi Winter Certifies that this is the approved version of the following Dissertation:

Coarse-grained deep water, slope & basin-floor systems: Influence of tectonic processes on internal and external architecture

Committee:

Ronald J. Steel, Supervisor,

Cornel Olariu, Co-Supervisor

William L. Fisher

Charles Kerans

Craig Fulthorpe

Coarse-grained deep water, slope & basin-floor systems: Influence of tectonic processes on internal and external architecture

by

René Ravi Winter

Dissertation

Presented to the Faculty of the Graduate School of

The University of Texas at Austin

in Partial Fulfillment

of the Requirements

for the Degree of

Doctor of Philosophy

The University of Texas at Austin

May, 2018

Dedication

This Dissertation is dedicated to the people who have made this effort possible. My wife Latoya and son Alexander thank you for putting up with me while I have done this work. My mother who has been my number one fan from day one, this is especially for you. My sister Renata has pushed me when I have felt like giving up. And to my dad. You have inspired me in ways you did not know. And most importantly, to God, for blessing me with all these people who have helped me, and giving me the strength to keep going so many times I wanted to give up.

Acknowledgements

I would like to acknowledge my advisors on this project – Ron Steel and Cornel Olariu – who have been with me from day one of this journey. They gave me the opportunity, and although there were many challenges along the way, they have always been supportive and engaging in this endeavor. Thank you for inspiring me to think about Geology in the correct way.

To my committee William Fisher, Craig Fulthorpe and Charlie Kerans, you have also been with me on this journey from the start, and again many thanks for understanding my unique situation in completing this project and providing much needed critical reviews and guidance to shape the final product.

To Philip Guerrero, Mark Hess, Ty Lehman and Adrian Huh, your help over the years in navigating this journey will not be forgotten. I would like to formally acknowledge STATOIL for providing funding for field work in the Neuquén Basin, as well as my colleagues who shared an unforgettable two summers in Patagonia – Eugen Tudor and Nataleigh Vann.

Much thanks go out to BP America for providing me the freedom and subsurface data to work to add to this Dissertation, especially John O'Leary, Jacek Jaminski, Mario-Moreno Vega and Jonathan Evans.

Abstract

Coarse-grained deep water, slope & basin-floor systems: Influence of tectonic processes on internal and external architecture

René Ravi Winter, Ph.D.

The University of Texas at Austin, 2018

Supervisor: Ronald J. Steel

Co-Supervisor: Cornel Olariu

Internal and external architecture of a series of coarse-grained, deepwater deposits have been investigated and the role of intra- and extra-basinal tectonic forces on the sedimentary record has been highlighted within a source-to-sink context. Six hundred (600) meters of coarse-grained sediment gravity flow deposits of a submarine fan were measured in the Jurassic Los Molles Formation in the southern Neuquén Basin, Argentina. This fan is encased in a thick (km scale), fine-grained, hydrocarbon source-prone unit and is characterized by well-sorted, thick-bedded turbidite deposits in the axial and proximal parts of the fan, which transitions to more poorly-sorted and heterolithic facies on the fan margin and downdip fringe. Measured thinning rates of ~7m/km suggest a fan that is ~15km long, smaller than other systems with similar slope dimensions. Bed thicknesses are consistent across the fan but much larger numbers exist in the axial locations, suggesting stratigraphic truncation and fan confinement, probably the result of a structured basin floor inherited from syn-tectonic processes.

At the regional or basin scale, a combination of 3D seismic data, well log and core data were used to describe a relatively undocumented deepwater sedimentary system in the

offshore Veracruz Basin, Mexico. Sandstone-prone Miocene channelized fairways are present in the basin, downdip from an active plate boundary zone and active foldbelts. Deposits are poorly-sorted and exhibit similar spatially-controlled facies associations as the Los Molles Formation, however the depositional system is much more extensive, facilitated by regional tectonic forces and uplift in the hinterland resulting in extremely high sedimentation rates to the basin. A large channel complex, initiated by tectonic uplift on the margin and an eastward migration of the depocenter, which parallel's the migration of the deformation front in the hinterland, provide additional influence of tectonic forces on the resultant deepwater sedimentary systems.

Table of Contents

List of Figures

Chapter 1: Introduction

PROBLEM AND SIGNIFICANCE

The study of deepwater depositional systems over the last sixty (60) years has underpinned the successes of the hydrocarbon industry in exploring for and exploiting oil and gas reservoirs in the deepwater hydrocarbon province. Coarse-grained sandstones in these play fairways are of added importance given their high storage capacity and elevated reservoir performance. However, there exists a broad relationship between sediment grain size in a basin and the regional tectonic setting that defines the said basin: coarser deposits are typically synonymous with tectonically active margins, while finer grained deposits are associated with tectonically passive settings (e.g. Reading and Richards, 1994; Bouma, 2000). Thus, any study into the nature of deepwater, coarse-grained deposits must acknowledge the regional tectonic forces in play. For the hydrocarbon explorer, knowledge of the presence, extent and gross reservoir quality of the sandstone is important. For the hydrocarbon developer, a working knowledge of the facies successions and internal architecture of these associations is key. For both, understanding external controls and internal depositional mechanisms provides the predictive tool required to better predict the available sedimentary budget, the sediment transport and the spatial control on sedimentary process and deposition.

While investigation into the architecture of deepwater deposits driven by tectonic forces is not new (e.g. (Pickering et al. 1986; Demyttenaere et al. 2000; Deptuck et al.

2003; Samuel et al. 2003; Rowan et al. 2004; Adeogba et al. 2005; Ferry et al. 2005; Gee and Gawthorpe, 2006; Clark and Cartwright, 2009; Kneller et al. 2011; Mann and Escalona, 2011), not many studies have attempted to link the regional scale processes with detailed sedimentary responses, i.e. the conflation of basin scale dynamics with bed-scale, facies development. The well-exposed Los Molles Formation outcrops in the La Jardinera region, southern Neuquén Basin, Argentina and the Lower to Middle Miocene deepwater deposits in the offshore Veracruz Basin, southern Gulf of Mexico provide two excellent opportunities to investigate the effects of intra and extra basinal tectonic forces on deepwater sedimentary deposition. The coarse-grained (sandstone and conglomerate) deposits within the Los Molles Formation are unique in that they represent deepwater interbedded sandstones in an overall fine-grained, hydrocarbon source-prone interval. Historically, source rocks have been regarded as fine-grained reservoir systems, devoid of significant sandstone reservoirs, which can be fractured for hydrocarbon exploitation. Source rock intervals often tend to occur at major tectonic transitions (megasequence boundaries), which are easily identifiable on seismic profiles. Because of the change in tectonic state, deposits along megasequence boundaries are affected by the preceding tectonic forces and the new tectonic state. In the case of the Los Molles Formation in Neuquén Basin, deep marine deposits mark the transition between syn-rift extension within a backarc basin to postrift subsidence. Sediments entering the basin would have been affected by waning tectonic forces in the hinterland, associated with fault block extension, as well as an uneven seafloor, inherited by the rifting episode that initially generated the basin. The nature of the sandstone-prone fans within the Los Molles Formation thus offers

a unique opportunity to investigate coarse-grained sedimentation at megasequence boundaries and the resulting sedimentary deposit.

The deepwater Veracruz Basin in the southern Gulf of Mexico has recently been the focus of much industry success as proven onshore Tertiary-aged fields have begun to decline (Seelke et al. 2015). A convergent plate boundary and dynamic fold and thrust belt zones provides an extra-basinal tectonic element, not present in the Neuquén Basin, within which deepwater sedimentation can be studied. A multidisciplinary approach of integrating sedimentary core data, well logs and seismic offers insight on the detailed facies successions of coarse-grained deposits on a more regional scale than the Los Molles outcrops study provide.

OBJECTIVES

The objectives of this research are:

1) Characterise the internal and external architecture (geometry, scale) of coarse-grained, sandstone-prone fans in an overall fine-grained, source rock interval (Los Molles Formation), and the possible impact that a highly uneven basinfloor may have on external form/ geometry of the fan.
2) Compare and contrast the sedimentary response of a deepwater depositional system in a dual active-passive margin – the Miocene deposits of Veracruz Basin reservoirs - to end member systems, at both a regional, basin scale and detailed internal facies association assemblages.

3) Provide the initial sedimentological descriptions of deepwater sedimentary successions of the Los Molles in the La Jardinera region in a source-to-sink framework, incorporating the scale of the depositional margin and its control on the extent of the fan system and development of depositional facies.
4) Provide the first subsurface sedimentary description of the prolific Miocene (both lower and upper) reservoir systems in the Veracruz Basin within a source to sink framework, with emphasis on the extent of the fans and internal facies associations as a product of extra and intra- basinal tectonic processes.

METHODOLOGY

Investigation into the architecture of coarse-grained deepwater deposits at multiple scales requires a multidisciplinary approach; this study utilized sedimentary descriptions of cores (Veracruz dataset) and outcrops (Neuquén-Los Molles dataset), combined with high resolution aerial photographs and GIGAGPAN composite images of outcrops (Neuquén-Los Molles dataset), well lithology data (Veracruz dataset, Quaternary canyon dataset), routine core analysis data and 3D seismic data (Veracruz dataset). For the reservoir characterization of the Los Molles Formation in La Jardinera, sedimentary sections were chosen and logged to describe the architecture of the fan system in both depositional dip and strike perspectives. Aerial photographs and GIGAPAN images were used to define a semi-regional framework for the outcrops, from which the fan system was described. In offshore Veracruz, 270m of core were described and combined with grain size data to define the depositional fabric of the Miocene deepwater depositional system,

which was then combined with seismic interpretation and attribute analysis of over 9000km² of 3D seismic data in the basin.

OVERVIEW OF CHAPTERS

Chapter 2: Architectural and internal textural trends of a small, coarse-grained deepwater fan system, Jurassic Los Molles Formation, Neuquén Basin, Argentina.

This chapter describes in detail the facies associations observed in the Los Molles Formation in the La Jardinera region, their spatial characteristics and external form. It represents the first detailed sedimentological description of the exposed fan complex in the area at a system scale. This work was submitted to an international journal for publication, following an exercise of revisions from an initial submission in 2017. The facies characterization of the outcrops revealed a spatially controlled trend across the fan: proximal and axial regions were typically thicker and had better developed, thickly-bedded structureless and horizontally laminated sandstones. Toward the margin and fringe, the succession thinned dramatically and contained significantly fewer beds, suggesting a high degree of stratigraphic truncation. Depositional facies also transitioned to more debritic fabrics (sandy, muddy and linked debrites). This is similar to other cases of similar facies reported in other sand-rich lobes elsewhere and adds an important datapoint control for this relatively new depositional model.

Chapter 3: Architecture of deepwater depositional systems fed from a tectonically active catchment: deepwater Veracruz Basin, offshore Mexico, SW Gulf of Mexico.

Over the last decade, the deepwater Veracruz basin has been the focus of much successful exploration activity in Mexico, targeting Lower and Middle Miocene reservoirs. With the recent release of industry data, for the first time these deepwater depositional systems can be described and reported. Insight from the updip onshore basin describes a poorly sorted, coarse-grained slope to basin reservoir system. The offshore data confirms a continuation of these fan systems hundreds of km further into the basin. The Lower Miocene deposits are made up of channelized lobes, with a similar facies association to the Los Molles – structureless and horizontally laminated sandstones in the proximal axis of the fan which transitions to more heterolithic and debritic facies downdip and to the fringe. Thinning rates up to 6m/km suggest significant lateral thinning of the fan, suggesting an elongate fan system. This changes to a prograding slope in the Middle Miocene, where submarine canyons are formed by tectonic uplift of the shelf margin, which deliver sediment over 500km further into the basin, calibrated by DSDP wells. Together with an eastward migration of the depocenter that parallels the tectonic uplift of the hinterland, tectonic forces impart a profound influence on the nature and extent of these reservoir systems in the southern Gulf of Mexico.

Chapter 2: Architectural and internal textural trends of a small, coarse-grained deepwater fan system, Jurassic Los Molles Formation, Neuquén Basin, Argentina

ABSTRACT

Geoscientists exploring for sandstone-prone reservoirs typically focus on sandstone geobodies overlying source rocks, as deposition of coarse-grained material during times of fine-grained, source rock intervals is regarded as limited. The Lower Jurassic Los Molles Formation of the Neuquén Basin in western Argentina is an example of a proven marine, mudstone-dominated source rock that contains sandy fans. Sedimentary descriptions are combined with high-resolution aerial and satellite imagery to provide a detailed facies characterization of the Los Molles deepwater fan system in the La Jardinera region (southern Neuquén Basin). This reveals a sandstone-prone, fine to medium-grained basin-floor fan, made up of two 40-meter thick lobe complexes, separated by a regional mudstone marker ~15 meters thick. The fan exhibits an average thinning of ~7m/km away from the interpreted axial fairway toward the lateral fan fringe as well as downdip into the basin, while the constituent lobe complexes exhibit variable thinning rates in both directions. These measured rates suggest a small lobate fan that extends no more than 15km in both dip or strike direction.

For both lobe complexes, the axial zone of the fan is consistently thicker and contains more beds (both sandstone and mudstone) than the fan fringe, which suggests a high degree of stratigraphic pinch out or termination away from the interpreted fan axis. The relative coarse-grained nature of the deposits and an uneven basin floor, facilitated by synrift faulting, perhaps contributed to the restricted nature of the fan. The lobe complexes are made up of meter-scale thick lobes which can be sub-regionally correlated and show a

consistent facies trend of coarser-grained, amalgamated, structureless sandstones along the axis, that transition to finer-grained, heterolithic and debrite facies along the margins and in downdip positions. Well-defined channel geometries are rare on or within the well-exposed lobe complexes. Debrites occur both as sandstone-prone, stand-alone beds and muddy linked with turbidite varieties, and generally occur on the margins and distal fringes of the fans. One poorly-sorted, pebble conglomerate bed was regionally correlatable across the entire fan, except at the axial position. We interpret significant shelf-margin sediment supply (Lajas Formation) on a seismically active margin and high mud content of the Los Molles source areas as factors that facilitated mass wasting and promoted debrite accumulation. Coarser-grained debrites, but with sand-rich matrix, dominate several of the upper-middle slope channel belts that nourish the basinal fans of this study.

The Los Molles fan in the La Jardinera area exhibits other features typical of classic coarse-grained, sandy fans noted in both the modern and ancient rock record, e.g. areally restricted nature of the fan system, a coupled decrease in net sand and gross thickness out to the margins and downdip, prevalence of high density turbidites (structureless and horizontally laminated beds), texturally immature sands, absence of well-developed channels and dominance of depositional lobes. These observations suggest that coarse-grained deepwater reservoirs within source-prone intervals are similar to fans historically described in active/immature passive margins. The relatively small number of reported coupled source-reservoir systems worldwide suggests that this hydrocarbon play may have been underexplored. The sandstone-prone, coarse grained nature of these deposits, juxtaposed with mature source rocks, make them an attractive target.

INTRODUCTION

As the technology to drill deepwater hydrocarbon reservoirs has evolved, so too has the importance of understanding subaqueous sediment gravity flows, the sediment dispersal process that is dominant beyond the shelf-slope break. Deepwater reservoirs and source rocks have historically been studied separately. This is due in large part to the fact that coarse-grained, reservoir-grade, subaqueous gravity-flow deposits have been associated with conditions of falling and low stand of relative sea level, whereas fine-grained, oil-prone, marine Type 2 source rocks are the product of terrigenous starvation during times of rising and high stand of sea-level (Van Wagoner et al. 1988, Chandra et al. 1993; Wignall and Maynard, 1993). High quality oil-prone source rocks, by their very nature, are best developed in regions of limited terrestrial input (Katz, 2012). However recent work (e.g. Carvajal and Steel, 2006; Covault et al. 2007; Carvajal et al. 2009) documents significant sediment delivery to the shelf margin and beyond during times of rising and highstand of relative sea level, in supply-dominated systems. Covault and Graham (2010) used ODP and DSDP borehole data to illustrate the significance of submarine canyons as efficient sedimentary conduits systems during transgressive and highstand sea-level conditions over the last 36,000 years.

From an applied perspective, in some tectonically active basins, e.g. the Mesozoic North Sea Buzzard and Magnus fields (De'Ath and Schuyleman, 1981; Surlyk, 1987; Dore and Robbins, 2005) and early passive margins, e.g. Santos & Sergipe Alagoas of the Brazilian margin (Liro and Dawson, 2000; Mohriak et al. 2000), and the Gabon, Kwanza and possibly Congo Basins of West Africa (Katz and Melo, 2000; Brownfield and Charpentier, 2006), coarse-grained, deep marine sediments were deposited coevally with source rock intervals during prolonged, low-order eustatic highstand conditions. This conflicts with historical sequence stratigraphic models (e.g. Van Wagoner et al.1988) and

has resulted in sandstone-prone hydrocarbon reservoirs that are the first permeable sands in the basin, interbedded with or directly overlying the proven working source rocks, thus facilitating a diminished risk of charge access and volumetric loss through hydrocarbon migration.

This study introduces the excellently exposed Los Molles Formation of the Neuquén Basin in the Andean foothills of Western Argentina, which offers an opportunity to investigate the complete depositional profile of a coupled source-reservoir system. Coarse-grained, sediment gravity flows interbedded with deepwater mudstone source rocks are widely observed within the Los Molles succession (Howell et al. 2005; Paim et al. 2008; Paim et al. 2011). These continuous outcrops afford us the rare opportunity to document the detailed, internal architecture of reservoir-prone, sandstone geobodies at a scale beyond conventional wireline log sampling and seismic resolution. Additionally, the outcrops enable direct comparison of the larger-scale measured thickness and extent of the sandbodies to established models for coarse-grained deposits interbedded with mud-prone intervals.

Important to the study of such deepwater reservoir systems are the concepts of paleobathymetry and the regional depositional profile, as well as the fact that marine organic productivity and preservation is limited to ~1000 meters below sea-level (Katz, 1995). Thus, reservoir units within coupled source rock-reservoir systems must have been deposited under this limitation and similar paleobathymetric conditions. Research on modern and ancient submarine fans in the 1970's and early 1980's advanced our knowledge greatly on the morphology of fans (e.gs. Normark, 1970; Haner, 1971; Mutti and Ricci Lucchi, 1972; Tillman and Ali, 1982; Bouma, 1983 and 1984; Nelson and Nilsen, 1984; Bouma et al., 1985a; Mutti and Normark, 1987), however, the majority of these studies did not focus on the connection between deepwater fan evolution and sediment-

routing systems located up depositional dip. The importance of the regional depositional profile and its connection to deepwater fan evolution grew with our understanding of the relationships between basin geometry and accompanying sedimentary processes and deposits (Carvajal et al. 2009; Romans et al. 2016). With the advent of the quantitative source-to-sink theme for sedimentary systems (e.g. Granjeon and Joseph 1999, Syvitski et al. 2003; Allen, 2008b; Somme et al. 2009,) attempts were made to link deepwater systems to hinterland and basin characteristics, e.g. river length, climate and topography. Somme et al. (2009) illustrated the correlation between drainage basin size, river lengths, and slope extent with basin floor fan size. It is now generally accepted that margins with moderate slope relief (<1000m for maintenance of organic productivity) are typical of regions with modest drainage areas and small subaqueous fans, compared to more mature, large-scale passive margins (Donovan, 2003, Somme et al. 2009). Thus, fans deposited with coeval source rocks in syn-rift or immature, early postrift settings with incipient margin subsidence are generally areally small. These types of fans tend to also be coarse-grained and/or sand rich (Reading and Richards, 1994) and characteristic of tectonically active (foreland, backarc, synrift) margin (Barnes and Normark, 1985) settings.

The principal objective of this study has been to build upon the previous work done in the Mid-Jurassic succession in southern Neuquén Basin, describing in detail the architecture of the La Jardinera sandy fans of the mud dominated, source-prone Los Molles Formation. The coarse-grained nature of these sandy fans allows for additional insight into these types of deposits and comparison with other similar systems elsewhere. A second objective is to test the linkage between paleobathymetry and fan size of these types of coarse-grained fans, deposited in moderate basinal conditions (<1000m).

THE DEEPWATER LOS MOLLES FORMATION - SOUTHERN NEUQUÉN BASIN

The Pleinsbachian to Bajocian Los Molles Formation has been historically regarded as representing the late synrift to early post-rift fill of the Neuquén Basin of west Central Argentina (Howell, 2005). Total sediment thickness for the entire basin infill exceeds 7000 meters (Ramos, 1988). The southern Neuquén Basin is a triangular-shaped basin covering over 160,000km², bounded by the Andean Mountains to the west, the Pampeano-Sierra Pintada massif to the north and the North Patagonian massif to the south (Zavala, 1993; Fig. 2.1). The tectonostratigraphic evolution of the Neuquén Basin spans three phases: 1) a Late Triassic to earliest Jurassic syn-rift phase driven by intraplate extension and the deposition of continental to marine strata, 2) Early Jurassic to Early Cretaceous postrift phase associated with backarc subsidence driven by the oblique collision of the Nazca and Gondwana plates and characterized by fully marine sedimentation, and 3) Early Cretaceous to Cenozoic compression and foreland phase associated with the Andean Orogeny (Vergani et al., 1995; Howell et al. 2005).

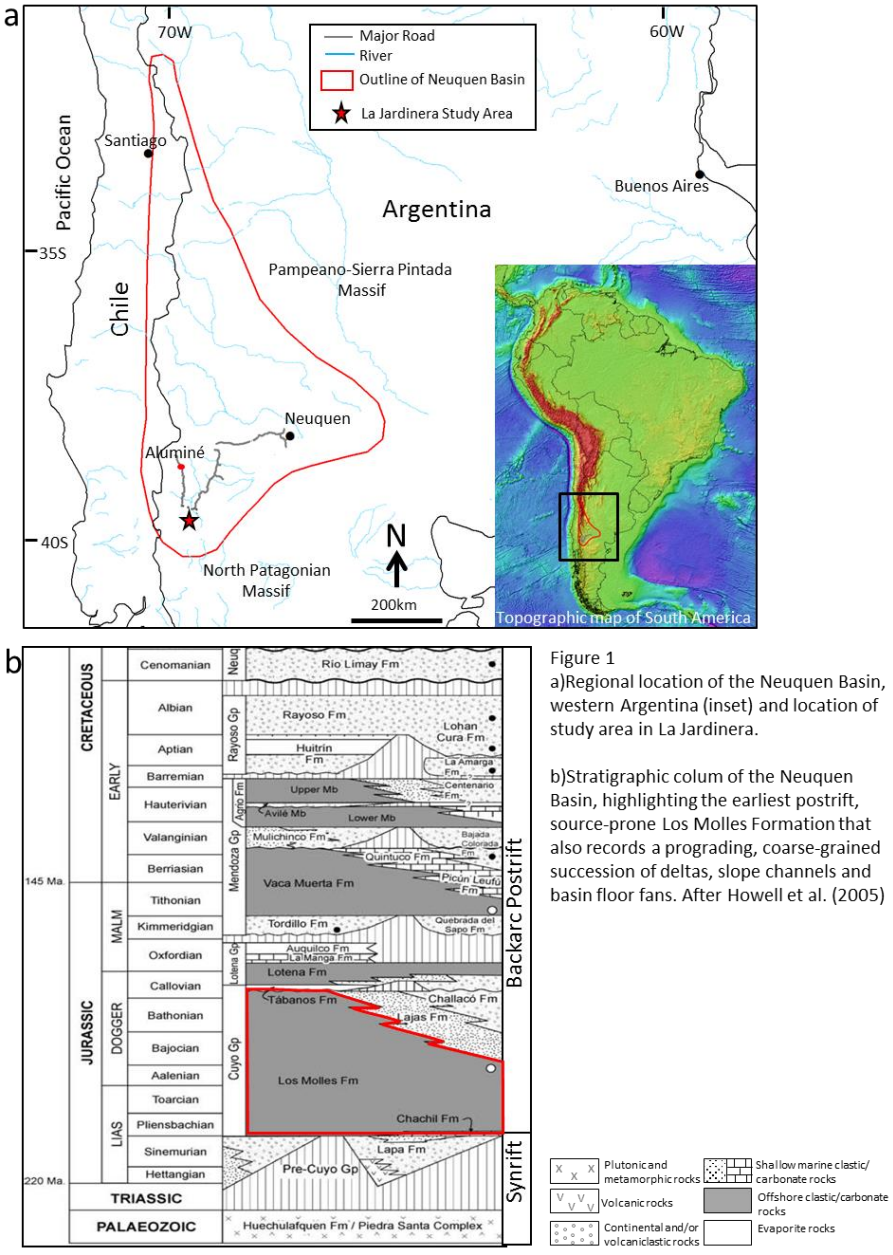

Figure 1
a)Regional location of the Neuquen Basin, western Argentina (inset) and location of study area in La Jardinera.

b)Stratigraphic colum of the Neuquen Basin, highlighting the earliest postrift, source-prone Los Molles Formation that also records a prograding, coarse-grained succession of deltas, slope channels and basin floor fans. After Howell et al. (2005)

Figure 2.1: a) Location of the Neuquén Basin, western Argentina and location of outcrops (star) on left. b) Stratigraphic colum of the Neuquén Basin, highlighting the earliest postrift, source-prone Los Molles Formation that also records a prograding, coarse-grained succession of deltas, slope channels and basin floor fans (right). After Howell et al. (2005)

The Triassic syn-rift stage of infill of the southern Neuquén Basin is reflected in interbedded volcanics, non-marine, lacustrine and shallow marine deposits, confined to half-grabens (Lapa Formation) with significant lateral variability in both facies and thicknesses (Howell et al. 2005). The deepwater dominated deposition for the overlying Los Molles Formation has been described by various authors (e.g. Gulisano et al. 1984b; Hinterwimmer and Jauregui, 1984; Carbone, 1988) within a lithostratigraphic framework. Vergani et al. (1995), using outcrop and early subsurface industry data, placed the marine deposition into a tectonstratigraphic context of transitional synrift to postrift setting of the underfilled Jurassic Neuquén basin system. Recent exploration of the Neuquén Basin, coupled with acquisition of new seismic data, has resulted in amendments to the previously proposed tectonostratigraphic framework for the basin. In the southern Neuquén Basin, including the Huincal High area, there is increasing evidence of continued syn-rift, sub-basin development into and through the Middle Jurassic, with the deepwater Los Molles Formation and its time equivalent shelfal Lajas Formation developing a thick growth succession between adjacent high blocks (Gulisano et al. 2001; Martinez et al. 2008). Burgess et al. (2000) documented the influence of inherited rift structures on overlying, basinal deposits, perhaps the youngest Los Molles Formation. This was also the first published detailed sedimentary descriptions of the coarse-grained fan systems. At a broader system scale, Gomez Omil et al. (2002) and Verzi (2005) described the Los Molles Formation strata as the distal deposits of a prograding marginal marine system that flanked the Neuquén Basin. It was the first attempt to place the early sedimentary succession of the basin in a linked chronostratigraphic framework. Paim et al. (2008), classified the coarse-grained deepwater deposits of the Los Molles Formation into 3 types of gravity flow deposits: channelized turbidites, hyperpycnal-driven deepwater flows and mass wastage

deposits within a sequence stratigraphic framework. Paim et al. (2011) further proposed a strong fluvial connection to the deeper water, downdip channelized turbidites.

In the La Jardinera area of southernmost Neuquén Basin, the outcropping Los Molles Formation is overlain by the shallow marine Lajas Formation, well described and constrained in this region (e.g. Martinez et al. 2008, Paim et al. 2008, and Rossi and Steel, 2016). Fig. 2.2 shows an aerial photograph of the La Jardinera study area, with an interpretation of the outcropping Middle Jurassic physiographic profile. Deltaic and other paralic deposits of the Lajas Formation, including a distributary channel complex, occur above the red line, which demarcates the vertical transition from shallower (sandy) to deeper (finer-grained) water deposits. Stacked decimetre-scale bedsets, often within channels with clearly defined pebble lags and high-angle cross-bedding are typical in this shallow-marine, tidal-fluvial system.

Stratigraphically below the red line in Fig. 2.2, an abrupt facies change to underlying muddier and deeper water facies with turbidite beds can be seen. This facies change can be traced on aerial photos across the entire study area and defines the litholologic boundary between the Lajas Formation and the underlying Los Molles Formation. Straddling this transition in several localities are large channel-form bodies, interpreted as shelf-margin/upper slope channel belts (Fig. 2.3), which act as sedimentary conduits delivering coarse grained material from the shelf-edge deltas to the deepwater slope. The upper-slope channel belts contain cobble and pebble size sandy debris flows and is associated with very coarse to medium-grained sandy turbidite beds, a direct indicator of the calibre of sediment being shed to the slope and basin floor part of the basin.

The succession below the shelf edge is otherwise mud-dominated, ~300 meters thick and is interpreted as a deepwater slope deposits below the shelf break. This muddy deepwater slope transitions downwards to a >200m-thick sandstone-prone interval

(highlighted by the yellow line in Fig. 2.2), consisting of two over 100 m-thick each, regionally tabular units, interpreted as separate submarine fans (following classifications from Prélat et al. 2009 and Koo et al. 2016). The lower of the two sandy fans (Fan A, Fig. 2.4) is the focus of this study. The regional paleoflow direction was defined by integrating previous research in the area (e.g. Paim et al. 2008, 2011) with more recent field observations of the shelf, slope and basinal facies and measurement of slope paleocurrent indicators as part of a wider field research effort by the Dynamic Stratigraphy Group of the University of Texas at Austin (e.g. Vann, 2013; Tudor, 2014; Shin, 2014; Olariu et al. 2015; Steel et al. 2017).

As a working petroleum system, the predominantly fine-grained, Los Molles has been regarded as a secondary source rock interval to the more prolific upper Jurassic Vaca Muerta Formation (Martinez et al. 2008). Hydrocarbons have historically been produced from both the fine-grained fraction (unconventional) and the coarser grained turbidites that are encased in the regional siltstones and mudstones. Present day exploration and production activity attempts to exploit its reported 275 trillion cubic feet of recoverable gas and 3.7 billion barrels of oil (US EIA, 2013).

DATASET AND METHODOLOGY

The Lower to Middle Jurassic Los Molles outcrops of the La Jardinera region are well exposed in the Andean foothills of western Argentina. Cenozoic Andean orogeny, to the west of the Neuquén Basin, has uplifted the frontal Andes region along the length of the mountain chain. The study area is located in the La Jardinera area at the corner of Route 46 and 24, on the road from Zapala to Alumine, in the southern Neuquén Basin, western Argentina. (Fig. 2.2). In the study area, the Mesozoic rocks were folded into a broad

anticline-syncline structure, uplifted and eroded. The remnant outcrops sit on opposing limbs of the anticline, with Sections S1-S4 dipping ~20º to the south and Sections S5-S11 dipping ~20º to the north.

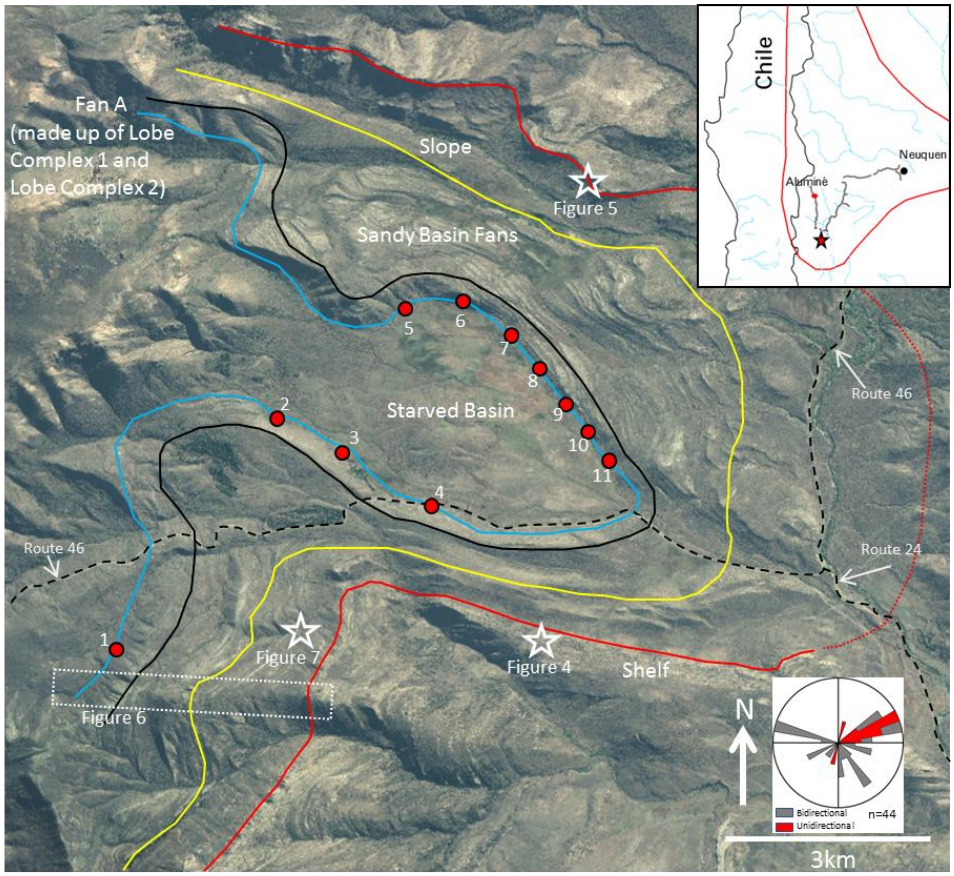

Figure 2.2: Satellite photo of the study area (red star on inset map) showing an interpretation of the Lower Jurassic depositional physiography (shelf, slope and basin) in the La Jardinera area: The shelf to slope transition is shown by the RED line and the slope to basin transition is shown by YELLOW line. These lines are defined by combining field observations of shallow marine, deepwater slope and basinal facies and extrapolation across the study region. Fan A (this study) is outlined by the BLUE and BLACK lines, interpreted from field observations and satellite photographs. The location of sedimentary log sections 1-11 are shown. Regional paleocurrent indicators, measured by Vann (2013), Tudor (2014) and Shin (2015) shown in lower right. Depositional Dip is to the northeast.

Eleven sites (S1-S11) were chosen along the regional outcrop exposure of Fan A based on accessibility, to characterize the facies and the internal architecture of the fan complex. A lithotype scheme (Fig. 2.5) was devised for the sedimentary logging and is used for bed- scale rock description based on lithology, sedimentary structures and grain characteristics and forms the smallest scale of rock description. The abundance and vertical assemblage of these lithotypes are used to interpret larger-scale facies associations within the fan complex. These facies associations represent the broad lithological variability of the fan and they reflect the groups of sedimentary processes that are typical of sub-depositional settings on the fan and basin floor.

With the main depositional facies of the fan documented, the detailed internal architecture of the correlated system is then described at various scales, following the hierarchical classification of Prélat et al. (2009) and Koo et al. (2016): i) fan scale (up to 100m thick), ii) lobe complex scale (up to 50m thick) and iii) lobe scale (<10m). In order to characterize the architecture of the sandy fan systems at different scales, the measured sedimentary sections and observed field relationships were integrated with high-definition satellite images, aerial photographs and a digital elevation model (DEM) of the region. The DEM was used as a high resolution, 3D model of the La Jardinera region to view the outcropping exposures from different perspectives than the aerial photographs and field observations provided. At all scales of description, spatial trends and internal architecture of the deposits are described with emphasis on gross interval and constituent bed thickness trends, correlation of sedimentary facies, spatial net sandstone trends and grainsize characteristics.

The observations and interpretations of the fan are then placed in its regional context within the basin, specifically the characteristics of the shelf and slope margin. This enables the direct comparison of the Los Molles fan in the La Jardinera region to other systems with

similar regional settings and fan characteristics, i.e. sandy basinal fans deposited coevally with fine-grained, source-prone deposits.

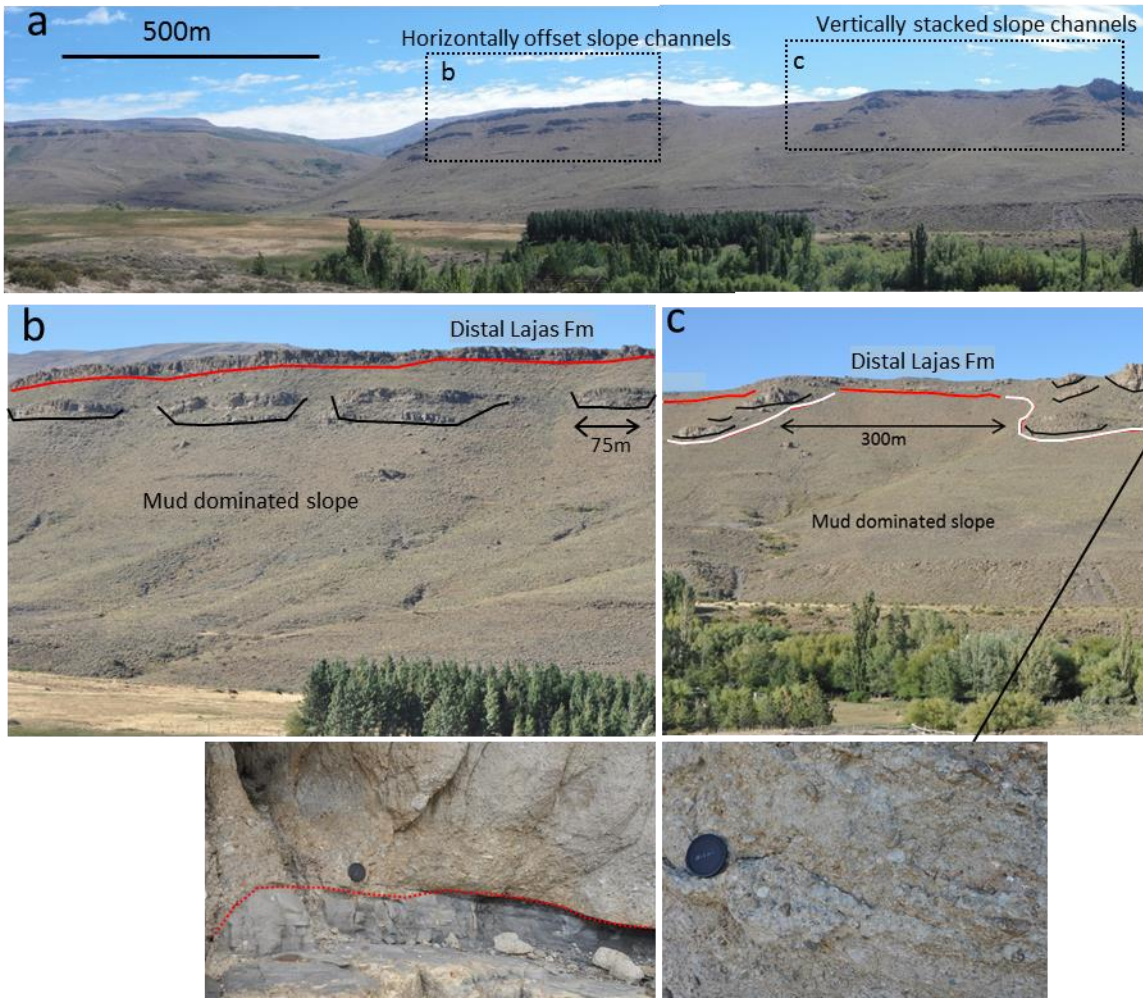

Figure 2.3: Architecture of the interpreted Upper slope channel systems, stratigraphically below the RED line of Fig. 2.2. View is toward the north. Note the coarse-grained nature of the sandy channel deposits. These are interpreted to be the source of the sediments observed on the basinal fan. See Fig. 2.2 for location of photos.

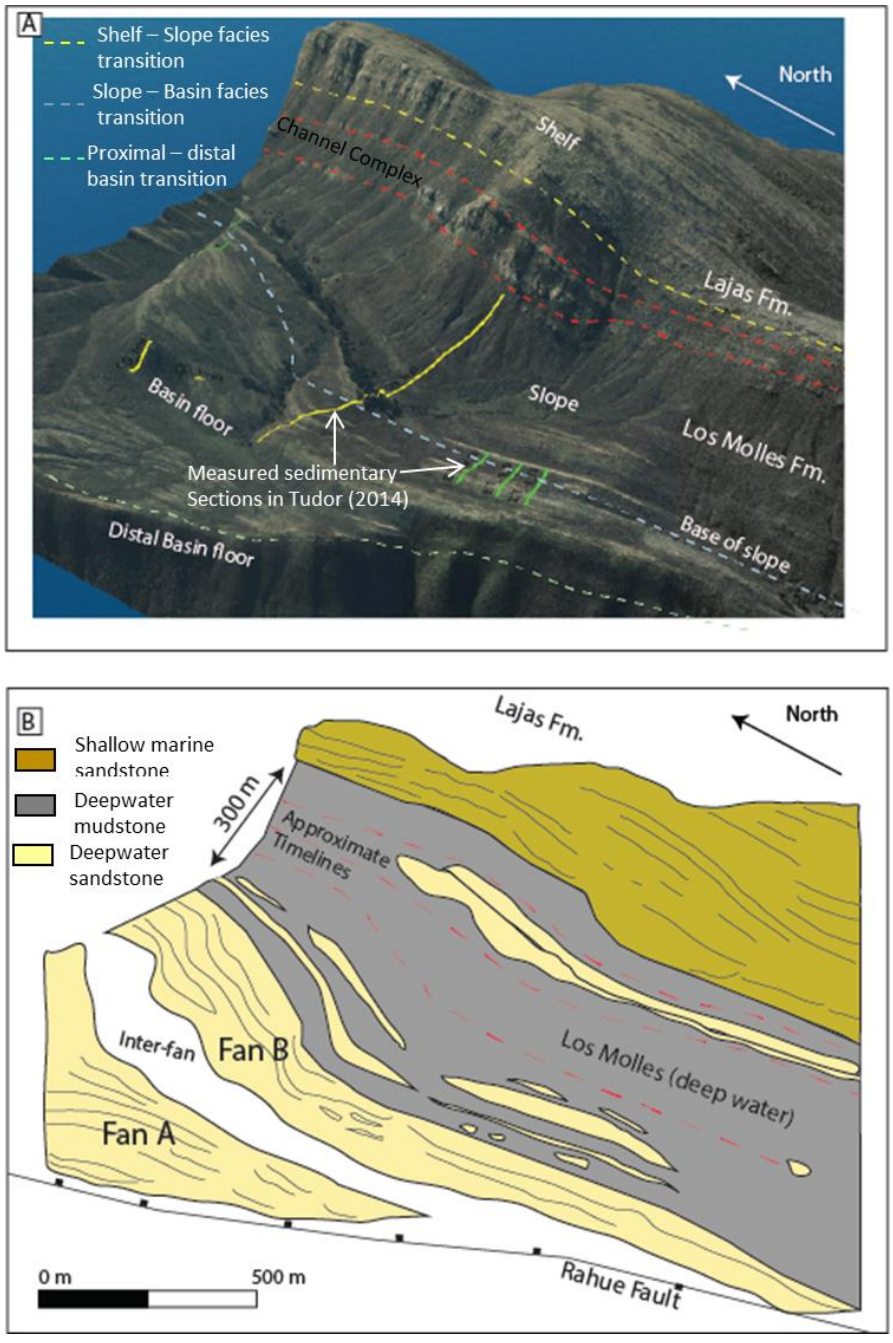

Figure 2.4: a) Oblique "birds eye" view of satellite image draped over high resolution Digital Earth Model, showing shelf, slope and basinal fan successions in the La Jardinera region. b) Interpretation of physiographic elements in photo above, highlighting Fan A. Modified after Tudor, 2014. See Fig 2.2 for location of image.

LITHOTYPES AND FACIES ASSOCIATIONS OF FAN A

Eleven sedimentary sections were chosen and described at 1:200cm scale, in order to document the internal character of Fan A, in both depositional dip and strike-oriented perspectives (Fig. 2.2). In Sections S2-S4, a consistent vertical facies transition from laminated, mudstone-dominated lithotypes to subtle coarsening- upward units is observed (Fig. 2.9), which marks the initiation phase of Fan A. The top of the Fan A is characterized by a vertical transition from sandstone-dominated lithology to heterolithic and muddy facies, and represents the shutdown and abandonment phase of Fan A deposition in the area. Approximately 3.5km northeast of sections S2-S4 the deepwater succession is repeated along the northeastern limb of an adjacent anticline, and sections S5-S11 are located along an exposed ridge 6km in length (Fig. 2.2). The regional anticline renders this ridge an ideal depositional strike exposure for the fans in a more downdip position. However, based on regional correlation on satellite photos, most of the exposed outcrops on this ridge are the upper part of Fan A, with the exception of Section S6, where rock exposure is of sufficient quality to describe the entire fan.

Twenty-two (22) lithotypes have been identified from the sedimentary sections recorded in the region, summarised in Fig. 2.5. Some of the more common types are also shown in Fig. 2.6.

Lithology	Lithotype	Sedimentary Log	Description	Interpretation	Example
Muddy	Mm		Structureless mudstone, beds can form 10's of m thick intervals, especially below Fan A.	Pelagic basinal deposition	
	Ml		Laminated (mm thick) mudstone, beds can form 10's of m thick intervals, especially below Fan A.	Pelagic basinal deposition	Fig. 6j
Silty	Slthl		Horizontally laminated (<1 cm thick) siltstones, beds form m-thick intervals.	Hemipelagic basinal deposition	Fig. 6k
Muddy Heterolithics	Mh		Dm thick units, with cm to dm-thick interbedded sandstones and mudstones. Net Sand % <40%	Low density turbidites	Fig. 6m
	Mhsl		Dm thick units, with cm to dm-thick interbedded sandstones and mudstones with contorted/slumped bedding. Net Sand % <40%	Low density turbidites on inclined topography	Fig. 6m
	Mho		Organic rich dm thick units, with cm to dm-thick interbedded sandstones and mudstones. Net Sand % <40%	Low density turbidites	
Sandy Heterolithics	Sh		Dm thick units, with cm to dm-thick interbedded sandstones and mudstones. Net Sand % >40%. Rare flute and flow marks and present.	Low density turbidites	Fig. 6l
	Sher		Dm thick units, with cm to dm-thick interbedded sandstones and mudstones with erosive bases. Net Sand % >40%. Rare flute and flow marks and present.	Low density turbidites	Fig. 13a
	Shpg		Dm thick units, with cm to dm-thick interbedded sandstones and mudstones. Graded pebble intervals commonly observed at sandstone bed bases. Net Sand % >40%	Low density turbidites	
Sandy	Ss		Structureless sandstones, frequently dm-scale in thickness, amalgamating to m-scale. Grainsize varies between fine to coarse-grained. Rare flute and flow marks and present.	High density turbidites	Fig. 6c
	Sr		Structureless sandstones, frequently dcm-scale in thickness, amalgamating to m-scale. Grainsize varies between fine to coarse-grained. Rare flute and flow marks and present.	Low density turbidites	
	Sx		Cross-bedded sandstones, dm-scale in thickness. Grainsize typically medium to coarse-grained.	Low density turbidites	Fig. 6c
	Shl		Horizontally laminated sandstones, frequently dm-scale in thickness. Grainsize typically fine-grained.	High density turbidites	Fig. 6c
	Sc		Sandstones exhibiting convolute bedding (wavy & dewatering structures), frequently dm-scale in thickness. Grainsize varies between fine to medium grained.	High density turbidites	
	Smgmc		Massive sandstones, dm-scale in thickness, with graded mudclasts. Sandstone grainsize varies between fine to coarse-grained.	High density turbidites	
	Smp		Structureless sandstones with ungraded pebble granules. Beds are cm to dm thick. Sandstone varies between medium and coarse-grained.	High density turbidites	
	Smpg		Structureless sandstones with graded pebble granules. Beds are cm to dm thick. Sandstone varies between medium and coarse-grained.	High density turbidites	Fig. 6b, d
	Smdps		Poorly sorted muddy (matrix) sandstones. Beds are cm to dm thick. Sandstone varies between fine and coarse-grained.	Debrite	Fig. 6e
	Sps		Poorly sorted, structureless sandstones. Beds are cm to dm thick. Sandstone varies between fine and coarse-grained.	Debrite	Fig. 6f
	Smpsp		Poorly sorted, structureless sandstones with pebbles. Beds are cm to dm thick. Sandstone varies between fine and coarse-grained.	Debrite	Fig. 6g
	Sig		Inversely graded sandstones, sometimes with pebble bases. Beds are cm to dm thick. Sandstone varies between fine and coarse-grained.	High density turbidites	
	Sigp		Pebble-rich, structureless sandstones. Beds are cm to dm thick. Sandstone varies between fine and coarse-grained.	High density turbidites	Fig. 6a

Figure 2.5: Lithotype scheme used in the description of Los Molles Fan A in La Jardinera. Images of common lithotypes are shown in Fig. 2.6

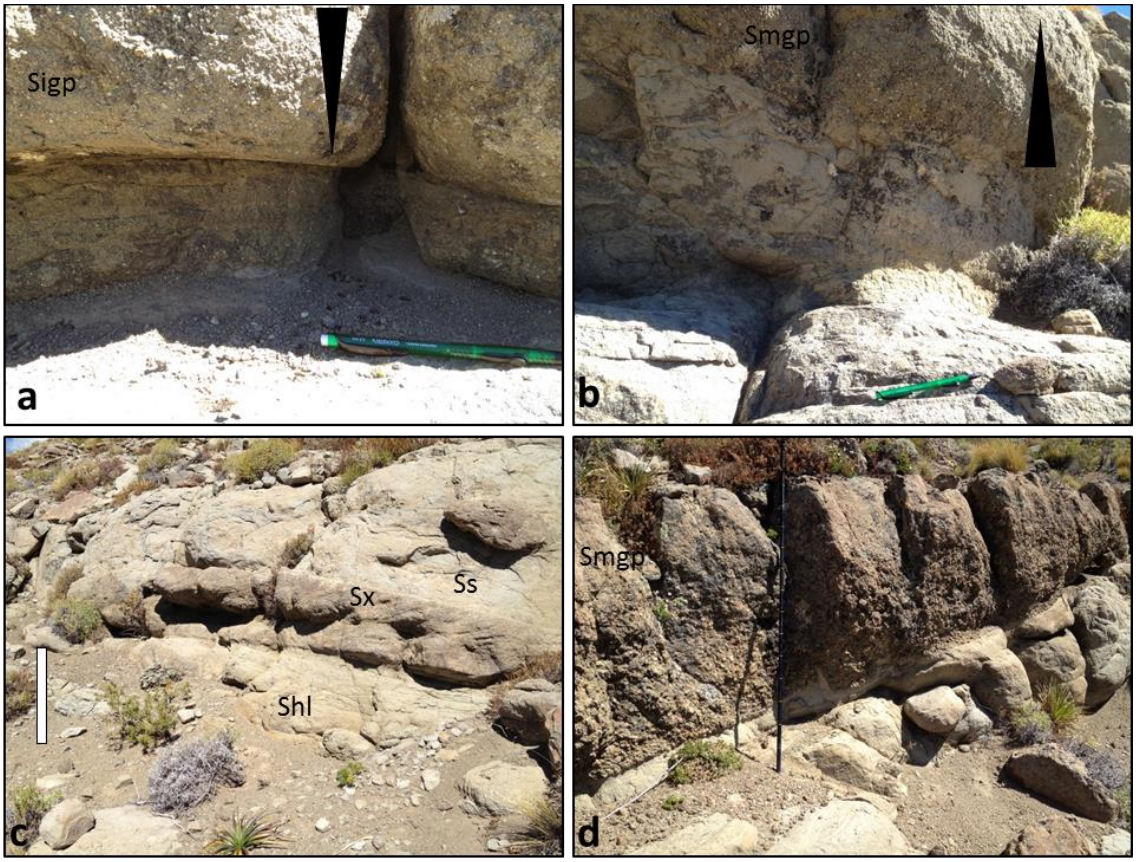

Figure 2.6: Examples of common lithotypes within Fan A, La Jardinera region. a- inversely graded, pebbly sandstone (triangle), b- normally graded pebbly sandstone (triangle), c- cross-bedded sandstone overlying horizontally laminated sandstone, in turn capped by structureless sandstone, d- weakly normal-graded, pebbly sandstone.

e – muddy, poorly sorted sandstone , f- poorly sorted sandstone overlying structureless sandstone, g- structureless, poorly sorted sandstone with abundant pebbles and clasts, overlying structureless sandstone with erosional contact (red line), h- poorly sorted pebbly sandstone between two structureless sandstone beds, i- poorly sorted pebbly, muddy sandstone in a large-scale erosional bed (red line represents the erosive base), j- laminated mudstone,

k- horizontally laminated siltstone, l- sandy heterolithics, m- slumped, muddy heterolithics overlying undeformed, muddy heterolithics. Pencil is 15cm wide. Hammer is 30cm long. Jacob's Staff is 1.5 meters long. Where no scaled object is present, white boxes are 1m.

These lithotypes were then grouped into five (5) facies associations, based on lithotype abundance and vertical assemblage trends. These facies associations correspond to the main depositional elements of the Los Molles Formation in the region.

FA1 - *Well sorted, structureless and horizontally laminated sandstones*

Description. FA 1 is characterized by well-sorted, structureless sandstone beds, and these occupy about 25% of beds in the measured fan successions. Grainsize varies from very fine to coarse, with small extra-formational clasts sometimes present. Beds are typically decimeter to meter-scale thick, with upper bounding surface either sharp or gradual. Basal surfaces are sharp and usually erosive. Normal grading is common, along with internal grading of clast sizes where present. Horizontally laminated beds are rare, but typically occur in close association with the structureless beds. Dewatering structures are rare. This facies association is best developed in Sections S3 & S4.

Interpretation. The well-sorted, structureless character of beds and presence of normal grading of both sand-sized grains and clasts suggest turbulence during transport and incremental deposition from rapid sediment fallout of near-bed processes (traction carpet collapse, Lowe, 1982). Beds that display horizontal lamination can also form in a similar manner, with slightly reduced sediment concentration, but can also be the product of low amplitude bedforms (Best and Bridge, 1992). The sharp to erosive bed bases suggest that they were indeed formed by high-density turbidity currents, where elevated sediment concentrations diminish turbulence at the base of the flow resulting in the general suppression of bedforms (Lowe, 1988).

Depositional Setting. FA1 occurs in the proximal parts of the depositional system, within low-relief channels and in proximal sediment lobes beyond channel mouths.

FA 2 – Poorly sorted sandstones

Description. A wide variety of poorly sorted sandstones are note in the Los Molles succession. They occur in 2 main types – a) mud-rich and mud-poor sandstones with sharp or erosive bases and b) mud-rich varieties with gradational bases, underlain by well-sorted sandstone beds.

FA2a - *Clean and dirty, poorly sorted, conglomeratic sandstones with erosive bases.*

Description. Structureless, poorly sorted, conglomeratic sandstones are common (up to 10% of beds in fan successions), especially in Sections S2, S3 and S5-S11. Clean (mud poor) sandstone beds are characterized by inverse grading at the base of beds, though the clasts in the beds show no obvious grading. Beds are centimeter to decimeter thick, with characteristic erosive bed boundaries. A 1-meter thick, non-graded to normally graded conglomeratic bed is observed in S2 and S3 that is tentatively correlated to the distal sections. Similar poorly sorted beds but with higher mud content (deeper grey colour) also occur, with similar scales of thickness to the cleaner beds. In both instances, the sandy fraction of the bed is significantly coarser than the underlying and overlying beds. A thick muddy, cobble-sandstone bed is also observed in a highly erosive setting at Section S4, incising more structureless, better sorted and cleaner FA1 sandy beds. Cobble-sized particles are randomly distributed within this unit, varying in shape from angular to sub-rounded. Sedimentary structures are typically absent in all beds.

Interpretation. These poorly-sorted pebbly sandstone beds suggest deposition by *en masse settling*, as the flow comes to an abrupt halt (freezing) and are interpreted as debrites (Talling et al. 2012). The random alignment of clasts also supports rapid sediment deposition. The cleaner sandstone beds with pebbles represent non-cohesive sandy debrites, possibly deposited by liquefied flows, while the rarer muddy (dirty) sands

represent more cohesive debris flows, capable of supporting larger clasts in the matrix (Talling et al. 2012), as seen in Section S4. For these sandy debrites with their diminished clay content, flow behaviour straddles the cohesive and cohesionless spectrum (Shanmugam, 1996). Deposits are typically characterized by poor sorting, inverse grading of clasts and irregular bounding surfaces and the presence of floating outsized clasts (Shanmugam, 1996).

Depositional Setting. FA2a beds occur most commonly near the interpreted distal and marginal parts of the fan.

FA 2b - Bipartite units of structureless, well sorted sandstone and overlying, poorly sorted, muddy sandstones

Description. FA2b occurs as repeated bi-partite units containing (1) a basal, cm-dm thick, fine to coarse-grained structureless sandstone bed with occasional basal clasts and sometimes soft-sediment deformation and (2) an overlying, poorly-sorted muddy sandstone with some granules or clasts. The boundary between the two parts of the bipartite unit is gradual or sharp. The nature of this sandy-muddy or sandy to argillaceous sand is key in differentiating this Facies Association from FA 2a, which displays similar erosive bases but not the consistent, underlying structureless sandstones. The upper boundary of the muddy sandstone is typically gradational to an overlying mudstone or occasionally contains very thin, fine-grained or laminated mudstone.

Interpretation. The consistent occurrence of a decimeter-thick, poorly sorted muddy sandstone lithotype, with occasional clasts, overlying a structureless sandstone bed is similar to reported "linked debrite" deposits of other fan systems (e.g., Haughton et al. 2003). The capping debrite is considered as genetically related to the underlying turbidite sandstone and differs from the stand-alone debrites of Facies Association 2, because of the

linked, underlying high density turbidite. Other indicators of co-genetic flow conditions include evidence for soft sediment deformation (water escape) near to the bed boundaries as well as the absence of hemipelagic or turbiditic muds between the 2 lithotypes.

Depositional Setting. FA2b occurs in the distal or marginal areas of the fans.

FA 3 - *Cross-stratified sandstones with basal mudclasts/pebbles in close association to structureless or horizontally laminated sandstones*

Description. Well sorted, cross bedded sandstones are rare, but where present, usually occur in beds with a characteristic basal mudclast conglomerate or pebbly interval. Basal bed boundaries are erosive to sharp-based and are typically decimetre thick. Grainsizes are notably coarser than other beds. The units are typically underlain and overlain by structureless and horizontally laminated beds, characteristic of FA1. This association is only observed in Sections S2 and S3.

Interpretation. Cross stratified sandstones suggest the presence of cut-and-fill structures or possibly the migration of bedforms (dunes or ripples) in sedimentary conduits or channels (Harms et al. 1982; Boggs, 2006). The adjacent structureless sands are interpreted as high density turbidites, deposited as FA1 beds, but within channels.

Depositional Setting. FA3 occurs mostly in the higher energy locations such as proximal and axial regions of the fan.

FA 4 – Interbedded, fine-grained sandstones and mudstone

Description. In some sedimentary sections, 40-50% of beds are represented by centimetre-thick interbedded fine-grained sandstones and mudstones within units which can reach 5 meters in total thickness. They are subdivided into sandy and muddy varieties, determined by a threshold of ~ 40% net sand estimation of the unit. Sands are typically

well to moderately sorted, structureless, or horizontally laminated. Internal clasts are occasionally present. Intervening mudstones are typically structureless or bioturbated.

Interpretation. Well sorted, structureless sandstones are likely to represent turbidity currents deposited by near-bed traction carpet collapse and fallout from suspension in turbulent flows (Lowe, 1982). The thin, repetitive nature of these beds suggest intermittent deposition from sediment pulses, during times or in locations of overall limited sand supply. This potentially explains the high frequency occurrence of cm-thick sand beds. Interbedded muddy beds represent periods of suppressed delivery of sand-rich flows to the basin floor. The non-amalgamated nature of these deposits suggests a position in the basin where the flows are mostly depositional with decreasing sand concentrations and relative low energy flows that are not able to erode muddy beds.

Depositional Setting. FA4 occurs mostly in distal and marginal fan areas.

FA 5 – Organic rich, laminated siltstones and mudstones

Description. Volumetrically the most abundant deposits in the La Jardinera area, it is made up of black, organic-rich, laminated siltstones and mudstones. Thicknesses vary greatly between decimetre thick beds to >100meters below measured sedimentary sections S2-S4. Units are fairly homogenous, with occasional cm-scale sandstone laminations. Bioturbation is difficult to discern.

Interpretation. These deposits represent the hydrocarbon source-prone, background fine-grained Los Molles Formation in the basin. The lack of sand sediment suggests a sediment-starved basin condition, with regional siltstones representing the times of terrestrial input. The black, organic-rich nature of the deposits is similar to other reported descriptions of the regional Los Molles Formation (Burgess et al. 2000, Martinez et al.

2008, Paim et al. 2008) and represents deposition and preservation of significant organic material to the basin.

Depositional Setting. FA5 is representative of times of diminished sediment delivery to the basin.

DEBRITE DEPOSITS IN THE LOS MOLLES FAN SYSTEMS.

On both the lateral and frontal fringe of Fan A, sandstone-prone (stand-alone) and linked debrites make up ~12% of the total beds. The former is more common (ca. 75% of total debrite beds) than the linked "hybrid" beds and represents sediment gravity flows that were typically generated via mass wasting and slumping on an unstable slope, with redeposition onto the lower slope and basin floor. As their name suggests, they are regarded as separate deposits to the much more frequent (background) high-density turbidites on the fan, based on their interpreted plastic rheology and flow behaviour (Dott, 1963). Deposition is not incremental as in conventional and high density turbidites, but rather *en masse* (Talling et al. 2012).

In the Los Molles Formation, the spatial occurrences of the debris flow deposits suggest either distal flow transformation from turbulent flows or proximal non-preservation of regionally deposited sandy debrites. Facies transitions from sandy, high density turbidites to downdip sandy debrite beds have been documented in the Marnoso Arenacea Formation (Talling et al. 2012). These distal beds are believed to have been formed by flow transformation, where sustained, high rates of deposition by turbulence produce a near-bed sandy layer whose thickness grows more rapidly than the layer can consolidate. Talling et al. (2012), also proposed a model for the generation of regionally extensive sandy debrites: incorporation of small amounts of basinal muds resulted in

increased fluid viscosity and decreased sediment settling rates. This model of more regional deposition and non-preservation of these debrites in the proximal axis of the fan is supported by the observation of a regionally correlatable, pebble-conglomerate debrite bed in the upper part of the Fan, which is noted at all locations except Sections S2 & S3 (Fig. 2.7c). At these two locations, amalgamated high-density structureless and horizontally laminated sandstone beds are common, suggesting high rates of erosion and non-preservation. A source of cohesive, marine muds to increase fluid viscosity for these regional debrites is readily available in the mud-dominated, source-prone Los Molles Formation. A single, well-exposed and highly erosive mud-rich, sandy debrite seen at Section S3 provides another example of these large-scale, stand-alone deposits.

The other type of debrite deposits seen in Fan A are linked debrites (Facies Association 2b). These differ from stand alone, sandy debrites in that they are typically muddy/finer-grained and are regarded as genetically part of the same flow of the underlying sandy turbidite. This spatial occurrence is of particular interest in that they deviate from established conventions (e.g. Bouma, 1962) which predicts increasing fine-grained deposits and thin-bedded turbidites in the distal fan as conventional turbidites diminish in sediment concentration as it travels down-system and sediment fallout occurs. Haughton et al. (2003) and Talling et al. (2004), suggest 3 possible mechanisms for flow transformation from turbulent to cohesive flow behaviour: i) downdip transformation of the flow via the entrainment of argillaceous material from bed erosion in the basin ii) interaction of submarine flow with irregular slope and basin topography which promotes erosion/slumping and incorporation of muddy substrate and iii) downdip partial-flow transformation from an initial debris flow. Mechanisms i and ii rely on the incorporation and flow intake of elevated muddy substrate, which changes the viscosity, yield strength

and flow state of the subaqueous event and subsequent transition from turbulent to cohesive/laminar controlled deposition.

QUANTITATIVE ANALYSIS OF LOS MOLLES FAN A DEPOSITS

Cross sections A-C (Fig. 2.7) show a series of sedimentary profiles across the Los Molles Fan A in both depositional dip and strike (proximal and distal) perspectives. These panels show both lateral and basinward thinning of the entire system from an observed maximum at S4. This confirms that the proximal part of the fan occurs in the south (in the region of S4) and transitions downdip to the middle/outer fan in the northeast. It also suggests that the axial part of the system occurs in the proximity of S4 (proximal) and S6 (downdip) with the fringes on either side of these. Fig. 2.8 summarises the spatial distribution of the textures and lithotypes described in the previous section across Fan A.

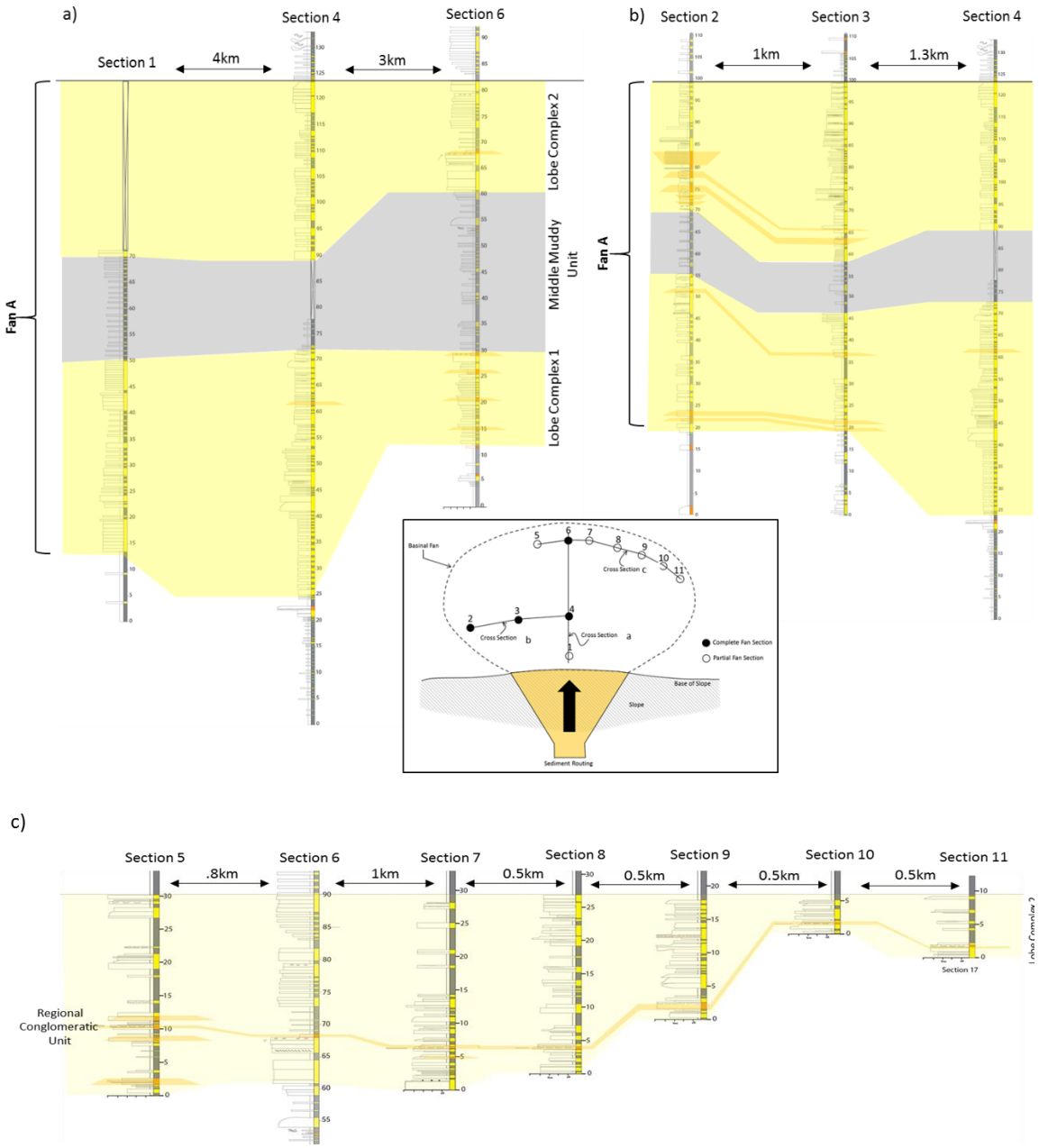

Figure 2.7: Cross sections through Los Molles fan in the La Jardinera region.
a)Depositional dip section, b) proximal strike section, c) distal strike section.

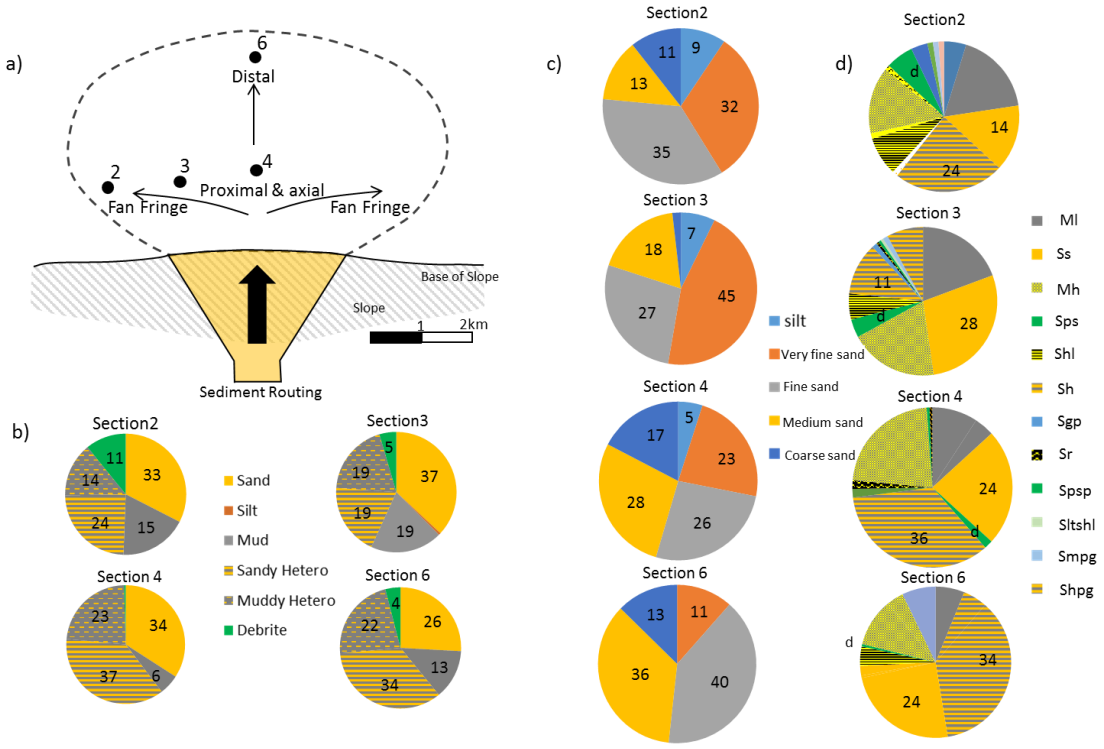

Figure 2.8: Summary of textural features of the Los Molles Fan A in the La Jardinera region. a) Location of sedimentary sections that describe the entire fan, b) Gross lithology of these locations - showing decreased mud content and increased sandy heterolithics toward the axis of the system (Section 4), compared to muddier heterolithics and debrites on the fringes and distal parts of the fan. Numbers represent % of given gross lithology, c) Grain size trends between sedimentary sections showing increasing grain size (medium & coarse-grained) toward axial positions (Section 4), d) Summary of lithotypes in the fan system, note the dominance of Structureless Sands (Ss) and Sandy Heterolithics (Sh) facies in the axis of the system vs. Pebbly Sandstones (Sgp) & Poorly Sorted Sands (Sps) which are interpreted as debrites on the margin and distal locations. See Fig. 2.5 for full lithotype descriptions

Thickness Trends. Using S4 as the reference point for the proximal and axial fan position, Fig. 2.7 shows an overall fan thinning rate of ~6.5-7m/km in both the depositional-strike and depositional-dip directions, from a maximum of 100 meters at S4.

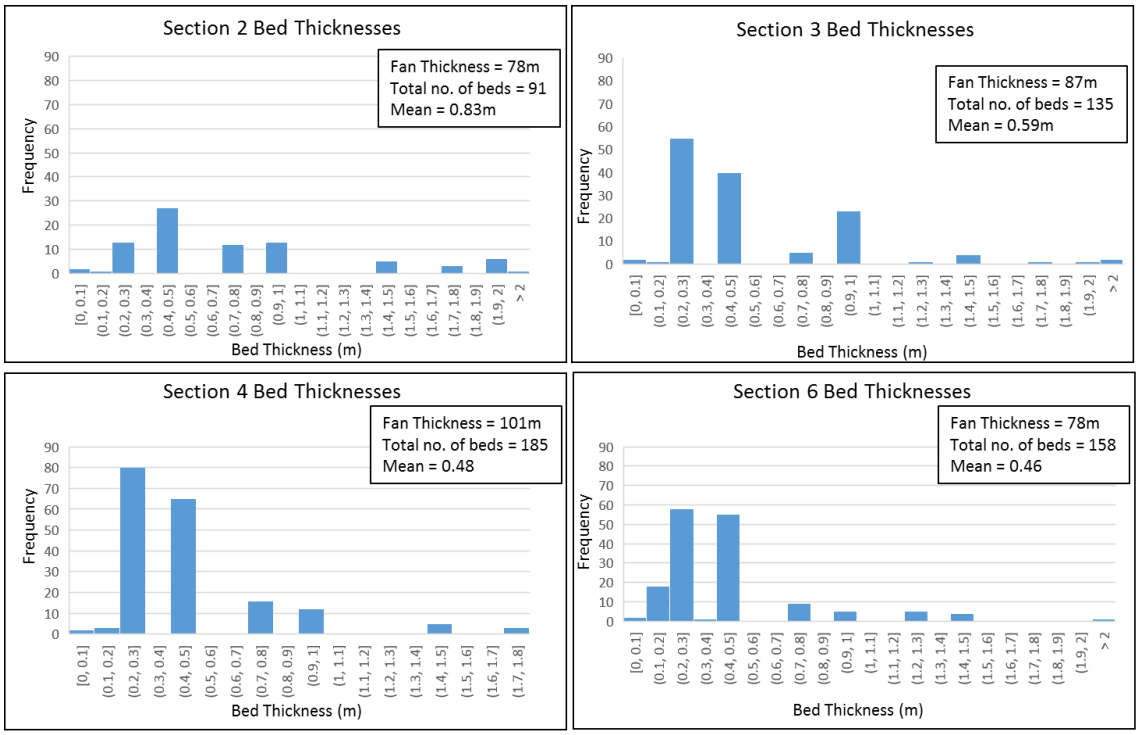

Figure 2.9: Histograms of bed thicknesses for Sections S2, S3, S4 and S6, that sample the entire fan. Note the greater number of beds in sections 4 and 6 (fan axis).

To investigate the controls on these observed rates, individual bed thicknesses for all 11 sections were recorded. For all sections, there were more sandstone-prone beds (total 544) than mudstone-prone ones (total 405). However, mudstone beds are thicker – mean 0.6m compared to a mean 0.46m for sandstone beds. The majority of beds at all sections have a thickness that does not exceed 1 meter.

Fig. 2.9 shows a series of bed-thickness frequency distributions for sections that sampled the entire fan succession (S2, S3, S4 and S6). The interpreted axis of the system

(S4 and S6) contains significantly more beds (50%) than the margin of the fan, suggesting that the fan thickness maximum is the product of the number of beds rather than greater bed thicknesses. A consequence of the number of beds variability is that some of the axial beds will thin and pinchout or will be truncated laterally or down-system.

Grain-Size Trends. The main lithotypes encountered in Fan A include: (1) structureless sandstones (Ss); (2) heterolithic sandstones (Sh); (3) muddy heterolithics (Mh), and (4) laminated mudstones, Ml (Fig. 2.8c). In the axial and proximal part of the fan, location S4 is dominated by the sandstone-prone lithotypes Sh and Sm with relatively minor volume of Mh and Ml. However, this trend changes to the northwest, where the mud-prone lithotypes become more prominent at the expense of the sandier ones. This trend is reflected by a modest system-scale reduction in net sand, shown in Fig. 2.8 (66% --> 52%).

In a depositional-dip direction, structureless and sandstone-prone heterolithics at S4 transition to mudstone-prone heterolithics at S6. There is also a marked increase in laminated mudstone facies thickness in the downdip direction. These changes are reflected in a corresponding decrease in net sandstone (~66% to 50%), which is a proxy for the overall diminishing of sand from the proximal to the distal reaches of the fan.

For the volumetrically minor lithotypes, a marked increase in poorly sorted sandstone (Sps) lithotypes is observed from section S4 toward S2 (lateral fringe). There are 2 lithotypes that are exclusive to S4: sandstone-prone heterolithics with erosional bed boundaries (Sher) and structureless, normally graded sandstones with mudclasts (Ssgmc), suggesting some channelization and preservation of mudclasts, probably within confined, turbulent flows. Additionally, graded beds are rare in Section S2 compared to S3 & S4. A

similar increase in poorly sorted sandstones (Sps) facies is observed in the downdip Section S6 compared to S4.

With regard to grainsize, sandy lithotypes show a coarsening from very-fine to medium-grained sandstone toward the axis of the system (Sections S2 to S4). There is a coarsening toward Section S5 downdip, where medium-grained sandstones dominate the thinner, lower net-to-gross section, highlighted in Fig. 2.8c. Much of these coarser-grained sandstone beds occur in the poorly sorted, sandstone-prone lithotypes (debrites).

LOBE COMPLEXES AT LA JARDINERA.

Using the hierarchical classifications of Prélat et al. (2009), and Koo et al. (2016), Fan A can be subdivided into two sandy units that are interpreted as lobe complexes (LC1 and LC2) both approximately 40 meters thick and separated by a 15-meter-thick, regionally correlative mudstone unit, observed both in the field and on gigapan images (Fig. 2.10).

a

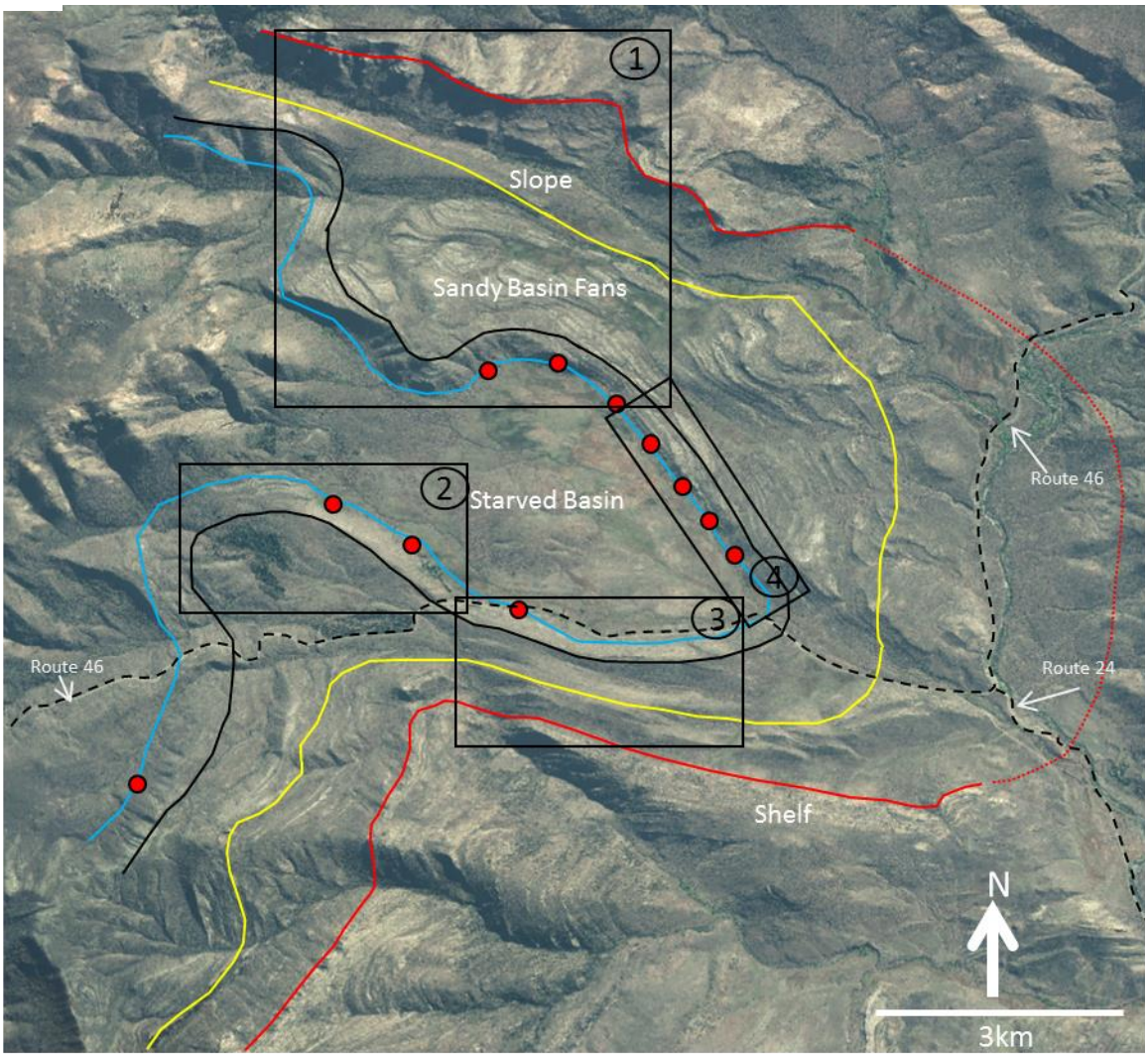

Figure 2.10: a) Satellite Photo of the study area showing interpretation of the Lower Jurassic depositional outcrop physiography. Black boxes represents Gigapan images in Fig. 2.10b and red circles are the locations of the logged sedimentary sections. The shelf to slope transition is shown by RED line, slope to basin transition is shown by YELLOW line. Fan A (this study) is outlined by the BLUE and BLACK lines.

b

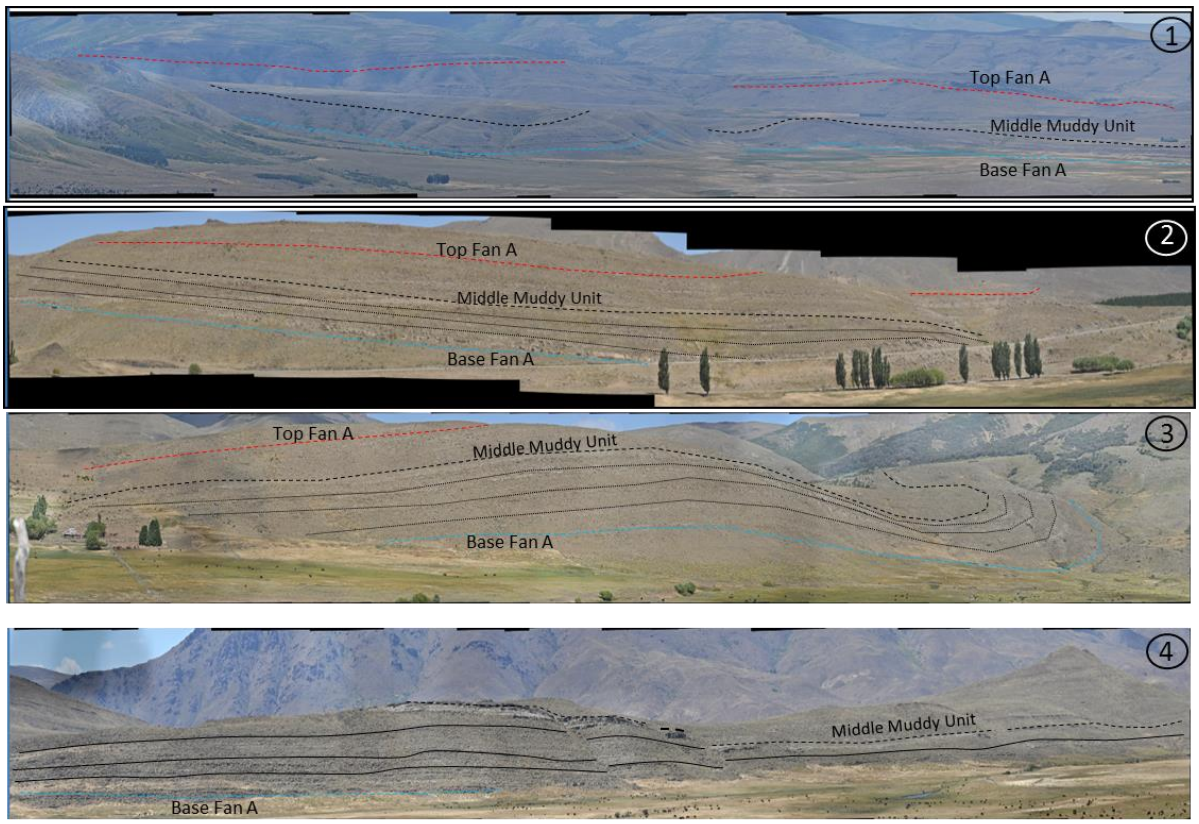

b) High Resolution Gigapans acquired in the field to aid correlation between sedimentary sections and across the AOI. Coloured lines are described in Fig 2.10a. The middle muddy unit separates Fan A into two (2) separate Lobe Complexes (LC1 and LC2). Black solid lines highlight the constituent Lobes within the lower LC1.

Although the lithologic changes can be observed directly in the field and calibrated to individual high resolution gigapans, the regional correlation on satellite photos introduces a level of irreducible uncertainty in correlating between the proximal sections (S2-S4 and the distal sections (S5-S11). Additionally, the lack of regional correlation outside of the La Jardinera area results in uncertainty as to the nature of this mudstone unit, i.e. whether it represents a regional shutdown of coarse-grained sedimentation to the basin,

or a local avulsion event. Outcrop exposure limits the description of the lower LC1 to Sections S1-4 and S6, whereas LC2 is described in Sections S2-4 and S5-11.

LC2 differs from LC1 in that it lacks any basal coarsening-upward package, instead being characterized by a sudden change from the mud prone middle section to decimeter-thick beds in a high net-to-gross unit (Fig. 2.7). The sandy unit of LC2 is capped by a sharp transition to a muddy heterolithic package that is interpreted to represent the final abandonment of the fan in the region.

LOBE COMPLEX LC 1 – THICKNESS & GRAIN-SIZE TRENDS

LC1 exhibits marked stratigraphic thinning from a maximum thickness of 47m at Section S4 to 33 m in the northwest (S2), similar to the regional fan trend described above. In a depositional dip direction sense, significant thickening is observed from Section S1 (36 meters) toward S4, which then switches and exhibits a significant thinning to the distal S6 (24 meters). These give thinning rates of ~6 m/km in a lateral sense from the axial position of the fan, and ~ 9 m/km from the proximal S4 to the distal S6, shown schematically in Fig. 2.11a.

Frequency distribution diagrams of individual bed thickness (both sandstone and mudstone) in LC1 are shown in Fig. 2.11b, which suggest that more beds occur in the axial and proximal positions of LC1– Section S1 and S4 – compared to the margins and distal part of the system.

Although a simultaneous increase in both thick sandy and muddy beds is noted in the axis of LC1, this location maintains the highest net sand proportion (67%). This is consistent toward the proximal Section S1, however a larger sand fraction occurs in the heterolithic (Sh) lithotype, compared to the more prevalent structureless sandy (Ss)

lithotypes observed at Section S4. Net sand decreases significantly to the thinner lateral fringes (average 40% sandstone) and distal reaches of the unit (60% sandstone), albeit the downdip decrease in sandstone proportion is not as significant as the lateral reduction.

In general, finer grained sands dominate the fringes and distal parts of the lobe complex compared to the axial and proximal parts of the system (Fig. 2.11a). Axial positions show an increased amount of coarse-grained sand at the expense of fine-grained sand which dominates the lateral fan fringe.

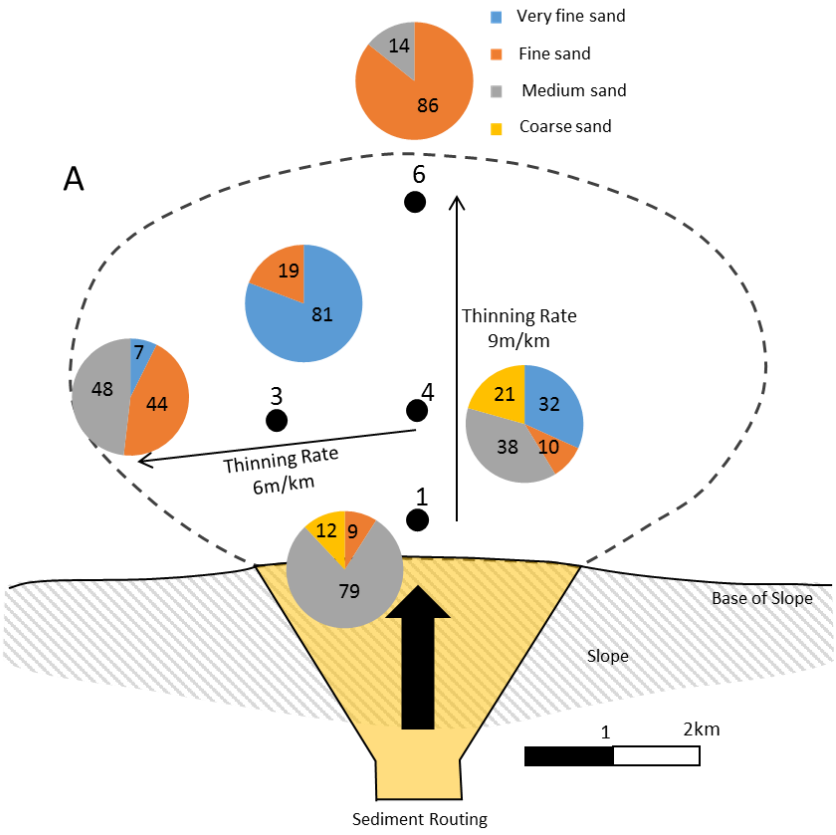

Figure 2.11: Thinning rate, grain size and bed thickness analyses for Lobe Complex 1.

a) Note greater thinning rate to the distal fan compared to lateral fringe from axis. Also, the increasing coarse-grained sands in axis of system vs finer-grained sands on the margin and distal setting. Grainsize percentages are shown in all locations.

B

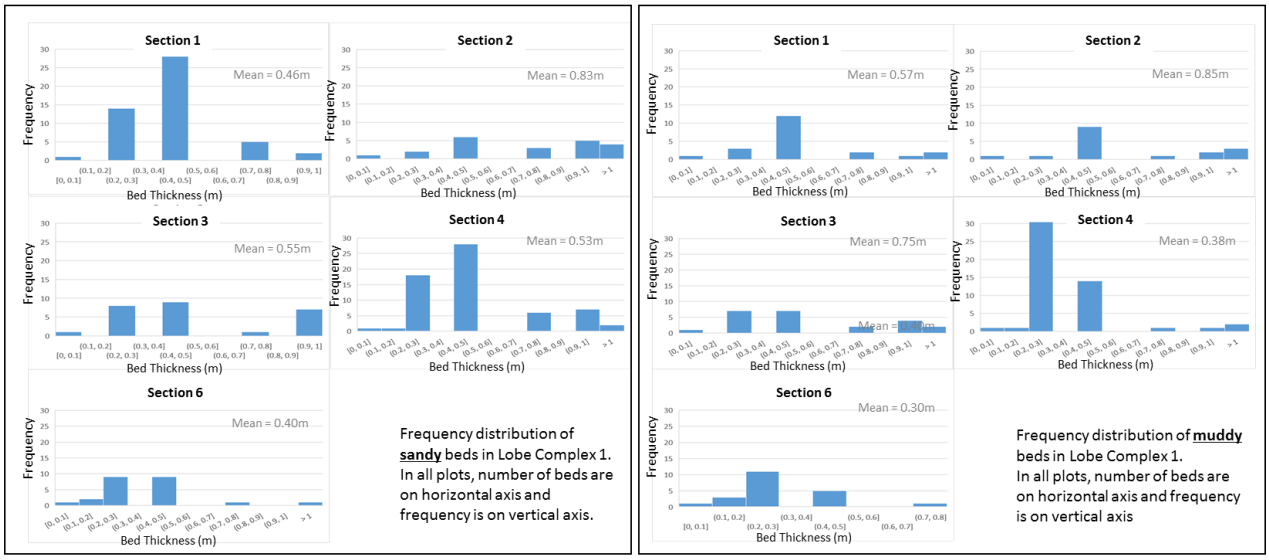

b) Bottom – Frequency distribution of both sandy and muddy beds in LC1. Note greater number of beds in the axis (Sections 1 & 4) of the system vs elsewhere on fan.

HIGH RESOLUTION (LOBE-SCALE) CORRELATION OF LC1

In the field, three (3) distinct units within LC1 can be traced between the measured sedimentary sections: an upper and lower sandy unit separated by a relatively sand-poor interval. Fig. 2.10b shows the identification and correlation of these units around the La Jardinera area. Following the hierarchical classification of Prélat et al. (2009), and Koo et al. (2016), these intra-LC1 packages are referred to as lobes (1A, 1B, and 1C) illustrated in Fig. 2.12a. Beneath lobes 1A-1C is an underlying heterolithic unit, marked by interbedded

sandstone, siltstone and mudstone. The individual sandstone beds thicken up to 1 meter, and in the case of Section S4, can exhibit subtle channelization (Fig. 2.13a and b). Deposition was dominated by thinly bedded, structureless sandstones against a background of laminated siltstone. Subtle coarsening and thickening upward bedding can be seen.

Lobes 1A-1C

The lowermost unit, lobe 1A is dominated by structureless, ungraded sandstone beds with minor, poorly sorted, muddy sandstones. A high degree of amalgamation is seen in Section S4 (proximal and axial), where the lobe is thickest (~27 meters, Fig. 2.12). Lenticular, non-amalgamated, compensationally-stacked beds are observed at Sections S2 and S3, suggesting a lower degree of amalgamation. Sandy debrite beds are also seen exclusively at Section S2. Basinward, this lobe is difficult to define. However, a marked increase of individual, thin, poorly sorted sandstone beds, interpreted as stand-alone debrites, are noted that correlate to the structureless sandy lithotypes observed updip.

Lobe 1B exhibits a marked decrease in sand volume in Sections S2 & S3 but S4 is dominated by amalgamated, structureless sandstone beds, some of which are downcut by a large scale, erosional, debris flow (Fig. 2.13c). This confined flow is made up of very poorly sorted muddy sands, with cobbles, pebbles and coarse-grained sand all chaotically arranged within a muddy matrix that erosionally truncates the underlying sandstone. In the distal S6, this debris flow deposit is tentatively recorded as a smaller, channelised flow (Fig. 2.13d). The thickest occurrence again occurs at Section S4, but does not exceed 10 meters. Unlike

the underlying 1A, this correlation suggests that these debris flow events are regional in scale and correlatable across the fan.

The overlying Lobe 1C is characterized by similar thickness to 1B, structureless, ungraded sandstone lithotypes across all sections which thin downdip to Section S6. At S2,

multiple occurrences of poorly-sorted sandstone beds with low mud content, that erode the underlying massive sandstone beds are observed. These are interpreted as stand-alone, sandy debris flow deposits. However, no evidence of these deposits is seen downdip.

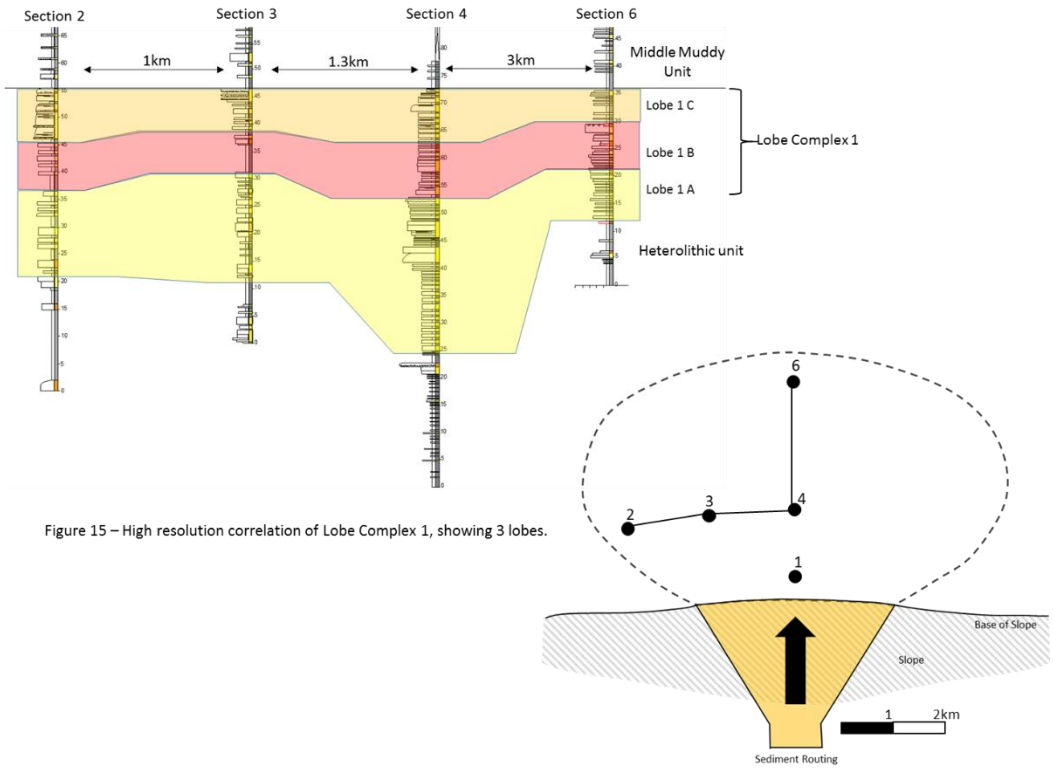

Figure 15 – High resolution correlation of Lobe Complex 1, showing 3 lobes.

Figure 2.12: High resolution correlation of Lobe Complex 1, showing 3 lobes.

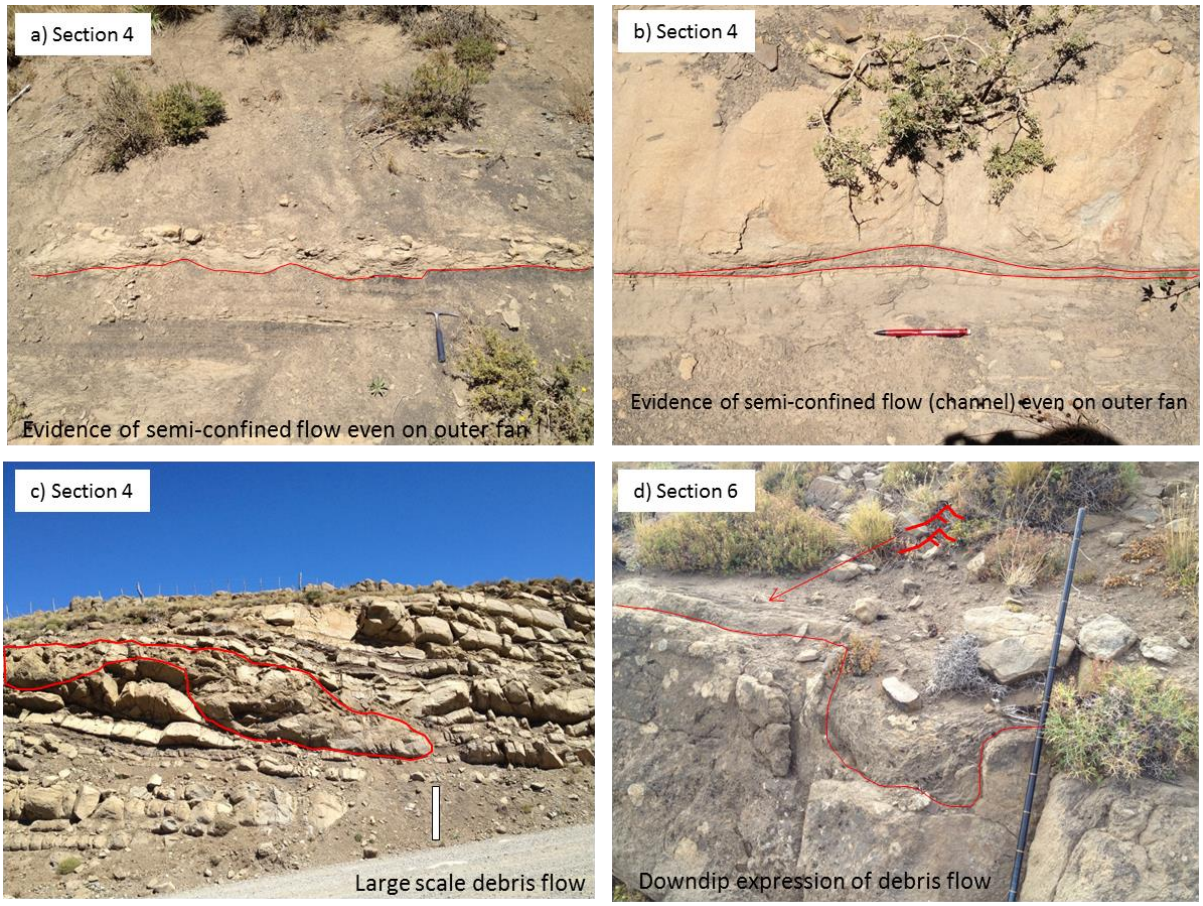

Figure 2.13: Examples of channelization seen in axial location of LC1, Fan A, a) cm-scale scale erosion within sandy heterolithics in distal reaches of the fan (hammer is 30cm long), b) subtle, cm-scale channelization of thick (1m) beds (pencil is 15cm long), c) Large scale debrite channel incising tabular, high density turbidite units (white box is 1m long), d) Distal expression of debris flow observed in Section S4 (yellow graduated lines on Jacob's staff are 10cm intervals)

LOBE COMPLEX LC 2 – THICKNESS & TEXTURAL TRENDS

At all locations, the upper LC2 is recorded as a sudden change in deposition from the underlying middle muddy marker unit to coarse-grained, sandy beds. This upper

complex is observed in Sections S2-S4 and S5-S11 (Figure 2.7) and shows a maximum thickness at Section S3 of 37.5 meters. Downdip thinning to S6 is ~3.5m/km, but higher rates are observed toward the fringes of the unit; in the proximal setting, a thinning rate of 11m/km is observed toward Section S2 and in the distal fan, a rate of 6.6m/km is calculated between Sections S6 and S11 (Fig. 2.14a). This reversal in thinning rate maximum suggests a switch from a more lobate-shaped LC1 to a more mounded geometry for the upper unit or a compensational switch with a re-orientation of the main axis.

Individual bed thicknesses were recorded and plotted via frequency distribution diagrams in Fig. 2.14b. These figures show a similar change in the interpreted axis of the system, with Sections S3, S6 and S8 recording the largest number of beds. Sections S3 and S6 are also the only localities where the majority of beds are equal to or greater than the mean bed thickness values, compared to the other sections where the frequency maximum is equal to or less than 0.25m. This mirrors the underlying LC1 where the interpreted axial position records a higher number of total sedimentary beds, as well as a higher frequency of thicker sandy and muddy beds. All beds showed a subtle thickness increase from LC1 to LC2 (mean 0.53m vs 0.59m).

The subtle downdip thinning results in an almost consistent net sandstone percentage trend compared to the significant thinning observed to the margins of the fan which results in a concomitant reduction in net sand. These observations, combined with similar LC1 trends, suggest a direct correlation between position on the fan and resulting sedimentary character: the axial fan is consistently the thickest part of the fan, with the highest number of thicker beds (both sandy and muddy), which results in the highest net sand percentage along the axis. Additionally, there appears to be a correlation with sand grain-size: the fringes of the complex are consistently finer-grained than the axial positions. One interesting observation noted at the fan scale was the apparent grain-size preservation

of the sandy sections in the distal reaches of the fan. LC2 shows this trend, with locally coarser grains in the interpreted sandy debrites in the distal part of the fan. A coarsening-upward grainsize trend is also observed between LC1 and LC 2 (Figs. 2.11a and 2.14a), especially in the distal portions of the fan.

A consistent transition from the sandy fan facies to an overlying mud-dominated succession is observed, and this can be traced on aerial photographs. At Sections S1 & S2, this unit is made up of repetitive, thinning upward, massive sandstones interbedded with mudstones (Mh and Sh). At Section S4, evidence for slumping and bed deformation can be observed (Fig. 2.6i). This provides further evidence for being adjacent to an unstable deepwater slope and a likely mechanism for deriving debrites from this slope onto the fan lobes.

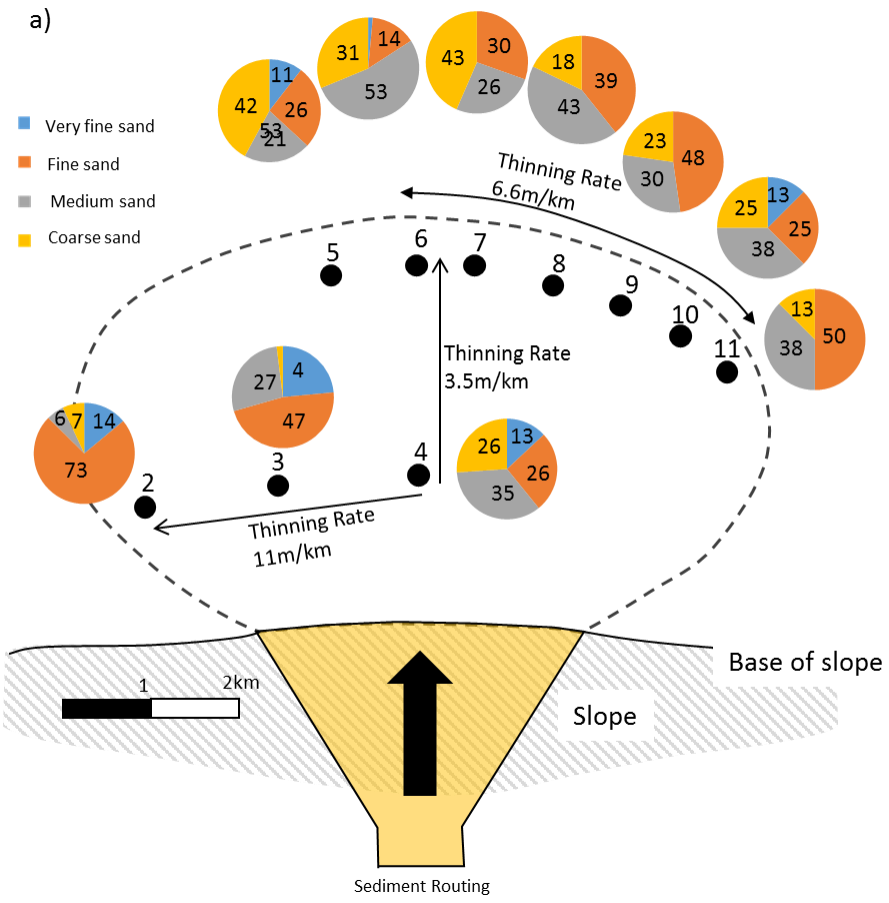

Figure 2.14 : Thinning rate, grain size and bed thickness analyses for Lobe Complex 2; a) Schematic profile of LC2, showing spatial trends of thinning and grainsizes. Note greater thinning rate to the lateral fan fringe compared to the distal fan from the axis. Also note the larger proportion of medium and coarse-grained sands in the axial locations of the fan vs very fine and fine-grained sands on the margin (both in the inner and outer fan).

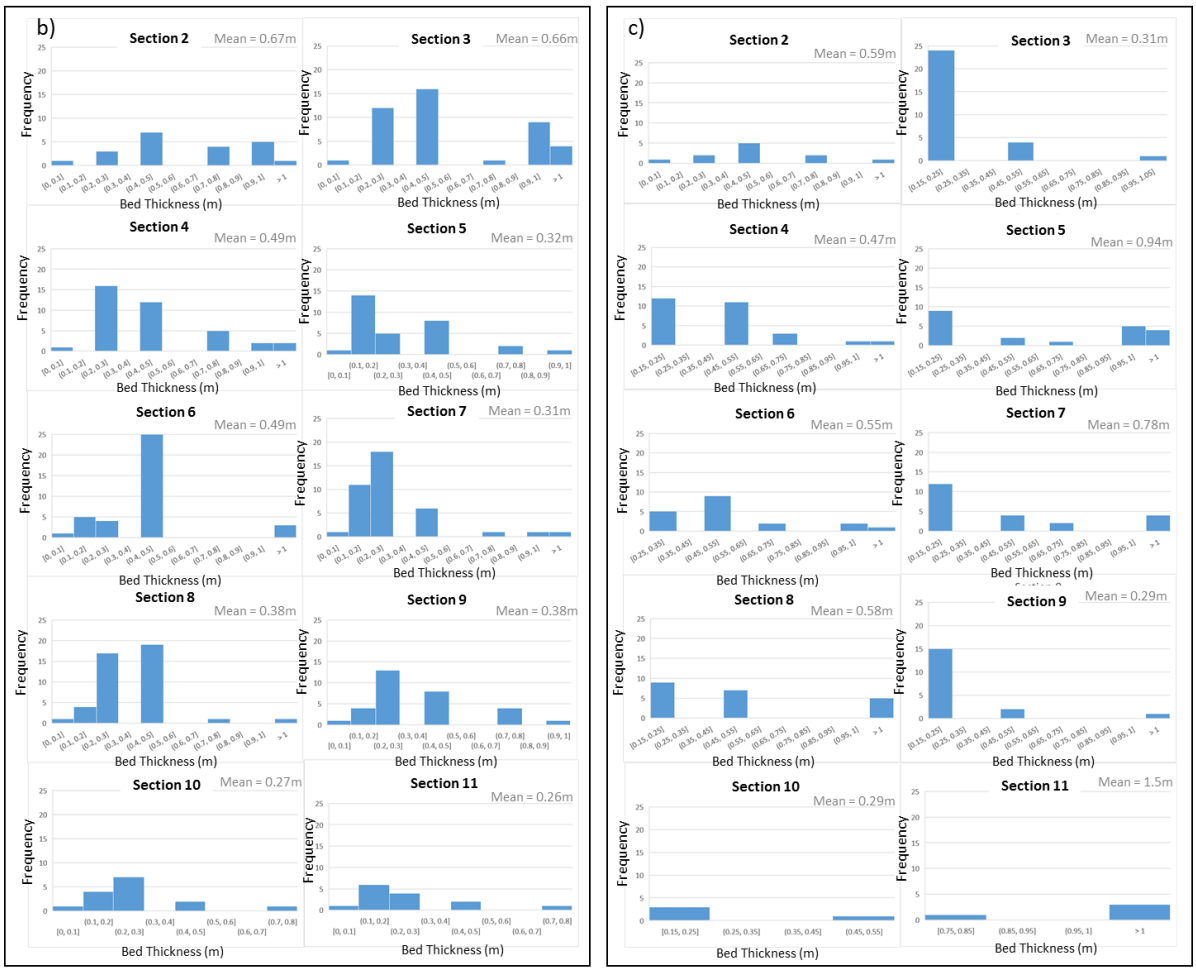

b) Frequency distribution of **sandy** beds in Lobe Complex 2. In all plots, number of beds are on horizontal axis and frequency is on vertical axis; c) Frequency distribution of **muddy** beds in Lobe Complex 2. In all plots, number of beds are on horizontal axis and frequency is on vertical axis.

HIGH RESOLUTION (LOBE-SCALE) CORRELATION OF LC2

LC2 was divided into 3 lobe units, observed in the sedimentary sections (Fig. 2.15) and supported by interpretations on high resolution gigapans; a lower, debrite-rich unit (2A), a middle mudstone-prone interval (2B) and an upper sandstone-prone interval (2C), seen on high resolution images as two distinct sandstone-prone benches.

Lobes 2A-2C

In the proximal parts of the Fan A, lobe 2A is characterized by a debrite-rich interval on the fringe of the fan (Sections S2 & S3) which transitions to a sandy, debrite poor succession at S4. The debrites are a combination of linked and stand-alone types, with the former only seen at S2. A 1-meter-thick, pebble-rich debrite is observed at the top of the unit (Fig. 2.6d) which transitions to three separate, decimeter-scale beds at Section S3. This unit is not seen at S4. Similarly, the underlying debrites show a marked decrease in occurrence toward the axis of the system (Section S3), instead replaced by sandier lithofacies. Lobe 2A can be tracked with reasonable confidence to the distal reaches of the fan at Sections S5 & S6 (thicker and axial). Here the thick-bedded debrites seen in S2 & S3 are observed, especially in S5 (Fig. 2.15). The debrites all appear to be stand-alone (erosive/sharp bases, mud poor and poorly sorted with a chaotic character and outsized floating clasts). Just as in S2 & S3, the stand-alone debrites are overlain by the pebble-rich marker in S5 & S6, suggesting the regionally extensive nature of these intra-lobe beds. However, in these distal sections, the pebbly unit is much thinner than that observed at S2 and more similar to the individual bed thickness observed at S3. They also appear to be non-graded to poorly sorted in the distal settings. Fig. 2.15 shows the interpretation of Lobe 2A to the fringes of LC2 (Sections S7-S11). Although there is a decrease in the occurrence of the lower stand-alone debrites, the overlying pebble-rich, marker unit is observed in all

additional sections. The spatial relationships of these debrites and overlying marker bed are summarised in Fig. 2.16.

Unit 2B represents a fan-scale reduction in sand, with lithologies dominated by heterolithics (sandy and muddy) at all measured sections (Fig. 2.15). Thicknesses are highly variable, in the proximal locations this unit is 5 meters on the fan margin at Section S2 and expands to ~ 15 meters at Section S4. In the distal fan, the unit is best developed in Sections S5 & S6 and similar in character to the proximal settings. On the distal fringes, correlation is challenging as the section thins to the southeast.

Unit 2C represents a return to higher sand deposition, this time with a lack of debrite deposits and characterized by only sandstone lithotypes (mainly massive, with minor horizontal lamination and cross bedded sandstones). This sandstone-prone interval is predominantly aggradational, with variable thicknesses between the axis (20 meters) at Section S3 to 10 meters at S2 & S4. In the distal fan, a marked decrease in sand is observed, with lithologies dominated by thin massive sands and heterolithics. Like in Units 2A and 2B, this upper lobe is difficult to interpret in Sections S7-S11, where the upper parts of the fan are characterized by thin, massive sandy and muddy heterolithics, with occasional pebbles.

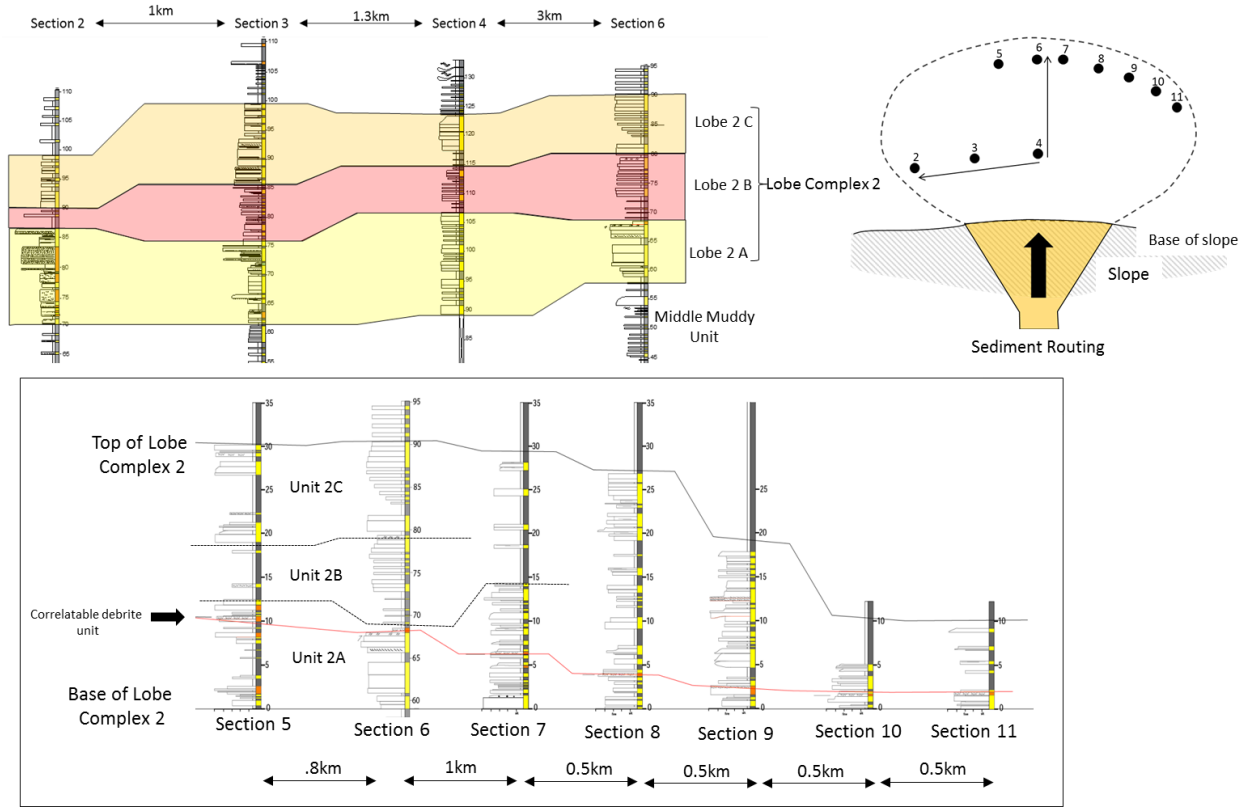

Figure 2.15: High resolution correlation of Lobe Complex 2, showing 3 lobes.

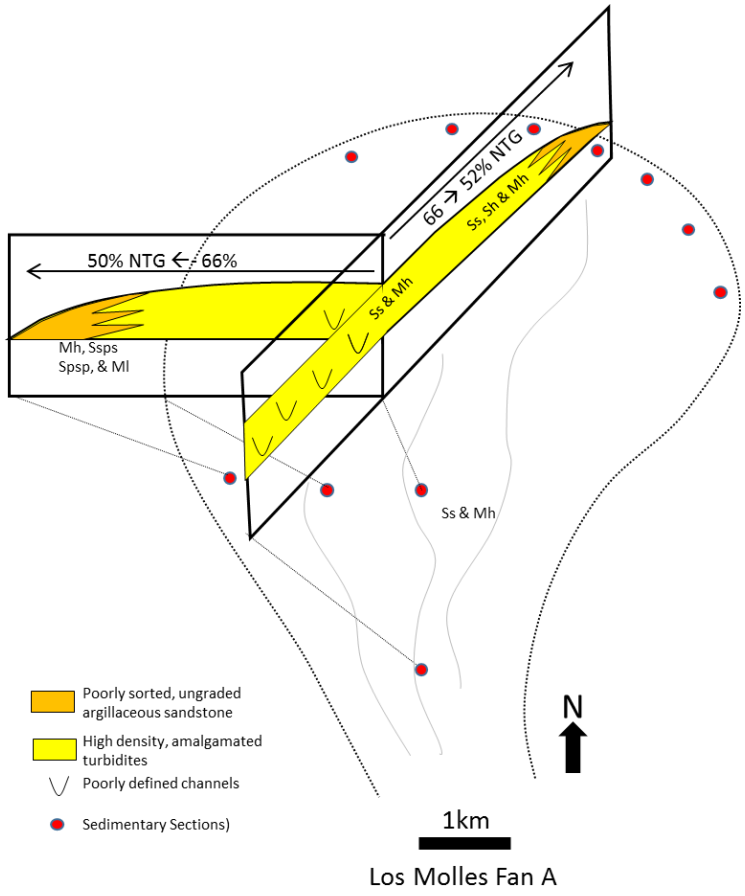

Figure 2.16: Cartoon showing distribution of debritic facies on the fringe and distal parts of Fan A vs turbidite beds which are characteristic of the proximal and axial locations.

PALEO-PHYSIOGRAPHIC PROFILE - EVIDENCE OF A RELATIVELY LOW-RELIEF, SHELF-SLOPE MARGIN

In order to place the observations of Fan A into their wider depositional context, the morphometric character of the La Jardinera shelf margin is described below. The system-scale correlation of the shelf to basin profile described earlier suggests, for two reasons, that the Lajas/Los Molles stratigraphy developed on a relatively low-relief, shelf-slope-basin margin:

i) Large-scale (~300m), north to northeasterly prograding, mudstone-prone, depositional clinoforms can be detected in places, crossing the Lajas-Los Molles lithostratigraphic boundary. In these places, conglomeratic deposits can be traced from the Lajas strata down-depositional-dip into the 300-meter-thick muddy slope (Fig. 2.17). The northeasterly trend of clinoform building is consistent with regional paleoflow observations of previous workers (Burgess et al. 2000, Paim et al. 2008).

ii) The vertical offset between the red and yellow lines in Fig. 2.2 is ~ 300 meters, and matches the relief of the clinoforms described above. Along the middle and lower reaches of the muddy slope, well developed isolated sandy channels are observed, and these are the downdip expression of larger channel-belts seen in the uppermost slope, containing large volumes of conglomeratic, sandy matrix-supported debris flow beds. In some areas, e.g. just above Section S3, well defined slumping can be seen. These, together with the abundant debris flows in the upper-slope channel belts (Steel et al. 2017), suggest a moderate slope gradient down to the basin floor fans.

The clinoforms passing through the Lajas- Los Molles stratigraphy are hundreds of meters in height (< 1km) and though contrasting with most continental passive margins (>1km), are comparable to slope clinoforms in other deepwater basinal settings, e.g. i) simple foreland basins (parts of the Magallanes Basin, Covault et al. 2009; Hubbard et al.

2010, or the Karoo Basin, Wild et al. 2009; Dixon et al. 2012; Poyatos-More et al. 2016); ii) thick-skinned foreland basins (e.g. Washakie Basin, Carvajal and Steel, 2006); iii) transpressional basins (e.g., Spitsbergen Basin, Steel and Olsen, 2002; Johannessen and Steel, 2005), iv) rift basins (e.g., Porcupine Basin, Ryan et al. 2009) or v) forearc basins (e.g., Tyee Basin, Santra et al. 2013).

Using a global average slope gradient of 2-4 degrees (Johannessen and Steel, 2005, Olariu and Steel, 2009), a slope length range of 4.3 to 8.6km can be calculated (Fig. 2.17c). This calculated horizontal extent of the slope (slope run) is the key physiographic element that links the shelf sediment-delivery system to the basinal depocenters. Quantitative data from Somme et al. (2009), using a global analogue database of 30 deepwater fans and their basinal physiography, predicts a fan length of 25-50km for the calculated slope lengths in the La Jardinera region. This calculated size is consistent with dimensions of small to moderate fans in active tectonic settings, as well as to the deepwater fans of foreland, backarc or rift basins cited above (Barnes and Normark, 1985). Additionally, small to moderate sized fans in active tectonic margins are characterized by coarse-grained, texturally immature, sand rich deposits (Reading and Richards, 1994, Mattern, 2005, Shanmugam and Moiola, 1988), similar to the calibre of sediment observed in the slope channels in La Jardinera (Fig. 2.4).

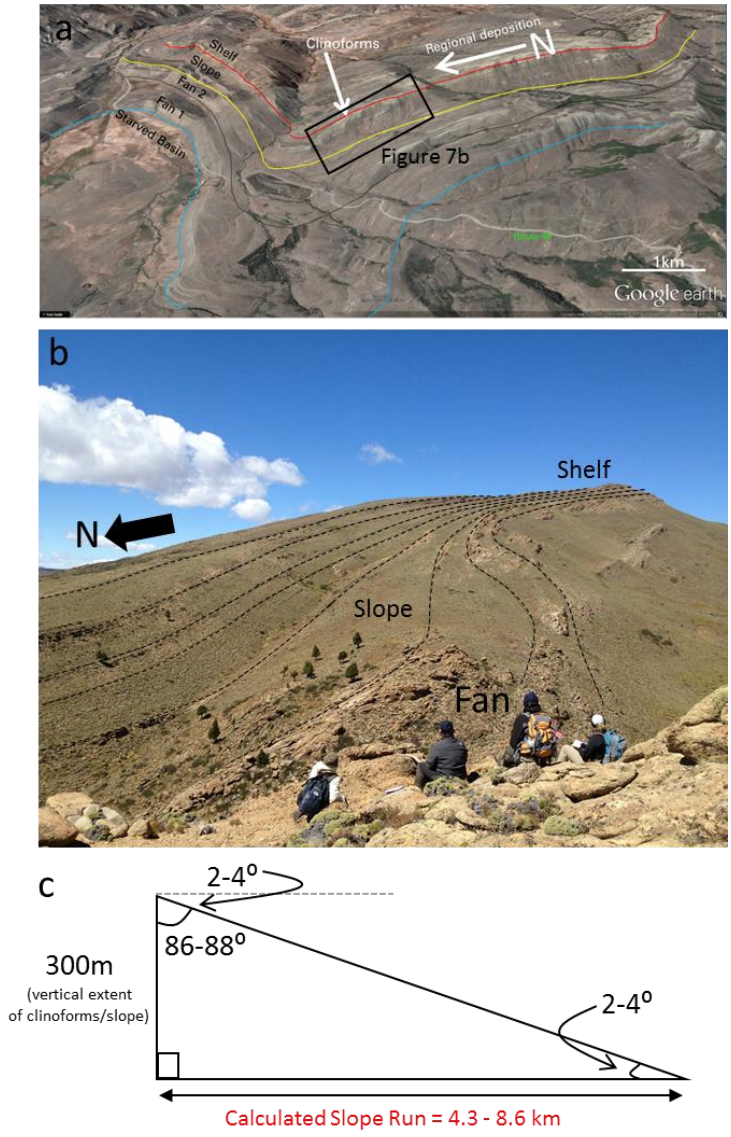

Figure 2.17: a) Google earth image showing the location of well-developed clinoforms observed from the Lajas Formation onto the upper slope of the Los Molles Formation. B) Closeup view of clinoforms prograding into the basin, c) Calculation of the slope run using measured clinoform height and average global slope gradient of 2-4 degrees. This is the physiographic element used to estimate fan size. See Fig 2.2 for location.

DISCUSSION

Comparison to other small, coarse-grained fan systems

The grainsize character of the Jurassic upper-slope channels and basin-floor fans of Los Molles Formation, coupled with computed fan and lobe complex thinning rates (Figs. 2.3, 2.11 and 2.14) suggest relatively small, coarse-grained submarine fan systems in this part of the Neuquén Basin.

The late synrift to early postrift setting of the Los Molles Formation conforms to the general observation that fan systems with these characteristics are typical of low efficiency fans in immature passive and active margin tectonic regions (Mutti, 1979, Shanmugam and Moiola, 1988). Examples of similar fans include the Precambrian Kongsford fan in Norway, the Lower Tertiary Balder fan of the North Sea, and the modern Navy and Monterey fans offshore California (Shanmugam and Moiola, 1988). These are all classified as sand-rich or mixed mud/sand rich fans (after Reading and Richards, 1994) based on net-to-gross ranges for the system. The 50-66% net sand percentage for the La Jardinera Fan A places it in the upper range of mixed mud/sand rich systems and the lower range of truly sand-rich fans (Reading and Richards 1994). A comprehensive summary of the scale of multiple ancient sandy fans was given by Mattern (2005) who documented fans on the order of 10's of km in extent with gross thickness of some 200-300m. The dimensions and thinning rates away from the Los Molles fan-axis are similar to those documented by Mattern (2005). Within this areally restricted context, there is also a concomitant reduction in net to gross toward the fringes and far reaches of the fan that parallels the overall thinning of such fan systems. Grainsize trends observed at the fan scale in the La Jardinera region are also similar to trends of decreasing sand size toward the margins and distal settings of many modern fans offshore California (Normark, 1970).

Small sandstone-prone fans are dominated by low-relief channels and depositional lobes (Shanmugam and Moiola, 1988), compared to fine-grained systems which develop more stable channels, with associated overbank levees and distal sheet-like deposits. As such, the general absence of well-developed channel forms in La Jardinera support a model of broad, shallow (difficult to discern) channels within sandstone-prone, coarse-grained lobe complex deposits. This can sometimes result in a braided fan morphology, e.g. the San Lucas and Navy fans (Normark, 1978). Braided fans tend to occur in active tectonic settings with elevated sand input and steep gradients (Shanmugam and Moiola, 1988).

These features directly control the resultant vertical facies association seen in these fans types; incomplete Bouma turbidite sequences are common in sandy fan lobes compared to much better preserved complete Bouma sequences seen in finer-grained, muddier systems with stable channel forms. The prevalence of structureless (Ta) and plane parallel-laminated sandstones (Tb) in the Los Molles Formation (Fig. 2.7) is interpreted to be representative of these mixed/sandy fan systems and similar to the axial Facies Association C of Mutti and Ricci Lucchi (1972). This interpretation is corroborated by a marked coarsening upward of grain size (Figs. 2.11 and 2.14) and subtle increase in bed thickness in lobe complexes of the Los Molles Formation. This is again typical of progradational depositional lobes in sand rich and mixed systems (Shanmugam and Moiola, 1988), in contrast to more tabular, sheet like and uniform textural and bed thickness characteristics of elongate, large-scale fine-grained systems (Reading and Richards, 1994).

Sandy debrites are a characteristic feature on the Los Molles Fan A. Similar deposits have been described in both in other small sandy fans e.g. North Sea Cretaceous and Paleogene Fans (Shanmugam et al. 1995) and the Brushy Canyon system (Gardner et al. 2003) as well as larger systems, e.g. the Marnoso Arenacea (Talling et al. 2004 and the

Karoo Group in South Africa (Van der Werff and Johnson, 2003). By definition, debrites are flows where grains and clasts are supported by dispersive pressure (particle collisions) with deposition by *en masse* frictional freezing. The scale of the deposit is directly related to the flow volume, with some deposits in the Marnoso Arenacea measured in the 10's of kilometres in extent. Terminal pinch-out edges tend to be abrupt, similar to debris flow deposits observed in other fan systems, on land and in experimental models (Johnson, 1970 and Major and Iverson, 1999). An important feature in the Marnoso Arenacea system is the characteristic distal fan setting of these sandy debrites and their updip transition to sandy turbidite deposits (Talling et al. 2012), similar to what is observed in the Los Molles. However, the model for their spatial occurrence differs in that proximal to distal flow transformation from turbulent to cohesive conditions are inferred for the Marnoso Arenacea deposits, while non-preservation in the proximal fan of more system-scale sandy debrites is suggested for the Los Molles Formation. The highly erosive nature of individual debris flows (e.g. S3, LC1, Fig. 2.13c) suggests an originating position close to the slope break, typically where many of these flows are triggered (slope over-steepening, instability and subsequent failure). The deepwater Saint-Antonin conglomeratic debrites of the Eocene-Oligocene Var River system in France are believed to be related to active tectonic activity on the shelf margin in the Maritime Alps (Stanley, 1980); the tectonic setting of the syn-rift to early postrift conditions in the southern Neuquén basin during times of late Los Molles deposition were perhaps still punctuated by occasional seismic episodes along the nearby fault systems that floor the Middle Jurassic basin (Burgess et al. 2000).

Although not as frequent as the ubiquitous stand-alone, sandstone-prone debris flows in the Los Molles, linked debrite deposits are a feature of the Los Molles fan system, similar to occurrences in other small, sandy fans , e.g. the Jurassic synrift North Sea (Haughton et al. 2003), the Cenozoic Forties Fan systems (Davis et al. 2009), the Marnoso

Arenacea Formation outcrops in Italy (Talling et al. 2004), the Carboniferous Ross Sandstone outcrops in Ireland (Pyles and Jennette, 2009), Skoorsteenberg Formation, South Africa (Hodgson, 2009) and the modern Agadir Basin system (Talling et al. 2004). These poorly sorted, argillaceous sandstones or mudstones are commonly deposited as bedcaps to turbulent driven sandstone event beds and tend to occur on the fringes and distal positions of the sand-rich fans. The early Neuquén Basin provides two independent conditions that can potentially facilitate the flow transition necessary for the deposition of the mudstone-prone linked debrites. The dominant and background fine-grained and sand-poor regional character of the Los Molles Formation provides a source of muddy substrate for nourishing the episodic turbulent event beds that characterize the sandy deposition into the basin, which facilitates flow transformation to debritic deposits. This is similar to the Ross Formation (Pyles and Jennette, 2009) where the Ross sandstone acts as the initial coarse-grained deposition into the deep basin and traversed an out-of-grade slope resulting in significant erosion of the underlying Clare Shale. Secondly, the Los Molles deepwater sediments are deposited in the late synrift to early postrift megasequence, where basin topography from active faulting may have influenced deposition. Burgess et al. (2000) highlights the effect of this highly structured basin floor, a direct remnant of the Late Triassic/Early Jurassic rifting episode, on variable paleocurrents observed in turbidite beds. This is not dissimilar to the irregular basin floor topography suggested for the Forties Formation and its constituent elevated debrite deposition (Davis et al. 2009). There are also other mechanisms of transformation and creation of muddy debrite tops. Current research is suggesting that initial deposition of the sandy bed can lead to water (including mud) escape and remobilization of the flow which causes a muddier portion of the unit (Koo, pers. comm. 2017).

Measurement and interpretation of the physiographic features of the La Jardinera margin offers insight into the scale of the regional slope (minimum 300m relief and <10km lateral extent). Using global analogues (Somme et al. 2009), this relatively small slope predicts a fan size of 25-50km. However, even the low-end estimate of these sizes is still significantly larger than the measured Fan A in La Jardinera, where the scale of the measured sections is less than 10km in a depositional dip orientation (Fig. 2.2). This suggests that Fan A possibly extends significantly further north of the study area, thus rendering Sections S5-S11 as representative of a middle fan setting rather than a distal position. Alternatively, Fan A may represent an anomalously smaller fan than empirical global datasets suggest, where the observed reduction in number of beds (50%) from the proximal fan axial to the lateral and distal fringes, coupled with the significant thinning rates and reduction in net sand, especially in Sections S5-S11, support the notion of a smaller fan. Hodgson et al. (2006) report thinning rates of 15-20m/km for Fan 3 of the Skoorsteenberg Formation in the Tanqua Depocenter, South Africa, attributed to subtle basin floor topography. Thinning rates of LC2, Fan A of the Los Molles Formation exceed 10m/km which suggests a similar basin floor topographic control on deposition and resultant fan size. A highly uneven basin floor, typical of synrift or transitional basins and reported by previous workers in the La Jardinera region (Burgess et al. 2000) would facilitate such stratigraphic relationships.

Importance for Hydrocarbon Exploration and Appraisal

Areally restricted, sandstone-prone fans are a key reservoir target for hydrocarbon explorers, with notable examples occurring in the North Sea, e.g. the Forties, Frigg, Magnus, and Balder fans (De'Ath and Schuyleman, 1981; Timbrell, 1993; McGovney and Radovich, 1985; Whyatt et al. 1991), as well as the Matilija, Stevens and Winters sandstone

units, California, USA (Scott and Tillman, 1981; Williamson and Hill, 1981; Link and Welton, 1982). Many other sandstone-rich deepwater reservoir units may possess similar characteristics to these classically defined sand-rich systems (Stow and Johansson, 2000). Their high net-to-gross character and coarse grain sizes make them especially appealing to hydrocarbon geoscientists, as high pore space volume and lack of architectural complexity (Mattern, 2005) contribute to high recovery of emplaced oil and gas. Conversely, the elevated occurrences of debrites on the edges of these fans is important in characterising reservoir properties; the poor reservoir performance of these types of deposits have been described by Amy et al. (2009). The quantitative data recorded from the Los Molles Formation in the La Jardinera region provides additional data on bed thicknesses, grain size trends and facies relationships in these types of settings.

As a small, coarse-grained deepwater fan deposited within in a fine-grained, source prone depositional interval, the Los Molles Formation provides additional evidence of source rocks deposited coevally with reservoir-grade deposits. Their direct juxtaposition to mature source intervals renders them low risk for charge migration. It is recommended that any exploration activity include source rock intervals as a primary coupled system and advanced seismic analysis be done on such intervals to define possible reservoir facies. As noted on many passive margins, source prone intervals lie close to the base of the postrift megasequence, near to the transition between the tectonically active synrift megasequence and the overlying, tectonically quiescent passive margin interval (Liro and Dawson, 2000, Mohriak et al. 2000, Katz et al. 2000 and Brownfield and Charpentier, 2006). Deposits in the lowermost part of the passive margin would naturally occur during times of continuous, but waning tectonic activity as early seafloor spreading progresses. It is not surprising that small, coarse-grained, sandstone-prone fans, which are typical of low slope relief, active tectonic margins, are found in these source-prone, early postrift settings. This is important

for deepwater hydrocarbon explorers who continue to explore deeper into sedimentary basins, many times with little or no existing well data to characterise possible reservoir units.

SUMMARY & CONCLUSIONS

The deepwater, sediment-gravity flow succession of the Los Molles basin-floor in the La Jardinera region form two separate submarine fans (each averaging 100m thick), separated by a ~30m mudstone. The lower fan (Fan A) is made up of 2 separate lobe complexes (each averaging 30-40m thick) separated by a 15m muddy interval (Fig. 2.7). Both lobe complexes are in turn made up of three (3) interpreted lobes, each averaging some 10m thick, containing sandstone-prone units separated by finer grained mud layers (Figs. 2.12 and 2.15).

The Lower Fan A shows conventional thinning in both a lateral and downdip direction, accompanied by a reduction in net sand. Consistently, the thickest part of the fan and lobe complexes had the largest number of individual beds, most of which recorded thicker (~0.5 meters and greater) sandstone and mudstone beds. Assuming a maximum fan thickness of 100meters (observed at Section S3) and using the observed average consistent thinning rate of 7m/km for the fan in both a dip and strike direction, and with the assumption that the thinning rate will not decrease, the Los Molles fan will not exceed 15km in either dip or strike extent. This is less than the 25-50km suggested by the quantitative scaling relationships of Somme et al. (2009) for fans with a ~300m slope rise. Sandy beds are primarily fine to medium-grained, normally graded sandstones and sandy heterolithics in the proximal axial location, and these transition to muddy heterolithics in the lateral positions of the system and to laminated mudstones with fine to medium-

grained, thinner sands in the downdip position. Poorly sorted beds, interpreted as both stand-alone and linked debrites, also occur frequently on the fringes and distal positions of the fans. Distal, sandy debrite beds typically exhibit coarser grainsizes than the background sandstone beds across the fan. Their apparent preferential occurrence on the fan fringe and distal position is possibly due to reworking and non-preservation across the proximal fan, based on i) the highly amalgamated character of structureless sands at these locations, ii) evidence of a single, regionally extensive pebbly-debrite observed in the upper fan and iii) the scale of the channelised debris flow at Section S4 which can be traced to Section S6 downdip. At the individual lobe complex scale, there appears to be a strong correlation between location on the fan and observed sedimentological texture; proximal axial positions have the largest number of beds, highest net sand ratios, and coarsest grainsizes, whereas the lateral fringe and downdip parts of the fan appear to be less sandy and finer-grained (Figs. 2.11 and 2.14). At the lobe scale for both complexes, similar facies trends of more debrite and heterolithic deposits are recorded on the fringe and distal part of the fan. These transition to thicker, structureless sandstones on the axis of the system. Unit 2A exhibits a single conglomerate-rich debrite, as seen in all sedimentary sections except Section S4, that is weakly normal graded in the proximal position, but appears ungraded to chaotic and thinner in the distal setting. The regional extent of this bed is remarkable, especially in the distal sections where it thins to 10-20cm. It is likely that this highly conglomeratic debrite was sourced directly from one of the mapped shelf-edge channel systems (Fig. 2.4).

The observations and data from Los Molles fans are similar to descriptions of other small, sandstone-prone submarine fans. The calculated extent of the Los Molles fan (15-50km) is consistent with other areally restricted, coarse-grained fans reported by Mattern, (2005). Depositional thinning toward the lateral fringe and distal reaches of the fan

(~7m/km) are accompanied by a reduction in net sand and decrease in grainsize. These trends are consistent with observations on modern fans offshore California (Normark, 1970). These lateral trends are accompanied by a facies transition from poorly developed channels in the proximal axis of the fan to depositional lobes that dominate the fan. The dominance of structureless and horizontally laminated sandstone beds, with very rare evidence of traction structures (ripples, cross bedding) is also consistent with deposits from high density turbidites in sand rich systems. A vertical increase in bed thickness and grain size at any location is also noted, which is characteristic of prograding depositional lobes (Shanmugam and Moiola, 1988). The presence of debritic facies on the fringes of the fan is consistent with reported occurrences of similar beds in sandstone-prone fans (e.g. the North Sea and Marnoso Arenacea fan systems).

Quantitative description and insights on the architecture of the Los Molles Fan A provide an additional analogue for hydrocarbon explorers working on areally restricted, sandstone-prone reservoir systems. Additionally, it proves additional evidence of coupled source-reservoir depositional systems, where significant coarse-grained deposition can occur during times of long-term diminished terrigenous sediment supply to the basin. These types of fans may have been historically overlooked in hydrocarbon evaluation on many early passive margin intervals.

Chapter 3: Architecture of deepwater depositional systems fed from a tectonically active catchment: deepwater Veracruz Basin, offshore Mexico, SW Gulf of Mexico

ABSTRACT

A convergent plate boundary less than 400km from the offshore Veracruz Basin, Gulf of Mexico deepwater basin sets up a unique, mixed active-passive deepwater margin. Recently acquired 3D seismic and well data (cores and logs) reveal a Lower to Middle Miocene, northward prograding, deepwater system that extended to the central Gulf of Mexico basin floor. Lower Miocene deposits are representative of a channelized fairway in the study area, characterized by a series of poorly defined, north-trending, subaqueous, deepwater channel systems, typically 10's of milliseconds (ms) deep and up to 2km wide. Interpreted overbank splays and terminal lobe-like deposits can be tens of ms thick and kilometers wide. These show an ordered, spatially-controlled facies occurrence: areas close to channels have amalgamated high density turbidite beds, that become thinner toward the fringes of the system and are replaced by heterolithics and debrites (sandstone-prone, mudstone-prone and linked "hybrid" varieties). This transitions to an overlying Middle Miocene slope setting with large, third-order sandstone-prone submarine channel complexes, up to 10km wide and 100's of ms deep. In the inter-channel areas, seismically defined sediment-wave bedforms, interpreted as formed by turbidity-driven cyclic step deposits, constitute an additional architectural element in the basin, but their grain size is unknown. Combined with the texturally immature character of the deposits, an eastward migrating depocenter that parallels the orogenic history of the hinterland and unusually long run-out channelized fairway, deposits in the deepwater Veracruz Basin illustrate the unique sedimentary response of this mixed active-passive margin setting.

INTRODUCTION

Continental margins are the site for much of the world's petroleum reserves (Wen et al. 2015). Deepwater deposits on these margins are controlled and shaped by a variety of intra and extra-basinal, regional processes that produce allocyclic (unsteady forcing) or autocyclic (steady forcing) responses in the stratigraphy. Tectonic forces operate in hinterland of the system as well as in the sedimentary basin. Coupled with climate, uplift and erosion in the hinterland define provenance regions and sediment supply while drainage networks control the magnitude and type of sediment flux to the basin. The morphology and sedimentary processes in the receiving basin control the accommodation space and the nature of the depositional products. In the petroleum industry, passive continental margin basins (e.g. Northern Gulf of Mexico, offshore Brasil, and West Africa) have historically been more prolific than active margin basins (e.g. Zarra, 2007; Snedden et al. 2012; Dailly et al. 2012; Thompson et al. 2015; Wen et al. 2015). Passive margins are typically the result of a rifted continental setting and subsequent generation of oceanic crust and crustal cooling (McKenzie, 1978), with active tectonic forces long extinct. Sites of deposition are also often far from active plate boundaries. Active margins by comparison occur along plate boundaries (Allen and Allen, 1990) and are frequently the site of orogenesis and dynamically evolving, smaller-scale sedimentary basins (Dickinson, 1974). Over 60 years of research on both ancient and modern systems have contributed to prevailing depositional models for both basin classes (e.g. Barnes and Normark, 1985, Reading and Richards, 1994, Bouma, 2000): passive continental margins feature large-scale, fine-grained depositional systems sourced from large drainage basins compared to tectonically active basins which are characterized by relatively small, coarse-grained, texturally immature deepwater deposits, often transported via submarine canyons and areally restricted drainage cells. Observations like this are in line with recent quantitative

"source to sink" research themes (Somme et al., 2009, 2013), where empirical data from modern and recent sedimentary systems suggest a direct correlation between drainage basin size and the resultant scale of the basinal deepwater system. These observations also agree with numerical modelling work (e.g. Syvitski and Milliman, 2007) which demonstrates the effect of increasing catchment size, relief (a product of regional tectonic processes) and climate (temperature and runoff) on increasing sediment flux to the oceans.

While end-member classifications and models like these are useful, they do not account for continental margins with characteristics of both active and passive margin conditions. The northern Gulf of Mexico basin is described as a tectonically quiescent, passive sedimentary basin (Hay, 1981; Pindell, 1985; Winker and Buffler, 1988; Allen and Allen, 1990), however the southwestern part of the basin, offshore Veracruz, Mexico, is adjacent to nearby active orogenic belts along an active plate margin (Guttierez Paredes et al. 2009). This creates a scenario whereby a relatively active, areally restricted hinterland is adjacent to a mature, oceanic-crust floored passive margin basin. Much of the sediment deposited in the northern passive basin is sourced from the North American continent; the present-day Mississippi has a drainage basin over 1,000,000km² and deepwater fan systems have been mapped for many hundreds of km away from their coeval shelf edges (Weimer, 1989). While many workers have characterised the nature of these deepwater systems (e.g. Fisher and McGowen, 1967; Winker and Buffler, 1988; Galloway et al. 2000; Radovich et al. 2007; Galloway et al. 2011), the nature of the deposits in the southern basin with its more active tectonic activity, has not been widely reported. Recently acquired subsurface data in the offshore deepwater Veracruz region, southern Mexico has for the first-time enabled researchers to study the ancient submarine deposits deeper into the basin. It provides a unique opportunity to investigate the deepwater sedimentary response of an adjacent active margin into a passive sedimentary basin. The aim of this study is two-fold:

i) to describe the sedimentary facies and architecture of the Lower and Middle Miocene, deepwater intervals in the offshore Veracruz Basin, and ii) Compare and contrast these deposits to other end-member continental margin types (active vs passive).

GEOLOGIC SETTING

The Gulf of Mexico (GoM) basin is a large, circular basin, bounded on the north by the North American plate, to the south by a series of microplates with complex tectonic histories, to the west by the Central Mexican Tampico Misantla province and the east by the Yucatan Platform (Fig. 3.1). The basin was formed by Jurassic extension and rifting of Pangea, followed by sea floor spreading in the Upper Jurassic (Callovian) to Lower Cretaceous (Sandwell et al. 2014). Since Lower Cretaceous times, the basin has been in a passive state, with sediments sourced from the surrounding regions. Large salt sub-basins exist in both the northern and southern parts of the GoM basin (e.g. Hudec et al. 2013), an artifact from widespread salt deposition prior to continental breakup (Pindell, 2009).

Major siliciclastic sediment entry points are located in the northern (Mississippi), northwestern (Perdido), western (Mexican Ridges), southwestern (Veracruz) and southern (Sureste) margins and some of them have been active since the Late Cretaceous. Sediment thicknesses in the basin exceed 12,000m (Winker and Buffler, 1988). Tithonian-aged source rocks provide most of the billions of barrels of hydrocarbons discovered over the last century (Klemme and Ulmishek, 1991), with clastic reservoirs ranging from Upper Cretaceous to Pleistocene in age (Galloway, 2000, Galloway 2011). These reservoirs were deposited in both paralic and deepwater environments. Much of the sediment flux in the northwestern GoM is Paleogene in age and is sourced from Texas coastal river systems (e.g. Galloway et al. 2000; Galloway et al. 2011) while the sediments from the ancestral

Mississippi in the northern Gulf of Mexico are dominantly Neogene in age (Galloway, 2011). Hinterland regions in North America include the Appalachian highlands in the east and the Rocky Mountains in the west. Although both these mountain ranges are the product of active plate tectonics, they occur on the peripheries of continental-scale drainage basins (>1,000,000 km²). In the case of the Appalachians, much of the mountain forming processes are long extinct. The nature and scale of the vast majority of the drainage basins (tectonically passive) combined with the tectonic quiescence of the receiving marine basin (northern Gulf of Mexico) results in the "passive" margin classification of the linked sedimentary system (Levell et al. 2011). In contrast, the southern GoM basin is adjacent to the convergent margin of western Mexico (Fig. 3.1). Throughout much of the Upper Cretaceous and Tertiary, convergence of the Cocos and Farallon plates beneath the North American plate (onshore Mexico) and eastward migration of the Chortis continental block along this margin have resulted in a long and active tectonic history of southern Mexico that continues today (Prost and Aranda, 2001; Pindell et al. 2009, Mandujano-Velazquez and Keppie, 2009). The results of this convergence are the Lower Tertiary Zongolica and Middle Miocene Chiapas fold belts (Fig. 3.1, inset) which are the source of much of the sediments delivered to the southern Gulf of Mexico (Guttierez Paredes et al. 2009).

The Veracruz Basin is regarded as an Early Tertiary, Laramide-aged foreland basin to the Zongolica fold belt, where the Mesozoic Cordoba Platform has been folded and uplifted (Prost and Aranda, 2001). Much of the Tertiary stratigraphic succession are deepwater deposits, comprising turbidites and debrites deposited through well-developed canyons onto the basin floor (Jennette et al. 2002). Lower to Middle Miocene reservoirs in the basin were first reported by Cruz-Helu (1977) who described conglomerate-rich, coarse grained deepwater deposits. He attributed the coarse material to the nearby folded Mesozoic and Lower Tertiary fold belt to the west, and to thrust sheets on the tectonically

active, steep depositional slope. However, much of the paralic and non-marine ends of the depositional system have been eroded or folded within the thrust front. Jennette et al. (2002), described both a slope and basinal sequence for the Lower and Middle Miocene intervals in the basin, which exceed 2km thickness in places. Jennette et al. (2002) also defined a NW-SE trending base of slope boundary within the Veracruz Basin (Fig. 3.1, inset) based on a multidisciplinary study of seismic and wells in the region. The Miocene slope was characterized by a series of submarine canyons which transitioned downdip to a proximal, sandy basin floor fan in the northeastern part of the onshore basin. Martinez-Medrano (2006) summarized the hydrocarbon prospectivity of the Miocene deposits, exploited in several onshore sub-basins (e.g. Cocuite, Apertura and Novillero fields). The eastern edge of the basin and the continuation of the depositional system into the offshore Gulf of Mexico have however not been well described. Prost & Aranda (2001) reported evidence of stratigraphic thinning of the Lower Miocene to the east, suggesting that there might have been some subaqueous topography during this time, possibly forming an incomplete barrier to the deeper GoM basin. Two large igneous complexes – the Anegada High and Los Tuxtlas Volcanic field (Fig. 3.1), attributed to backarc volcanism from the subducting Cocos Plate and dated at Middle Miocene to Present, may have had positive topographic expression between the onshore Veracruz Basin and the western GoM (Prost and Aranda, 2001). Other authors (e.g. Roure et al. 2009) have suggested a long-lived forebulge at the site of the coastal volcanics that may have also provided bathymetric relief to sediments entering the gulf at the northern edge of the onshore Veracruz Basin, however seismic sections published by Jennette et al. (2002) do not show evidence of thinning of Lower and Middle Miocene sequences to the east.

In the last decade, a series of offshore exploration wells in the deepwater Veracruz Basin, outboard of the coastal volcanic complexes, have found hydrocarbons in Lower and

Middle Miocene reservoirs, confirming the extension of the onshore reservoir systems further into the basin. Arreguín-López et al. (2011) provided a high-level summary of Eocene to Pliocene deepwater reservoirs in the basin, describing the Lower Miocene unit as representative of deepwater deposition in an unstructured basin, characterized by channel and overbank deposits. The Middle and Upper Miocene in contrast were controlled by the emerging submarine Catemaco fold belt (Fig. 3.1), the contractional toe-thrusts of updip, Middle Miocene margin extension (Mandujano-Velazquez and Keppie, 2009). Coarse-grained deposits have been described as texturally immature, representing a persistence of the textural fabric reported onshore (Cruz-Helu, 1977, Jennette et al. 2002, Dutton et al. 2002).

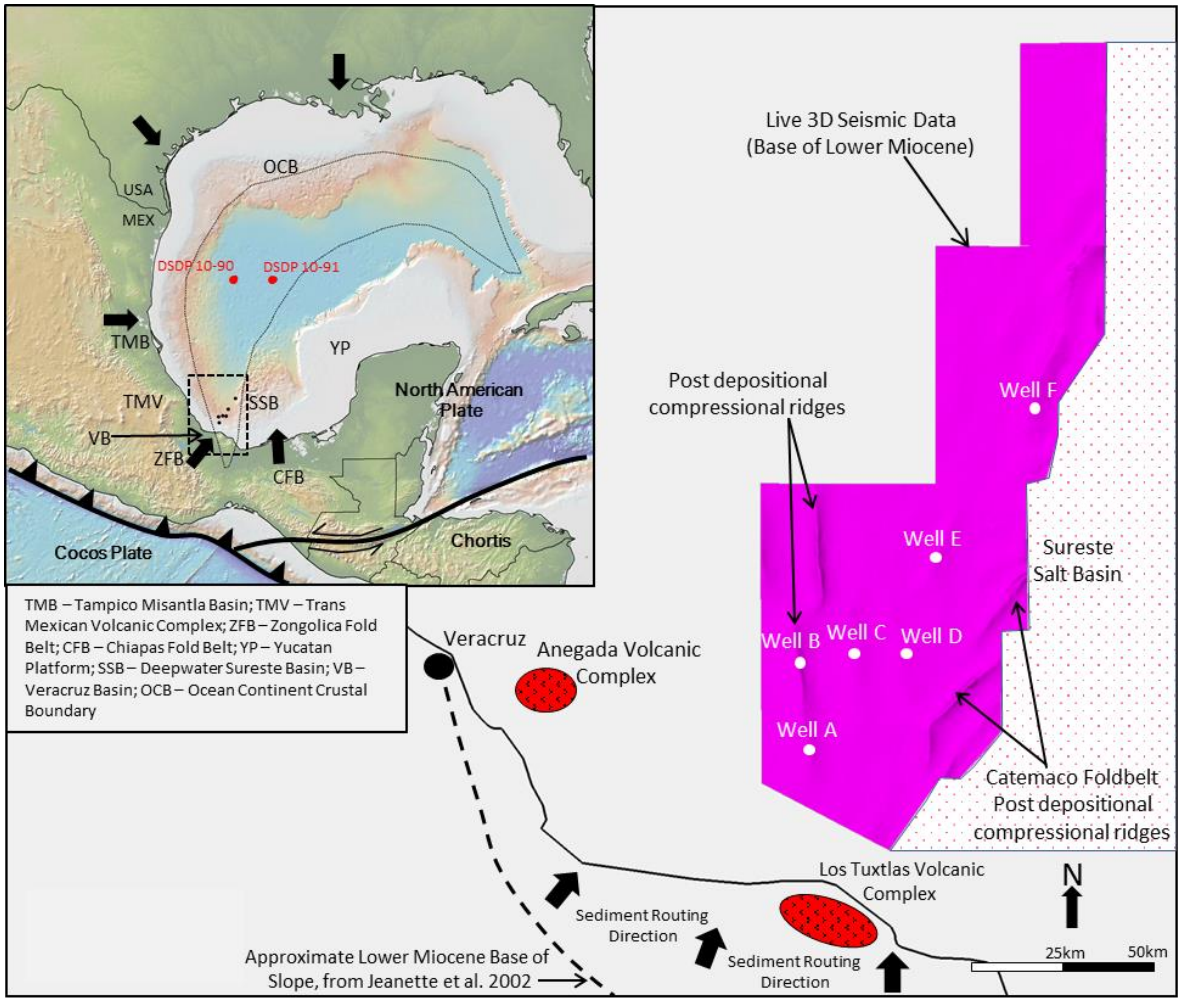

Figure 3.1: Regional Location map (inset) showing offshore Veracruz Basin in the Southern Gulf of Mexico. The study area is shown in the dashed black box. Note location of DSDP wells in relation to study area. Main regional structural elements also shown and labelled below the map. Black arrows represent major Tertiary siliciclastic sediment pathways to the GoM Basin. Map to the right shows the location of the 3D seismic data and wells used in this study. Note the Sureste Salt Basin (SSB) to the east of the study area. Lower Miocene basinal sediment routing direction shown by black arrows.

DATASET & METHODOLOGY

In order to characterise the Miocene deepwater deposits in the offshore Veracruz Basin, we use a multidisciplinary approach, incorporating ~270 meters of core, well log data from six (6) wells and 3D seismic data (two-way time) in the basin (Fig. 3.1). Cores were logged at 1:50 scale from which sedimentary lithotypes were defined based on gross lithology, sedimentary structures and grain-size data. These lithotypes are then grouped into Facies Associations (depositional elements) based on the occurrence, frequency and vertical succession of lithotypes. This interpretation allows for the identification of individual architectural elements and their approximate position on the deepwater sedimentary profile of the Miocene units.

These Facies Associations were then placed into the larger stratigraphic context, by calibrating the sedimentary cores with well log lithology curves and the intersecting seismic data. The seismic database is ~ 9000km² and is bounded to the east by the presence of the regional salt boundary, which corresponds to the transition to continental crust (Fig. 3.1). The top and base of the Lower Miocene, as well as two regionally correlatable mudstone markers, identified on logs, were mapped on the seismic dataset, from which regional structure, amplitude and isochron maps were generated. These two (2) regionally extensive and mappable mudstone units subdivide the Lower Miocene interval into three (3) intra-Lower Miocene Subunits (I-III).

Core coverage in the Middle Miocene is limited to a single 6m core, however inferences for this interval were made from the available well log data and seismic attribute maps. This approach of incorporating core-based sedimentary data, calibrated to seismic properties within a regional framework provides insight into the architecture of the depositional systems in the basin at multiple scales, which is then compared to other end-member continental margin types.

LITHOTYPES AND DEPOSITIONAL FACIES OF THE MIOCENE DEEPWATER UNITS

Approximately 270 meters of core were recovered from Wells A to E throughout the various Miocene intervals. The majority of the cores sampled the Lower Miocene (264m). Cores were typically 9m and 18m lengths and are of variable recovery quality. Laser Particle Grain Size (LPSA) analysis was used to aid the sedimentary descriptions.

Lithotypes are cm to dm-scale sedimentary units, defined by grainsize/lithology, sedimentary structures and degree of bioturbation. They are considered the building blocks of facies analysis. As such, they are then grouped into "Facies Associations", based on their frequency and vertical assemblage trends. Some lithotypes occur in multiple facies associations, however any interpreted facies association will contain a unique combination of these lithotypes. Fig. 3.2 shows the different lithotypes observed in the cored intervals with type example photos.

Seventeen (17) lithotypes were identified from the cores of Wells A to E. The most common are structureless sandstones, bioturbated mudstones and muddy heterolithics (thin silt, mud and sand alternations), which together account for almost 75% of the total lithotypes present (Fig. 3.3). Well B is the only well where sandy lithotypes dominate (graded and ungraded structureless sands). It is also the most homogenous core dataset, with these 2 lithotypes dominating the succession. The cores in other wells are more heterolithic with a more uniform distribution of lithofacies represented in the cores (Fig. 3.3). However, because of the apparent non-systematic nature of core sampling and lack of cored intervals across the entire reservoir interval in any single well, caution must be applied in drawing quantitative inferences and trends on lithotype occurrence across the dataset. Some wells may have inadvertently recovered more core across fine-grained lithologies, thus skewing the lithotype sampling for that well and interval.

Individual bed thicknesses were recorded for each lithotype across all 5 wells. The lithotype mean thickness for the dataset is 0.56 meters (n= 528). On an individual well basis, there appears to be 2 populations of bed thickness: Wells B & C have an average bed thickness of 0.94 and 0.70 meters respectively, while Wells A, D and E have thickness averages of 0.36, 0.37 and 0.35 meters respectively (Fig. 3.3).

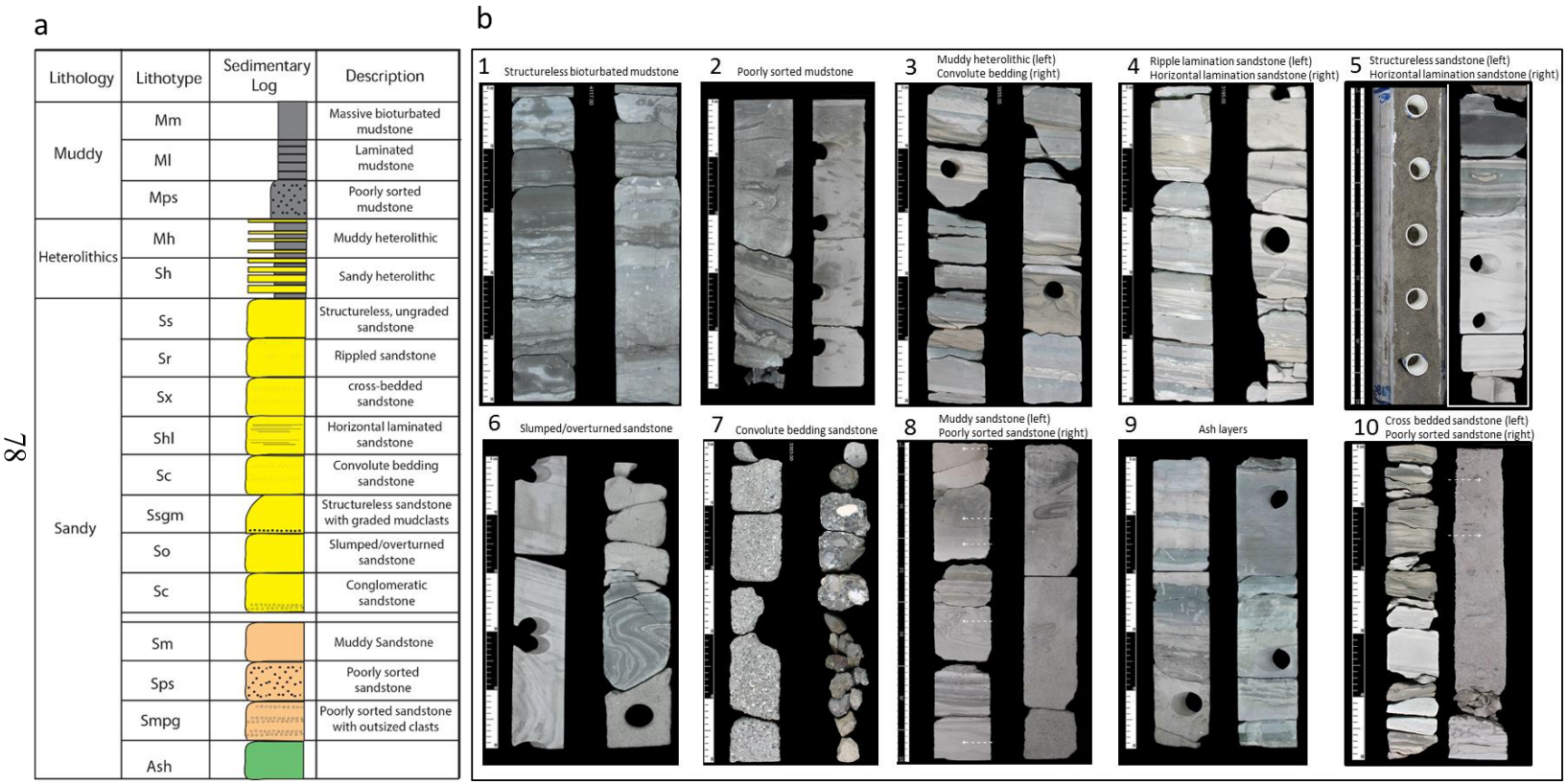

Figure 3.2: Lithotypes of the Lower and Middle Miocene, Deepwater Veracruz Basin, Mexico. Scale on the left represents 0.5m. a) Left – lithotype key of all rock types observed in subsurface core data.b) Right – examples of common lithotypes

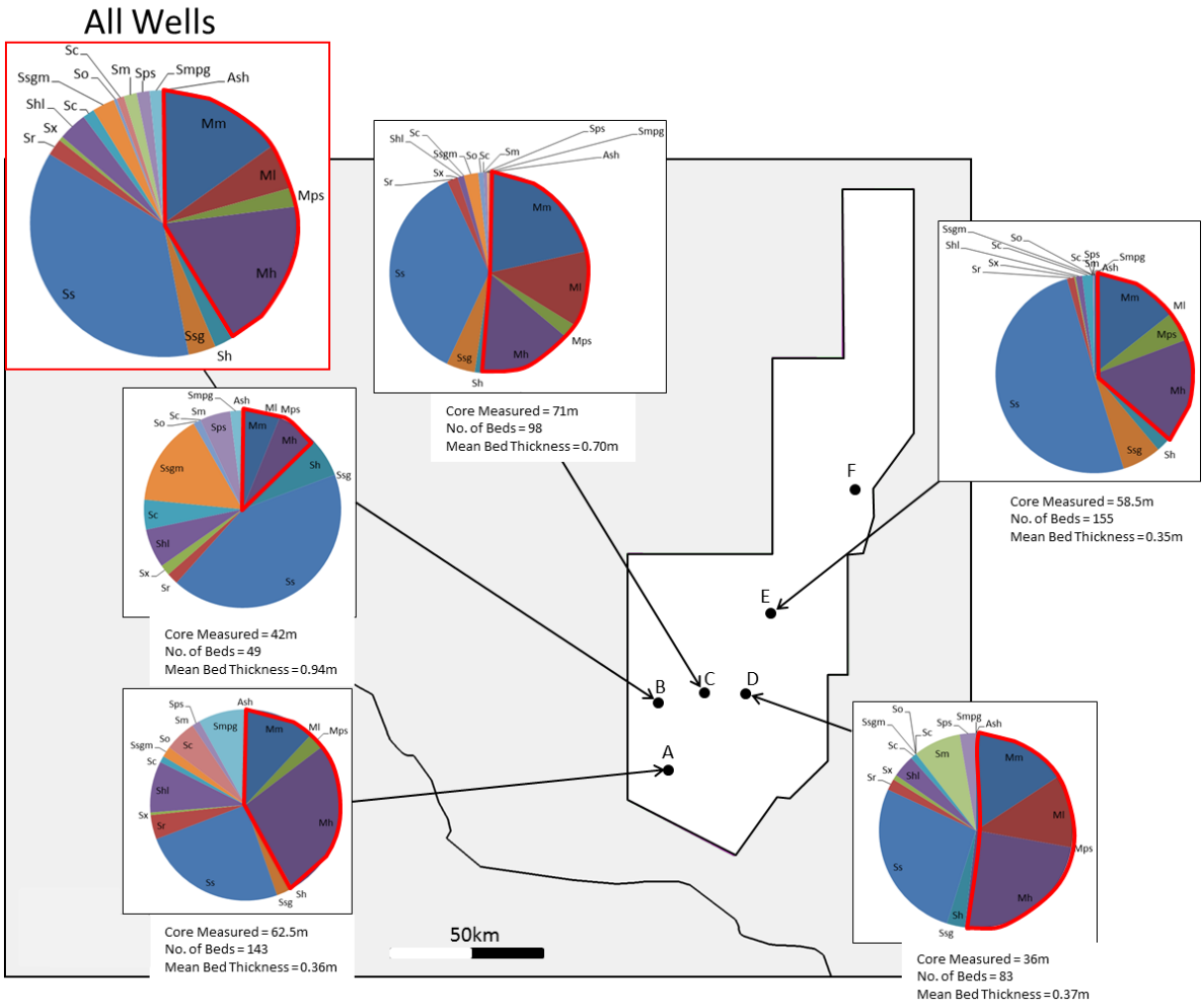

Figure 3.3: Spatial distribution of lithotypes in Wells A-E. Total distribution shown above. Note also bed thickness summaries for each well. Wells B & C show significantly thicker beds than other wells. In all pie charts, mudstone-prone lithotypes are highlighted in RED.

Facies Associations

Eight (8) Facies Associations were interpreted from the occurrence and vertical associations of the lithotypes described above and represent the main depositional elements observed in the core data.

1) Well sorted, structureless and horizontally laminated sandstone beds (Fig. 3.2b no. 5)

Description. FA 1 is characterized by well-sorted, structureless and horizontally laminated sandstone beds, which are the most prevalent sandy lithofacies in the cores studied. Grain size varies from fine to coarse-grained, with mud and pebble clasts sometimes present. Beds are cm to m-scale thick, with top bounding surfaces usually sharp but occasionally gradual. Bases are often erosive. Some horizontally laminated beds show normal grain-size grading, along with internal grading of clasts (if present). Where present, mud clasts are preferentially arranged in discrete intervals within the unit.

Interpretation. The well-sorted and structureless to horizontally laminated character of the sandstone units suggest sediment transport in turbulent suspensions with incremental deposition from rapid sediment fallout of near-bed processes (traction carpets, Lowe, 1982). The beds are interpreted as formed by high-density turbidity currents. Alternatively, these deposits can be the result of deposition from low amplitude bedforms (lower density turbidites, Best and Bridge, 1992). Mud clasts, where present, indicate that there were mud layers deposited, but then ripped up during passage of the turbidity current. The general lack of matrix mud within the well-sorted sandstone beds also suggests that mud was lofted out of the grain population as the early underflows were initiated (Zavala et al. 2006; Steel et al. 2017).

Type Section. Well B, No. 6 core, 3042.5m and Well C, No. 3 core, 4232m

2) Poorly sorted, ungraded, structureless sandstones (Figs. 2b8 and 2b10)

Description. Even with variable photograph quality, poorly sorted, clean (low mud content) structureless sandstone beds can be identified and confirmed by LPSA grainsize analysis. Typically, the grain variance is evenly changing throughout the lithotype, but can sometimes occur as discrete, small-scale, random occurrences, giving rise to a patchy grain size texture. Bed thickness varies from dm to m-scale. Often, these poorly sorted sands contain small mudclasts and volcanic rock fragments and minor outsized quartz granules. The quartz granules are scattered throughout the lithotypes rather than confined to discrete intervals. Median grainsize varies from fine to coarse-grained sandstones. Bed basal surfaces typically overlie muddy intervals and are frequently sharp-based. The top bounding surfaces are also sharp, being overlain by better sorted sands or muddy lithotypes. Sedimentary structures are typically absent. In some instances, this lithofacies assemblage is overlain by contorted bedding. Another common lithotype seen in this facies association are dirty, muddy sandstones, which have a dark, sometimes mottled appearance. LPSA grain size data confirms the elevated argillaceous material within these sandstones. These are confined to the distal Well E (Fig. 3.3). Within these intervals, larger clasts are sometimes seen, which appear angular to sub-rounded.

Interpretation. The poorly sorted, texturally patchy sandstones suggest deposition by en masse freezing or post-depositional grain realignment in situ, typical of poorly cohesive liquefied debris flows (Talling et al. 2012). The lack of grading observed in both the sandstone beds and constituent clasts also suggests deposition by en masse consolidation rather than incremental or traction carpet collapse (turbulent flow processes). Low mud content of the sandstone results in poorly cohesive flow process and a limit to clast size that is supported by the flow. However, in the “dirty, muddier” sandstones in the

distal well E, clasts are generally larger, suggesting a more cohesive flow, able to support larger clasts (Talling et al. 2012). In these dirtier flows there was no lofting out of the mud fraction at initiation, distinguishing FA2 structureless beds from structureless FA1.

Type Section. Well A, No. 2 Core, 3047m and Well D, No. 3 Core, 4658-4663m

3) Poorly sorted mudstones (Fig. 3.2b no. 2)

Description. FA3 consists of fine-grained, silty to muddy, poorly sorted lithotypes with randomly oriented internal clasts. Bed boundaries are typically sharp to erosive. Constituent clasts range from coarse quartz granules to cobble-sized mudclasts. The mudclasts are mainly angular.

Interpretation. The fine grain-size, poor internal sorting and lack of grading in beds or of the clasts suggest deposition by frictional freezing of a cohesive, muddy debris flow (Talling et al. 2012).

Type Section. Well E, No. 4C Core, 3946m, 3943m and 3940.5m

4) Cross bedded sandstones, with graded mudclasts/conglomerates (Fig. 3.2b no. 10)

Description. FA4 consists of graded or cross-bedded, clean sandstones occurring as individual beds or units, ranging between 20cm and 3 meters. The beds have internal, coarse-tail grading of mudclasts or conglomerate clasts, typically concentrated at the base of the unit. Sometimes mudclasts can be accompanied by large quartz granules which also show grading. Basal bed boundaries are erosive and sharp based. Upper boundaries are abrupt or gradational. Cross-bedding sometimes shows evidence for associated dewatering. Dewatering pipes are also observed in structureless, clast-rich beds which frequently occur in close association with the stratified beds. Grain-supported, normally graded

conglomerate beds are also observed. The composition of the conglomerates is highly variable, comprising both mudclasts and extra-formational granules. Rounding is also highly variable, from very well rounded to angular grains.

Interpretation. Erosive basal bed boundaries and normal grading of mudclasts and other clasts in beds suggest confined, turbulent-driven sandy flows, probably within channels. Cross -bedding is the result of cut-and-fill structures or dune migration within the channel (Harms et al. 1982; Boggs, 2006). Soft sediment deformation structures reflect high depositional rates (Lowe, 1975) and their association with interpreted channels suggest rapid sediment fallout, possibly at the terminal channel to lobe transition point as flows evolve from confined to unconfined. Thus, the facies association is probably representative of the spectrum of proximal to transitional (terminal) channel settings.

Type Section. Well C, No. 1 Core, 4096-4103.6m, Well B, No. 3 core, 2839-2841m and Well A, No. 5 core, 3200-3205m

5) Clast-rich mudstones with thinly-bedded, ripple-laminated sandstones (Figs. 2b2 and 2b3)

Description. FA5 consists of repetitive cycles of thicker mudstones with interbedded thinly bedded, ripple-laminated sandstones. Mudstone intervals can reach up to 50cm thick, while sandstone beds are typically 10-15cm and occur over a 3m interval. The mudstones vary from structureless to laminated and often contain angular mudclasts aligned in discrete zones. The interbedded sandstones are primarily fine-grained but can attain medium grain-size in discrete intervals. They frequently exhibit cross bedding/lamination and minor horizontal lamination and appear to be well-sorted. Unlike most other heterolithic type units, bioturbation is low to absent. Bed boundaries are typically sharp based between both lithologies.

Interpretation. Presence of ripple cross bedding and loosely imbricated clasts within the muddy lithotypes suggest confined flow within a possible mudstone dominated channel. The absence of bioturbation also supports an active depositional/erosional fairway (stressed environment).

Type Section. Well A, No. 2 Core, 3040-3045.5m

6) Bi-partite sequences of sandstone, capped by poorly sorted mudstone with clasts (Fig. 3.2b no. 8 and 12c)

Description. This facies association occurs as an alternation of sandstone and poorly sorted muddy sandstone or bioturbated muddy bed with occurrence of unsorted granules/clasts. The underlying sandy beds are cm to dm in scale, typically structureless and sometimes have evidence of soft sediment deformation. Grainsize varies between fine and coarse grained and the beds may contain basal clasts. The overlying, muddy units are similar in thickness. Textures vary from structureless, muddy sandstones to poorly sorted mudstones with coarse granules or larger angular clasts. Bed boundaries between the lithotypes vary from gradual to sharp based. Sometimes sand injections from the underlying lithofacies penetrate the overlying muddy interval.

Interpretation. The consistent occurrence of a poorly sorted mudstone or muddy sandstone lithotype, with ungraded clasts, overlying a structureless sandstone unit is similar to reported "linked debrite" deposits of other deepwater depositional systems (e.g. Haughton et al. 2003; Kane and Ponten, 2012). The overlying muddy debrite is considered as genetically related to the turbulent-driven flow of the underlying sandstone and differs to the stand alone muddy debrites of Facies Association 3. Main evidence of genetic flow conditions include evidence for soft sediment deformation near to the bed boundaries and

subsequent injection of sand into the overlying debrite, as well as absence of hemipelagic or turbiditic muds between the 2 lithotypes (hiatus).

Type Section. Well E, No. 6 Core, 4243.5 and 4244.5m, Well D, No. 4C core, 3949.5m

7) Heterolithics (Figs. 2b3 and 2b4)

Description. FA7 is a volumetrically significant facies association of intercalated, thin (cm to dm scale) beds of sandstones and mudstones and is subdivided into sandstone-prone and mudstone-prone varieties, by 40% net sand estimation of the overall interval, which ranges from dm to m-scale thicknesses. Sands are typically well to moderately sorted and vary between structureless, horizontally laminated or more often ripple laminated, similar to parts of the Bouma turbidite sequence (Bouma, 1962). Sometimes the sedimentary structures are deformed due to convolute bedding (dewatering). Internal clasts are rare to absent. Intervening mudstones are either structureless or bioturbated. Flame structures are common. Discrete ash layers are sometimes preserved within these heterolithics, especially in Wells A, B and C (western wells).

Interpretation. The abundance and frequency of incomplete "Bouma" units within the interbedded sands and muds suggests turbulent flow leading to low density turbidites and preservation of low amplitude bedforms (Bouma, 1962; Best and Bridge, 1992). The degree of sandiness depends on the sediment availability. Muddy beds represent the trailing wake of the turbidites together with background hemipelagic sedimentation (highly bioturbated). These thinly interbedded units are common on the lateral and distal fringes of depositional lobes of fan systems.

Type Section. Well A, No. 4 Core, 3194m

8) Bioturbated Mudstones (Fig. 3.2b no 1)

Description. FA 8 is dominantly black to grey bioturbated mudstones, sometimes interbedded with distinct green (ash) layers. Frequently heavily bioturbated with Planolites and Chondrites trace fossils.

Interpretation. The lack of internal lamination suggests dominantly hemipelagic deposition (non turbidite muds) or weak turbidity currents. The relative abundance and diversity of burrowing organisms and the presence of cm-scale ash beds also support depositional quiescence and bed preservation.

Type Section. Well C, No. 2 Core, 4114-4120m

The poorly sorted, texturally immature nature of a large number of beds in the cores from the 5 wells are similar to the observations of the previous study in the offshore basin (Arreguín-López et al. 2011), as well as the updip, onshore deposits (Cruz-Helu, 1977; Jennette et al. 2002; Dutton et al. 2002). Poorly sorted, sometimes clast-rich sandstones and mudstones, together with argillaceous sandstones are diagnostic of the debrite facies in the subsurface and make up to 12% of the measured core section (common in wells A and D, Figs. 2b2, 2b8 and 2b10). When present, individual outsized sand grains are relatively angular. In total, 3 types of debrites are observed – sandy, muddy and linked debrites (after Haughton et al. 2003). Sandy debrites are characterized by dm-thick, fine to coarse, poorly sorted sandstone beds, often with randomly dispersed (not coarse-tail graded) angular clasts. In some instances, these beds sometime have an elevated mud content, but still retain their sandstone-prone nature. In contrast, muddy debrites are mudstone-prone deposits, with dispersed angular clasts. Linked debrites are differentiated from stand-alone mudstone-prone debrites by the presence of an underlying, well-sorted sandstone that shows evidence co-genetic flow with the overlying debrite. Wells A, D and

E show relatively high proportions of these debris-flow facies compared to the other wells and are discussed further later.

The dominant sandstone lithotype in the well cores are the well-sorted, structureless sandstones (25-50%, Fig. 3.2b no 5). These are interpreted as the main constituent of channels and proximal lobes, delivered by high density turbidity currents. The occurrence of significant interbedded debrites suggests episodic alternation between sandy turbidity currents and debris flows. The second most common facies association in the cored intervals are the muddy and thin-bedded heterolithic facies (~30-40%, Fig. 3.2b no 3).

Wells B and C exhibit evidence for higher proportions of turbidite deposits and more interpreted channelized deposits. They also exhibit a lower degree of heterogeneity (larger bed thicknesses) compared to Wells A, D and E, which display more debrite and heterolithic facies. This suggests a level of spatial control on the depositional fabric. The presence and character of fine-grained material in the interpreted muddy channels (well A) suggests periods of terrigenous fine-grained deposition from the margin in an off-axis position to the deepwater.

REGIONAL STRATIGRAPHIC FRAMEWORK

In order to place the interpretations from the core descriptions into a wider stratigraphic context, a regional stratigraphic framework is established. A cross section showing the lithology of Wells A-F, flattened on the top of the Middle Miocene is shown in Fig. 3.4. The cross section represents a regional depositional dip section, as sediment routing direction is from the south and southwest to the north and northeast (Arreguín-

López et al. 2011), with these facies associations representing the downdip extension of the depositional systems described by Jennette et al. (2002).

From well data, the Lower Miocene is significantly thicker than the Middle Miocene in the basin, with thicknesses over 1000 meters in the proximal wells A-D. The Lower Miocene succession thins markedly to the distal Well F, which was drilled almost to the base of the Miocene, recording ~600 meters of sedimentary section. Two (2) regionally correlatable muddy intervals, up to 50 meters thick, are identified which defines three (3) sandy intra-Lower Miocene subunits. These mudstone markers are tied to the seismic data and shown on a composite seismic section between all 6 wells (Fig. 3.5). The sandstone-prone subunits bounded by these mudstones vary between 150-350 meters thick and are labelled as Subunits I, II and III on Fig. 3.4.The location of the sedimentary cores within this framework is also illustrated on Fig. 3.4 (red bars).

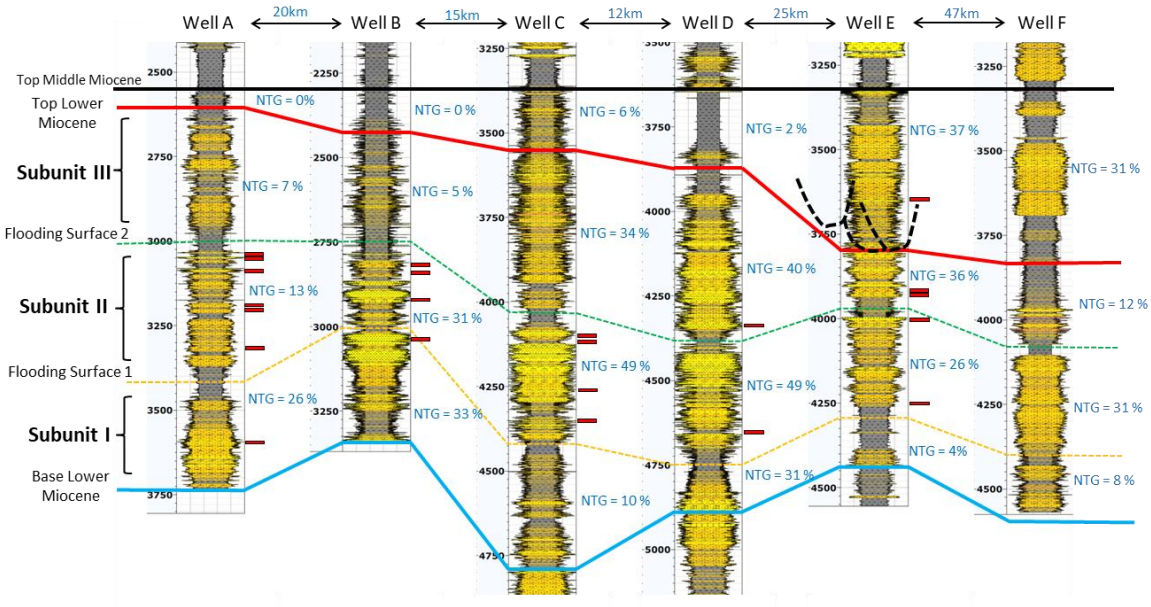

Figure 3.4: Cross Section Wells A-F, showing stratigraphic framework in study area. Yellow and Green lines represent the regionally correlatable mudstones that subdivide the Lower Miocene into 3 separate Subunits. Wells show lithology curves with sedimentary core depths. Petrophysical summations of each subunit also shown. All depths and thickness are in meters. Note interpretation of Middle Miocene channel complex CMM (dashed line) in Well E. See Figure 3.5 for well locations.

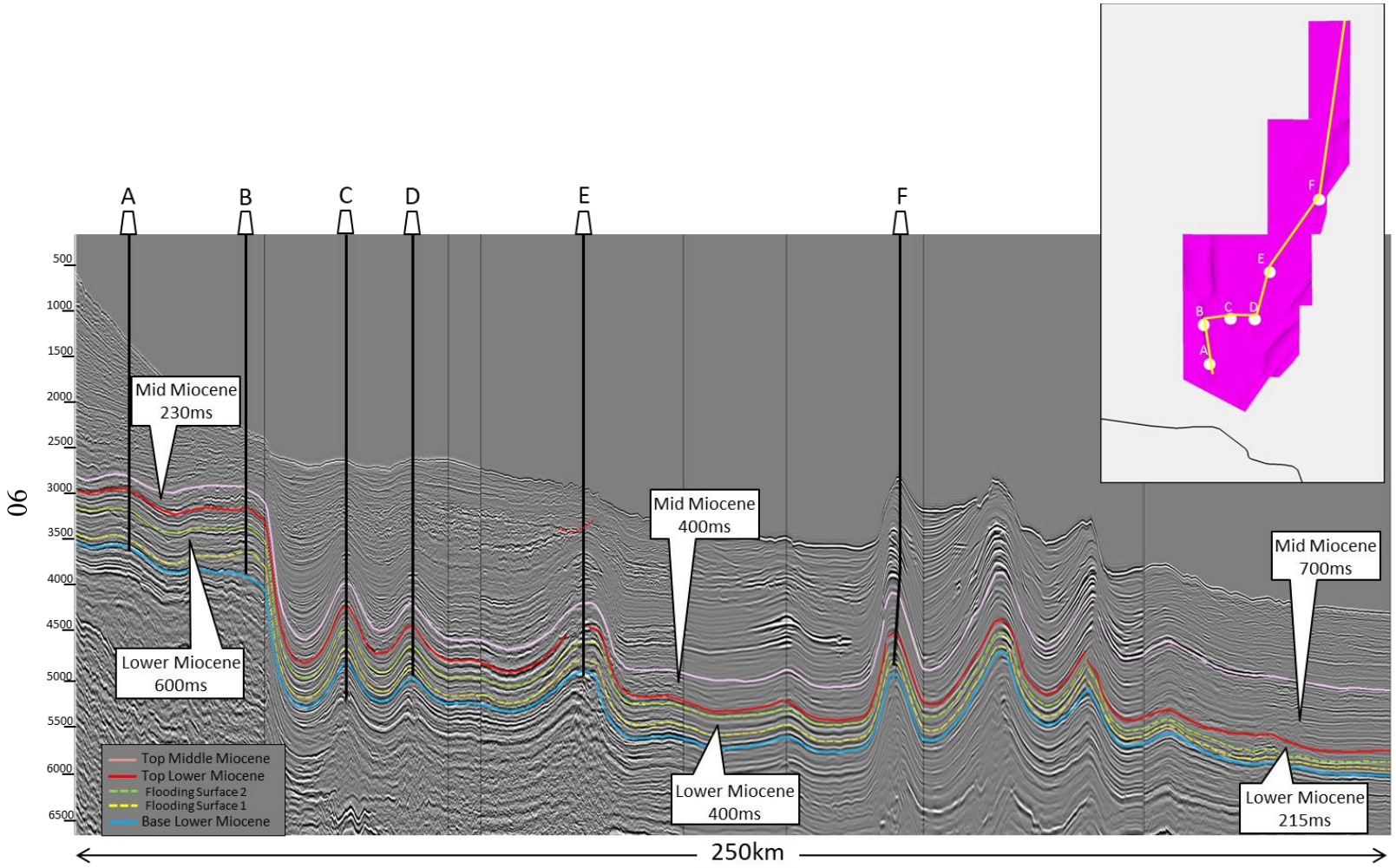

Figure 3.5: Composite seismic line with chronostratigraphic surfaces derived from well data. Inset map shows location of line. Note thinning of Lower Miocene and thickening of Middle Miocene into the basin. Compressional folds are all post deposition of Lower and Middle Miocene.

Fig. 3.6 shows an isochron (stratigraphic time thickness) for the Lower Miocene in the basin. This map shows a regional thinning of the depositional system to the north (distal), over a distance of 175km. Well data in Fig. 3.4 confirms a thinning of ~ 40% of the entire succession between the proximal wells and Well F. Accompanying this interval thinning into the basin is a concomitant reduction in net sandstone, from ~ 40% at Well D to ~ 20% at Well F (70km downdip). Subunits I-III also display similar thinning rates (Fig. 3.4) as the chronostratigraphic unit and a thinning rate of ~ 2-4m/km. These observations suggest a proximal to distal, sandstone-prone deepwater complex.

These trends contrast to the Middle Miocene, which shows a significant thickening from ~100 meters and less in the proximal wells to over 500 meters in the distal wells. The sandiness of the Middle Miocene also increases, from <10% in the proximal wells to >30% in the distal Wells E and F. Seismic isochrons of Subunits I-III are limited by a combination of the resolution of the thinner Subunits in the distal basin as well as the presence of post-depositional contractional folds (formation of the Catemaco foldbelt) which yield tectonically thickened values that are probably not representative of the depositional trends in the basin. Like the Middle Miocene we use thickness trends observed in the wells (Fig. 3.4) combined with seismic attribute maps which are generated for the individual Subunits and core data where available.

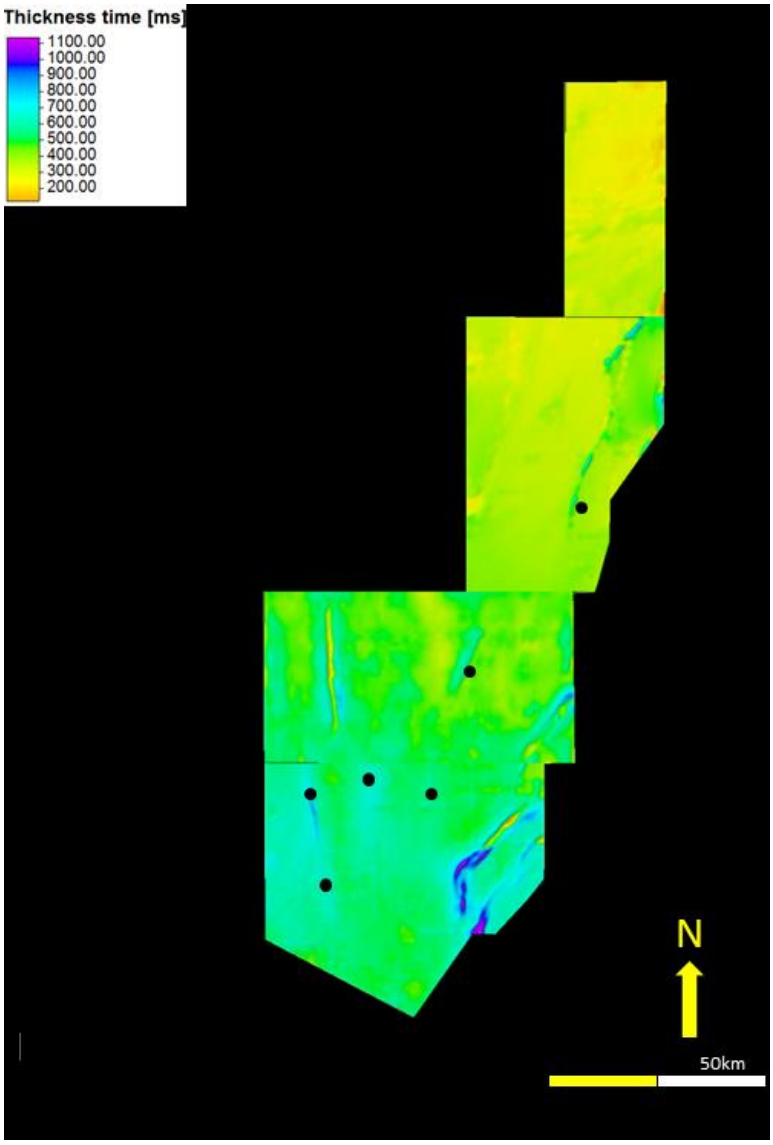

Figure 3.6: Thickness map of the Lower Miocene in the Study Area Showing regional thinning to the basin (north)

SUBUNIT I – LOWERMOST LOWER MIOCENE

This unit represents the lowermost interval within the Lower Miocene stratigraphic unit in the basin. It is the thinnest of the three (3) Subunits (Fig. 3.4), with a maximum thickness of 350 meters at Well C. The unit thins to both the east (Well D, 200 meters) and also to the basin (wells E and F, ~150 meters), suggesting a depocenter focused in the western basin that thins at a significant rate of ~ 12.5meters/km to the east and a much more subtle 1m/km in a downdip direction to the north. Lithology curves show a marked difference between the western wells which are dominated by a combination of coarsening-upward and fining-upward trends, compared to the dominant fining-upward trends of the eastern and distal wells.

With the top and base of Subunit I mapped, seismic amplitude maps were generated for the interval. Root Mean Amplitude (RMS) extractions, which display the high amplitude features within the mapped seismic interval, are shown in Fig. 3.7. These extractions were done over intervals of 100-250ms (150-350m). Amplitude maps extract and display the highest amplitude features within this interval. Stratigraphic features are constrained by seismic resolution, in this case the seismic volume has a peak frequency of 25Hz and an average seismic velocity of 2500m/sec, thus the limit of vertical resolution is ~25m. Of note are a series of north northeast-trending linear, elongate features, interpreted as submarine channels. Of particular interest is the single, large-scale feature on the western portion of the seismic amplitude map where Well B occurs. This interpreted channel (Ch1a) is observed to be the only feature to traverse the entire ~175km depositional dip runout. Fig. 3.8 shows a seismic line through Ch1a, which exhibits widths of 2-3km, and shallow thicknesses up to 50ms. To the east of this large system are a series of shorter-run, low-amplitude channels that also show a northerly trend. Although not as extensive as Ch1a in cross section these channels have comparable widths and thicknesses (Fig. 3.8).

Cores from Subunit I exist in Wells A and B (Fig. 3.9). Grain size trends are difficult to discern given the quality of the photographs and absence of grain size data. Well B appears to directly intersect Ch1a in Fig. 3.7, and displays a sandstone-prone, thickening-upward bed profile, that is characterized by the abundance of high-density turbidites, with clasts (basal and sometimes graded) and occasional crossbedding (Fig. 3.9). These have been interpreted as sandy channelized facies (Facies Association 3), which supports the amplitude extraction interpretations. The presence of overturned/slumped bedding is interpreted as channel margin collapse fill facies.

Wells A, C and D appear to test different seismic features – rounded to elongate terminal ends of smaller channel systems (Fig. 3.7)similar to terminal lobes of channels. Core data in Well A for this interval records 8 meters of thinly-bedded, heterolithic dominated facies (Facies Association 7, Fig. 3.9) suggesting this rock type may also exist at wells C and D which appear to test similar seismic features to the east.

Similar to Well B, Well E appears to lie in a seismically highlighted channel system (Ch1b), albeit smaller in scale and basinward of the previously described wells. No core exists in this interval but the well log shows poor sand development, probably representing a mud-filled channel in this part of the basin. A correlation between channel location, size, extent, amplitude and sandstone content appears to exist – proximal, longer, higher amplitude channels (Ch1a) tend to be sandstone-prone vs more basinward, lower amplitude, relatively smaller channels (Ch1b). When sandstone-prone, channel facies are dominated by stacked, meter-scale, well-sorted, high-density turbidites. By comparison, smaller, less apparent channels tend to be mudstone or heterolithic-prone, with occasional muddy debrites. Inter-channel regions observed in Subunit I may represent an amalgamation of channel overbank or terminal facies from multiple channels or underlying deposits.

Well F which lies further downdip shows marginally better sand development and occurs in an overbank setting, 5 km to the east of the muddy channel tested by Well E. The correlation between Ch1a and the presence of significant sand development in well B, coupled with the general decrease in sand in both terminal and overbank settings suggests a possible channelized lobe setting, where coarse-grained material is confined to the main channel conduits. The smaller scale channels in the eastern basin, represented by poorer sand development may represent smaller, less significant channel systems, supporting the model of the main sedimentary depocenter being focused in the western part of the basin. The muddy nature of Well E is interesting, as it demonstrates that not all channels are sandy. This may be due to significant volumes of muddy sediments delivered to the eastern region concomitant with coarse-grained sands in other channel complexes to the west (position of the depositional axis), or alternatively coarse-grained sediment bypass further to the basin. The first model is preferred, given the regional thickness maps which show consistent thinning to the north into the deeper basin.

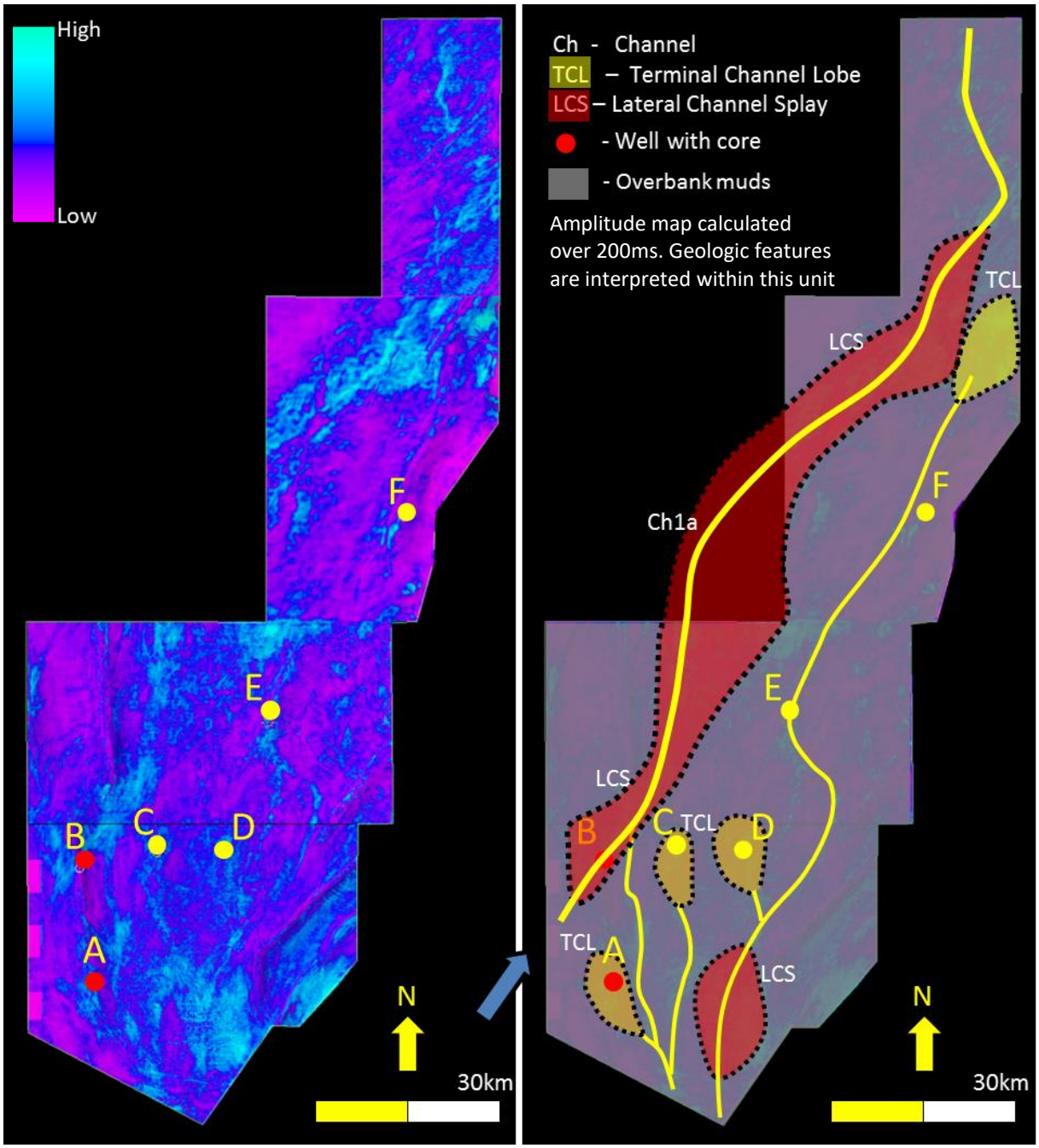

Figure 3.7 : Amplitude (RMS) map for Subunit I, Lower Miocene (between Base of Lower Miocene and Flooding Surface 1)

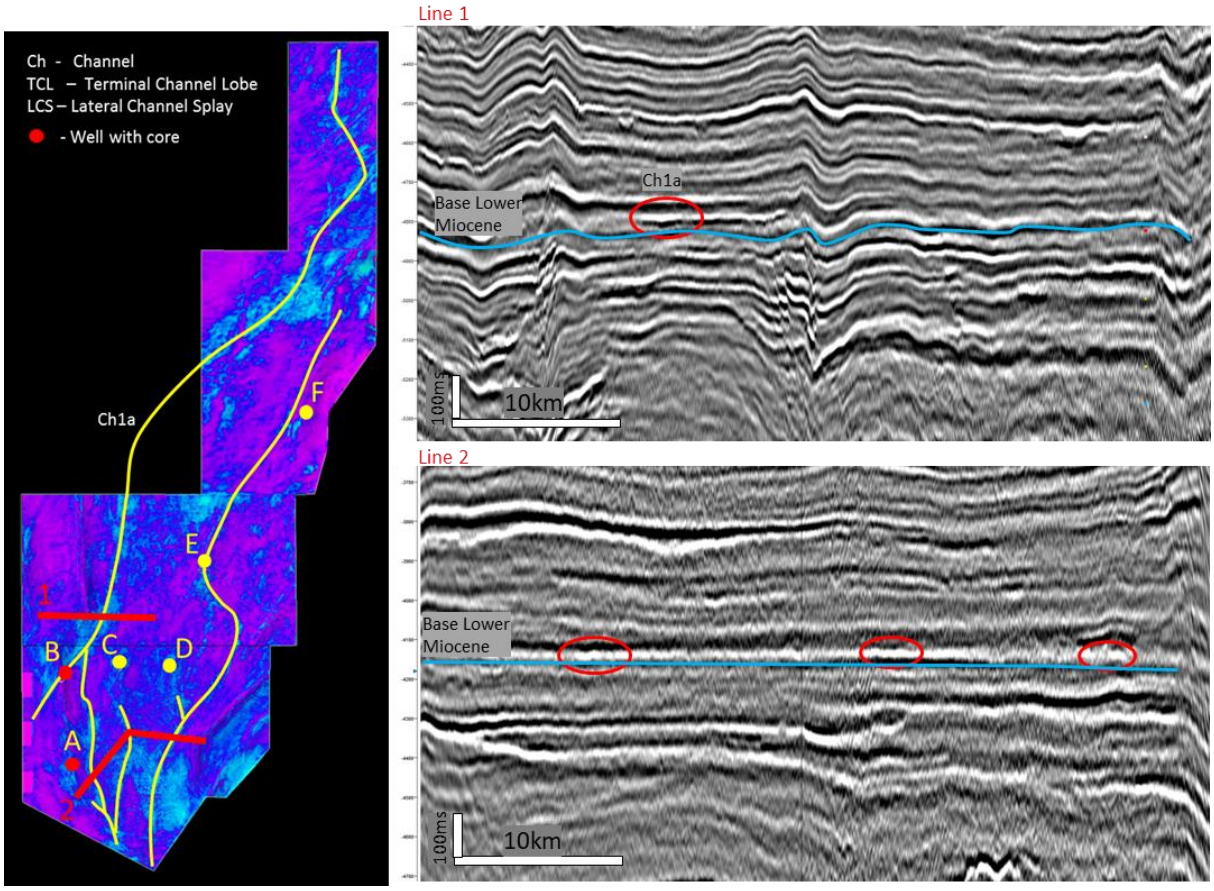

Figure 3.8: Channel systems of Subunit I. Very poorly developed channel forms, <50ms thick, 2-3km wide

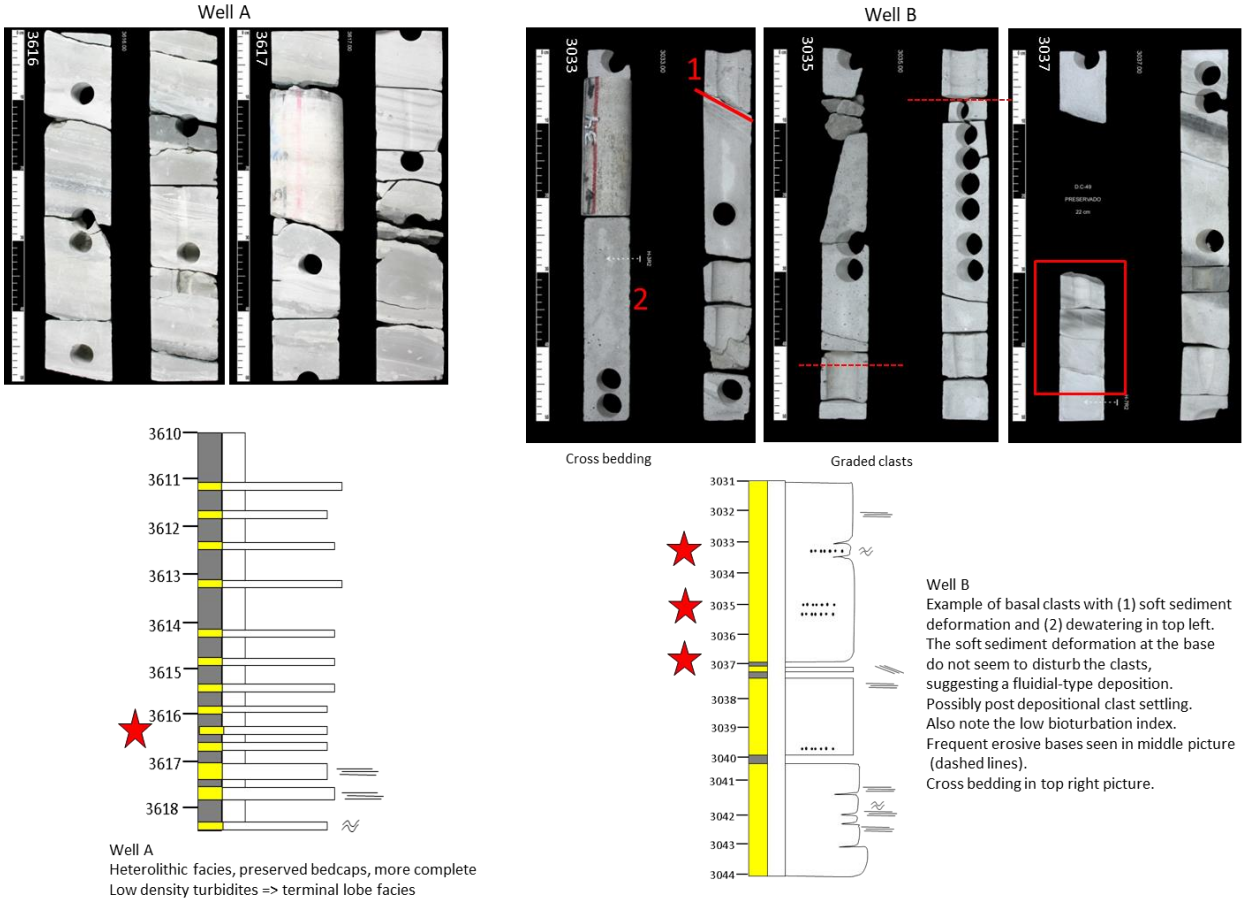

Figure 3.9: Core photographs showing common facies associations in Subunit I. Logged sedimentary sections are shown for reference. Red stars are location of photos

SUBUNIT II – MIDDLE LOWER MIOCENE

Subunit II is thicker than Subunit I, with Well C recording a thickness over 400 meters. From Well C, the section thins significantly in both lateral directions – 10 meters/km to the western Well B and 5.8 meters/km to the eastern Well D and more subtly at 2meters /km to the distal Well F. This distal thinning is not constant, as the thinning rate

to the medial Well E is significantly greater (5.8meters/km). This significant lateral thinning rate compared to the distal trend mirrors the underlying subunit, suggesting morphologically elongate depositional systems in the direction of the overall sediment transport.

Lithology curves for all 6 wells show both coarsening-upward and fining-upward log patterns. An RMS amplitude map of this seismic unit (Fig. 3.10) shows a prominent fan-like geometry of elevated amplitudes in the proximal part of the basin. This feature is made up of 3 distinct channel complexes in a strongly dendritic pattern, labelled Ch2a, Ch2b and Ch2c respectively. The central channel Ch2b passes just west of Well C (thickest and sandiest interval), with Ch2a further away from Well B and Ch2c occurring significantly away from Well D. The inter-channel regions are characterized by elevated, non-linear amplitudes in this proximal region, and are interpreted as overbank deposits or non-channelised, underlying deposits that are incised by Subunit II, due to the sandy, coarsening-upward nature of the well lithology curves. Further into the basin, Ch2a runs north outside of the data area, while Ch2c trends to the northeast and thins to the limit of resolution just east of Well E. The central Ch2b runs all the way north to the end of the regional seismic dataset, similar to Ch1a in the underlying Subunit and occupies a similar position in the basin. Fig. 3.11 is a seismic cross section showing the character of Ch2b compared to the underlying Ch1a. They are similar in scale to the channels in the underlying Subunit I, ~2km wide and up to 50ms deep. This long-run channel passes significantly west (~15km) of Wells E and F (Fig. 3.10). Because the coarsening upward motifs of Subunit 1 in the proximal areas tend to underlie major channels or channel belts of Subunit II, it is suggested that some of them represent progradational lobes that are eventually over-run by channels.

Subunit II is also the heaviest cored interval, with Wells A-E all having representative core and shown in Fig. 3.12. Well C, which lies closest to the central axis of the distributive channel system and records the thickest, sandiest interval, shows evidence for erosive bed bases with dispersed mudclast conglomerates (Facies Association 4) and interbedded (up to 7 meters) amalgamated, high-density turbidites (Facies Association 1, Fig. 3.12a). On average, the thickest beds of the Lower Miocene occur in this interval at Well C (up to 7m). Grainsizes do not show any apparent vertical trends between the cores, but textural immaturity is a characteristic feature of all analyzed samples, varying between very coarse to fine grained sandstones.

Wells A and B, which lie in the lower amplitude regions and to the west of Ch2a show a subtle decrease in mean grain size of the cored interval and marked decrease in sand content and individual bed thickness (Figs. 3.4 and 3.12b). Sedimentary cores in Well A, which lies 6km to the west of the main trunk channel, display thinly bedded heterolithics, with dm-thick bedsets of low density turbidites and preserved bedcaps (Facies Association 7), poorly sorted sandy debrites (Facies Association 2) and linked debrite deposits (Facies Association 6). Well B, which lies closer to a seismically identified channel system (3km west of Ch2a) contains heterolithics but also better developed sandy beds, interpreted as high-density turbidite deposits (Facies Associations 1). The frequent occurrence of dewatering and soft-sediment deformation structures in both wells (convolute lamination and flame structures, Fig. 3.12b) suggest rapid sediment fallout from the transition between confined and unrestricted flows, perhaps representative of overbank deposits associated with the nearby western channel system (Ch2a).

Well D, which is similar to Well A in terms of distance from the nearest channel (~ 6km from Ch2c) possesses a single core, which records a 10m mudstone-prone heterolithic unit overlying an argillaceous sandstone with cross-bedding and dewatering structures

(Fig. 3.12c), interpreted as a sandy debrite deposited on the distal fringe of the seismic feature. Further downdip, Well E which lies at the terminal end of Ch2c, displays significant development of muddy debrites (Facies Association 3) and linked debrites (Facies Association 6), with lesser evidence for channelized facies (erosive beds with mudclasts, Fig. 12d). Sandstone is texturally immature like the other wells and displays similar grainsizes to Wells A, B, and D, i.e. slightly finer-grained than Well C. These wells also display significantly thinner bed thicknesses than Well C (Fig. 3.4). Unfortunately, no core data is available for Well F, but the seismic amplitude and lithology curves show similar trends to Well E (Fig. 3.4) and are interpreted as the downdip expression of the terminal channel facies interpreted at Well E.

Combining the seismic observations and core data, Subunit II is markedly different from the underlying Subunit I in that the wells all test extra-channel parts of the depositional system, in varying distances away from the main trunk channel. The presence of significant sandstone development in these wells is also different to the observations from the underlying unit. There also appears to be a correlation between distance from channel systems and degree of sand development – wells that are farther from the channels are invariably muddier/debrite dominated (e.g. Wells A and D, Fig. 3.12) compared to wells closer to the channels (Wells B and C). Well E is interpreted to test the terminal channel seismic features of Subunit II, and like the underlying interval, record moderate sand development and similar facies. The thicker nature of these deposits relative to the underlying unit is perhaps a function of the overall higher volume of terrigenous sediment, noted in the overall thicker nature of Subunit II. The fan-like shape observed on the seismic amplitude map, combined with observations from the core data, strongly suggest Subunit II as being a proximal, channelised fan, made up of channel complexes, overbank splays and terminal lobes, in a moderate to poorly confined channel system. Further down-system

in the region of Wells E and F, the channels become less confined and transition into broader, more unconfined non-channelised seismic features. This evolution is probably the result of increased volume of terrigenous material which exceeds the carrying capacity of the channels further down-slope or downdip reduction in slope gradient, which results in more poorly confined channels downdip.

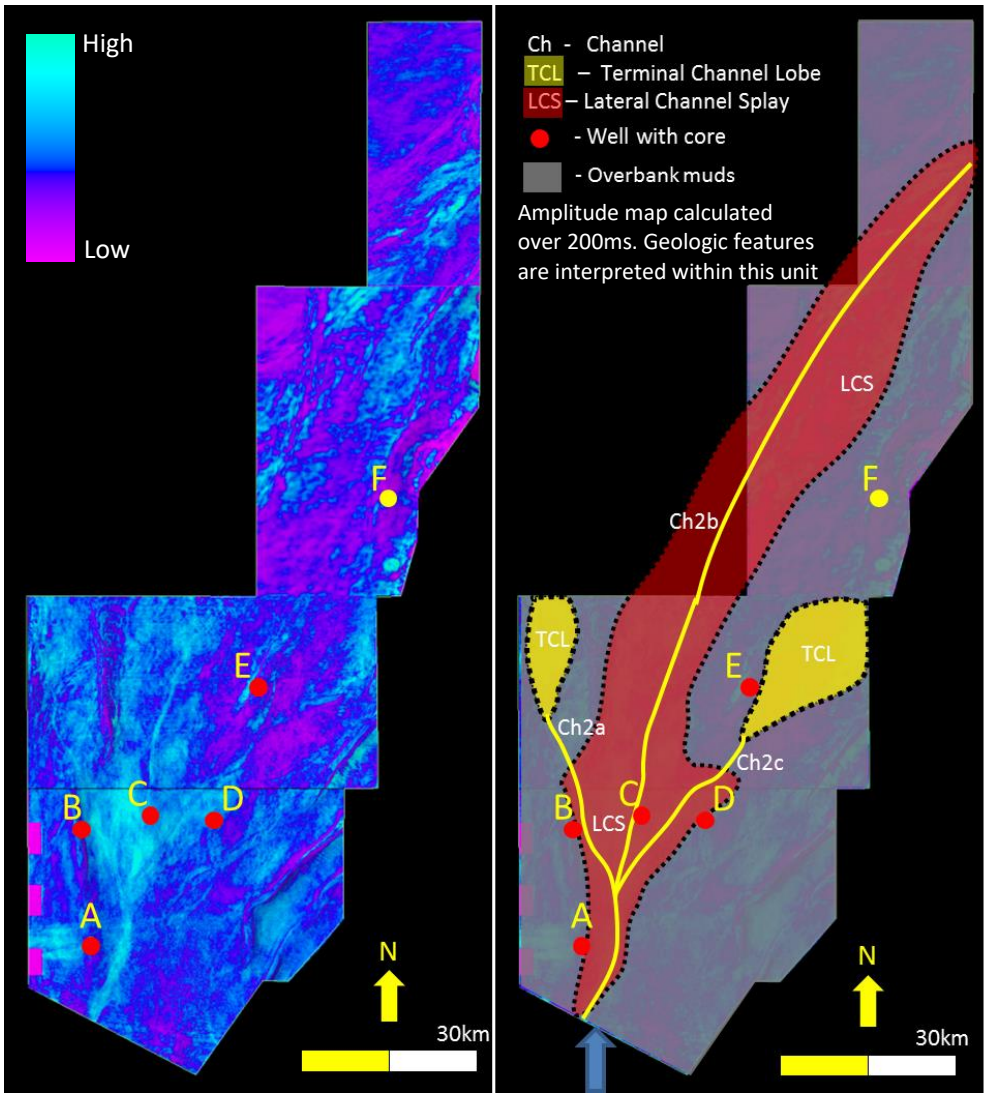

Figure 3.10: Amplitude (RMS) map for Subunit II, Lower Miocene (between Flooding Surface 1 and Flooding Surface 2)

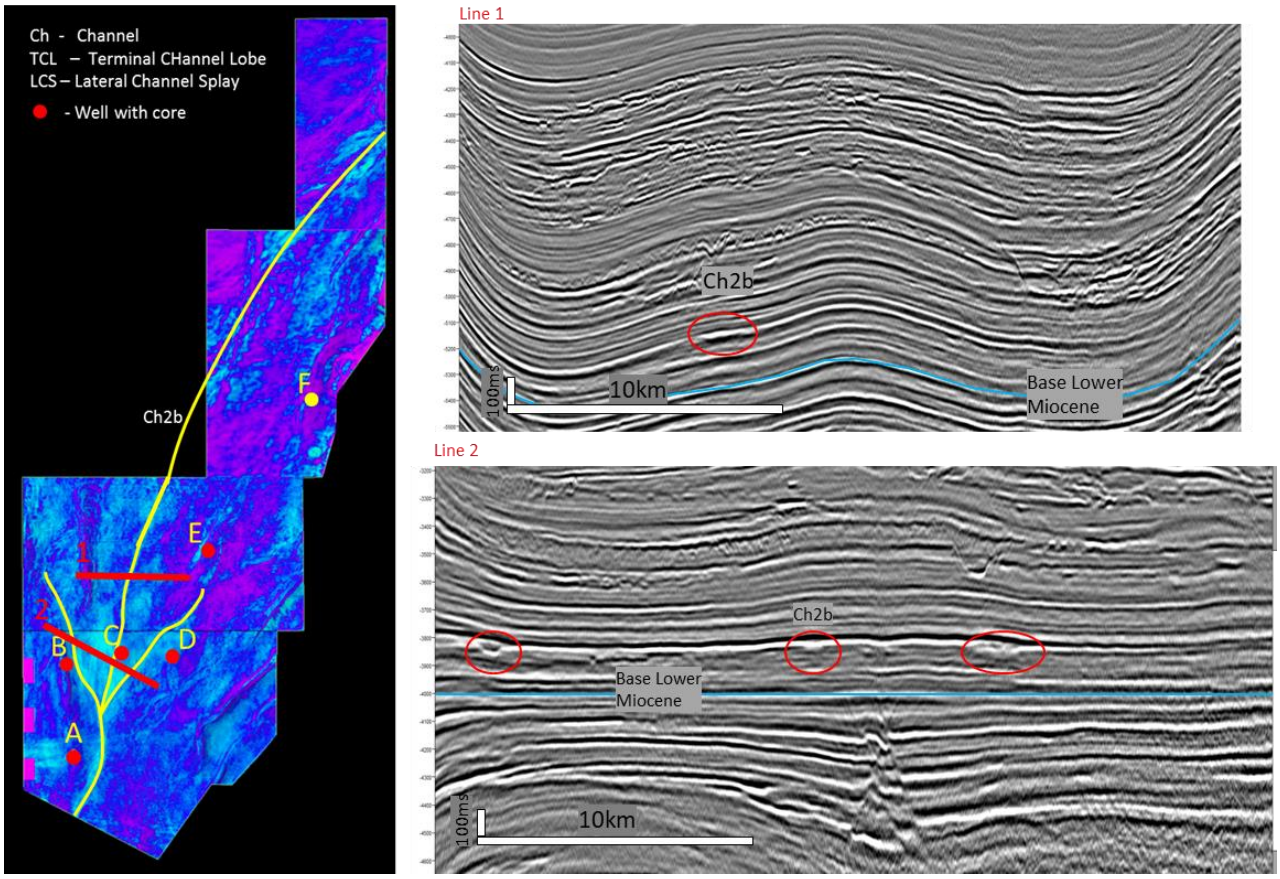

Figure 3.11: Channel systems of Subunit II. Poorly developed channel forms, but better developed than Subunit I.

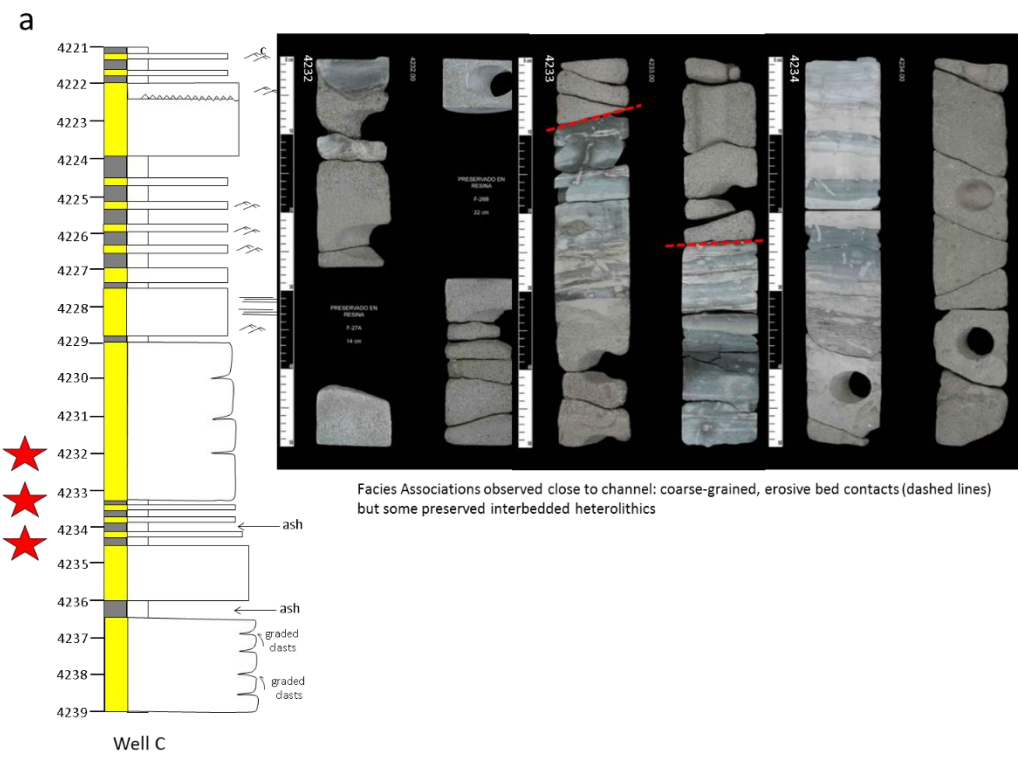

Figure 3.12: Core photographs showing common facies associations in Subunit II. Logged sedimentary sections are shown for reference. Red stars are location of photos. Well C showing common facies associations close to channel system (coarse-grained, erosive bed boundaries).

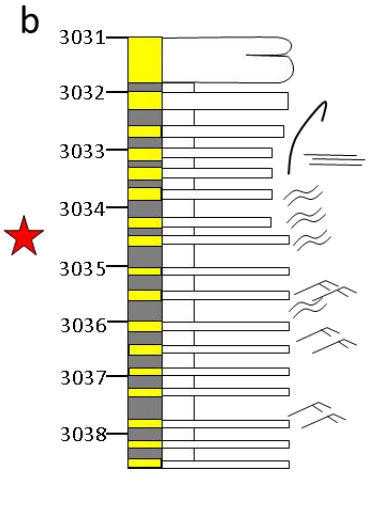

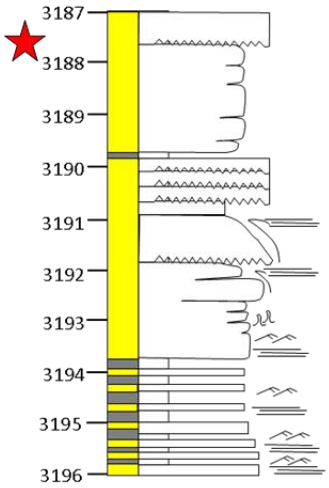

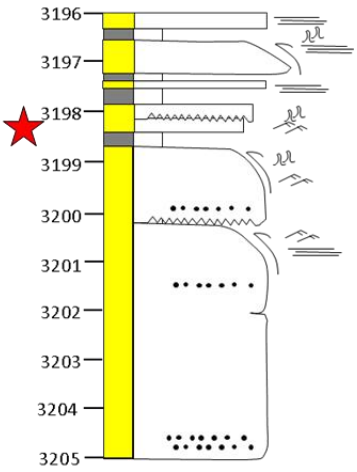

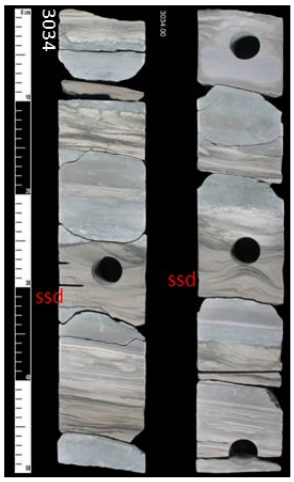

Well A – Heterolithic facies with preserved bedcaps. High bioturbation index and soft sediment deformation (ssd).

Well A – poorly sorted, sandy debrites

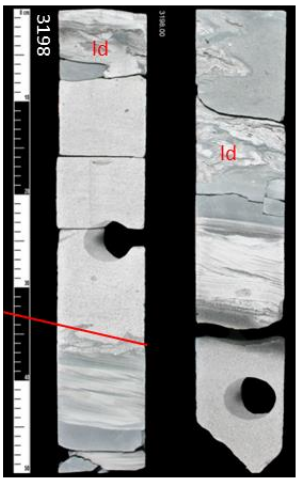

Well A – Linked Debrites (ld)

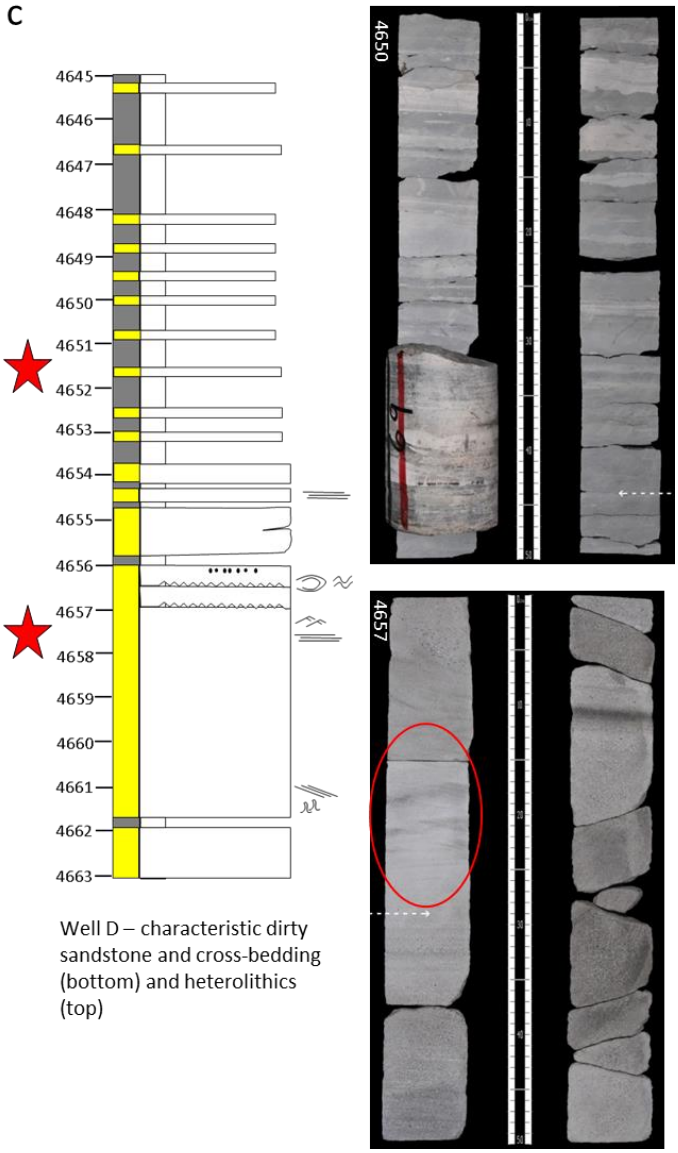

Well D showing additional facies for positions away from channels (stand-alone debrites and heterolithics).

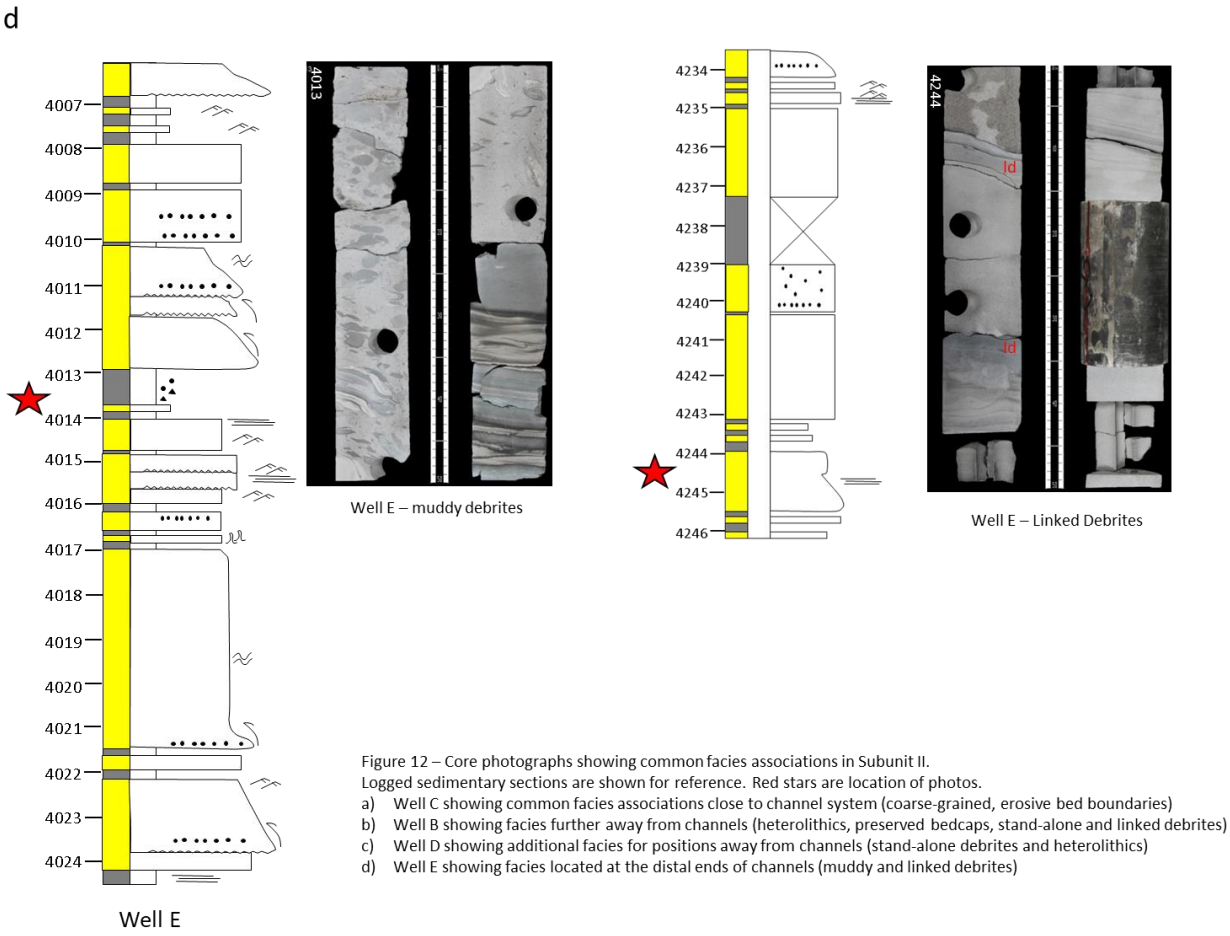

Figure 12 – Core photographs showing common facies associations in Subunit II.
Logged sedimentary sections are shown for reference. Red stars are location of photos.
a) Well C showing common facies associations close to channel system (coarse-grained, erosive bed boundaries)
b) Well B showing facies further away from channels (heterolithics, preserved bedcaps, stand-alone and linked debrites)
c) Well D showing additional facies for positions away from channels (stand-alone debrites and heterolithics)
d) Well E showing facies located at the distal ends of channels (muddy and linked debrites)

Well E showing facies located at the distal ends of channels (muddy and linked debrites)

SUBUNIT III – UPPER LOWER MIOCENE

This interval is the youngest and thickest of the Lower Miocene subunits in the basin, exceeding 500 meters in Well D and represents a progressive eastern migration of the depocenter throughout the Lower Miocene. Subunit III thins between 4-5 meters/km to the western wells and in marked deviation from the underlying intervals which show

very subtle thinning to the basin, with a thinning rate that is similar to the lateral rates of between 4-5meters/km. Well E displays an anomalously thin (~170meters, Fig. 3.4) interval as much of it has been removed by an overlying Middle Miocene erosional feature. The thickest preserved Subunit III occurs at Well D, which also records the highest net sandstone (Fig. 3.4).

An RMS seismic amplitude map of this unit (Fig. 3.13) confirms the interpreted eastward migration of the regional depocenter. The depositional axes of the individual Subunits can be defined in well data by the thickest Subunit intervals, which are always the sandiest, and display significant lateral thinning rates away from the axial well – Well B for Subunit I, Well C for Subunit II and Well D for Subunit III. These interpreted axes are also the regions of highest amplitudes. For Subunit III there are lower-amplitude, north-trending elongate morphologies in the western basin that replace the prominent channel systems of Subunits I and II, interpreted as smaller-scale channels that form in the vicinity of the muddy Wells A and B. The central region is dominated by a single, well defined, north-trending sinuous channel system, just west of Well C, labelled Ch3a. This complex persists for about 100km until the northern end of the seismic data. Unlike the channel systems in Subunits I and II, this complex is thicker, with erosional relief up to 100ms (Fig. 3.14). Channel widths are also slightly larger, up to 3km, and mirror the underlying channel system Ch2b which shows a downdip widening of the erosional complex. To the east, an even larger, sinuous channel complex, with a northwestern trend is observed, but this feature appears to be Middle Miocene in age and erodes into the upper part of the Lower Miocene (highlighted in Fig. 3.13 & 3.14). The eastern region is also characterized by a broad area of high amplitude with no discernable channel forms in the vicinity of Wells D, E and F. This region borders the post-depositional deformation, where seismic mapping becomes challenging, thus affecting the seismic resolution of the amplitude maps.

There is a general absence of channelized facies in the cores from nearby Well D and E; they are instead dominated by heterolithics (Facies Association 7). Well D displays evidence of linked and sandy debrites, while Well E contains beds interpreted as muddy debrites (Fig. 3.15). Given their location on the edges of a broad, high-amplitude region on the seismic amplitude map, these facies are interpreted as representative of the lateral and/or distal positions of a southeastern depocenter (Facies Association 3, 6 and 7). with updip feeder channels outside of the seismic coverage area.

No core data for Subunit II exists for the central and western wells. The poor sand development in Wells A and B that coincides with the smaller-scale channel system, coupled with the better sand development at Well C which lies to the west of Ch3a suggests a poor correlation between channel-forms and sand development for Subunit C in general. The western channels and Ch3a may be highly unconfined with most of the coarse-grained sediment deposited in overbank/inter-channel areas, with muddy/silty fills within the channels, or alternatively, late stage, muddy channel elements that incise a broad, unconfined sandy slope unit (Fig. 3.14). The narrow, highly sinuous nature of ChC1 is markedly different to the underlying channel complexes, which are much wider zones of confined downslope sediment transport.

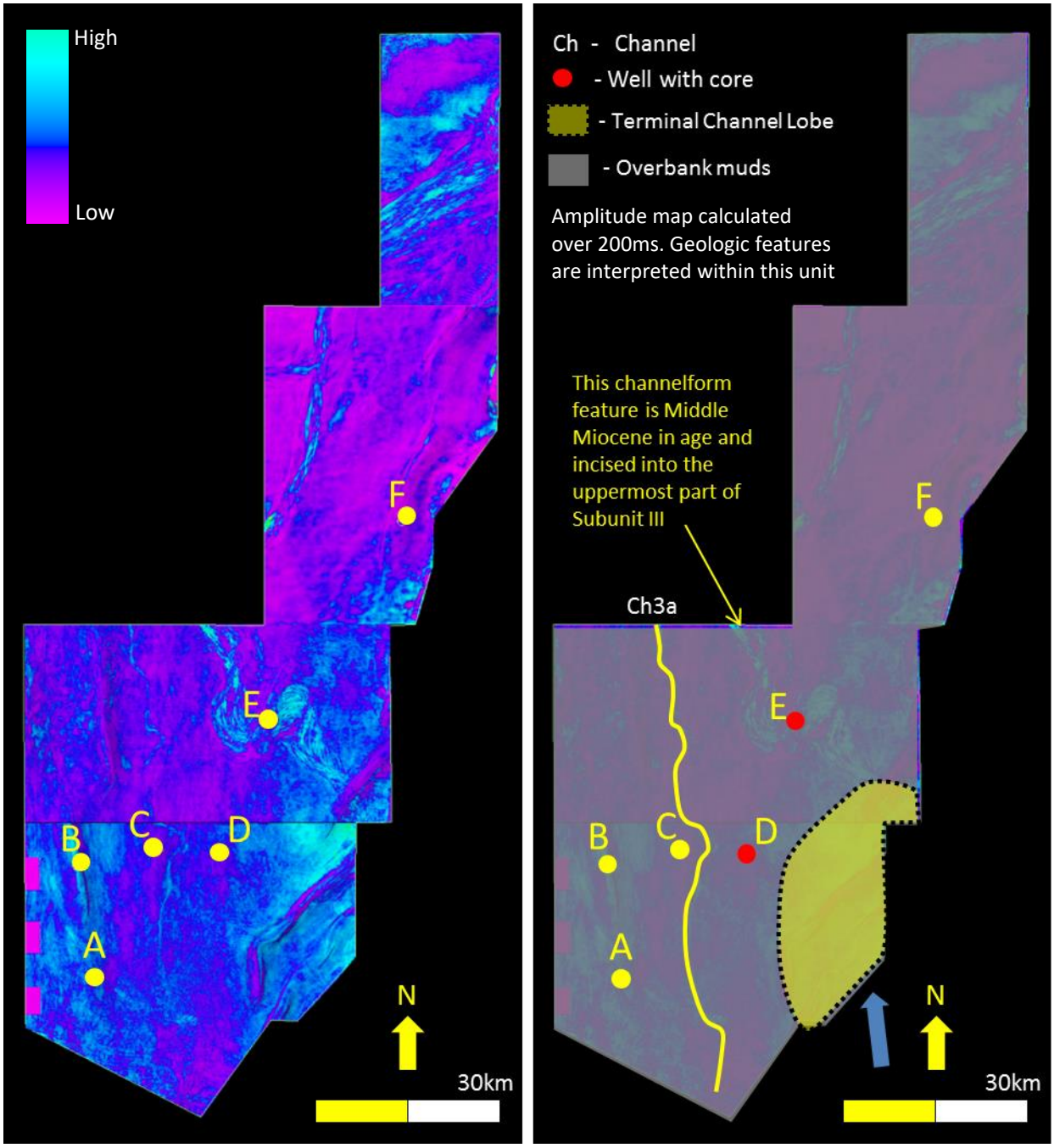

Figure 3.13: Amplitude (RMS) map for Subunit III, Lower Miocene (between Flooding Surface 2 and Top Lower Miocene)

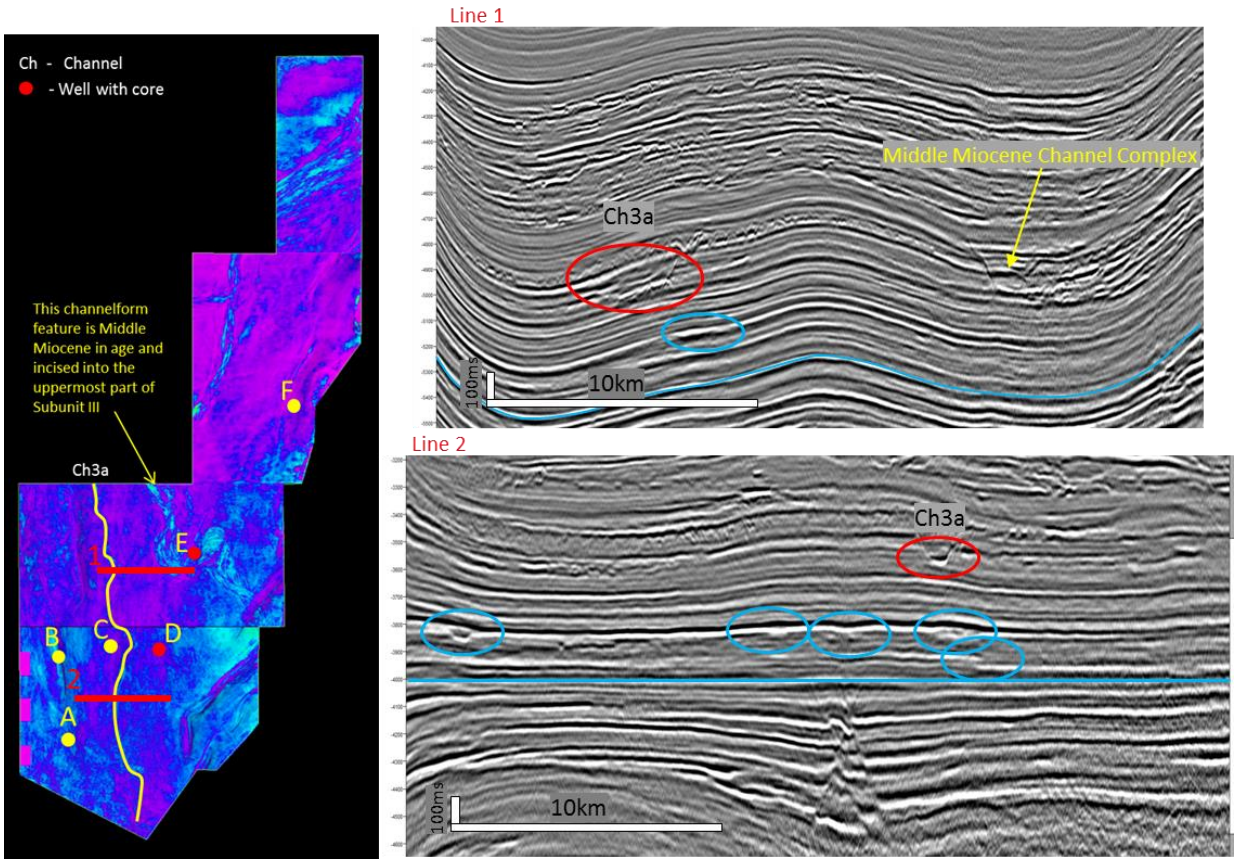

Figure 3.14: Channel systems of Subunit III shown in red circles. Note well developed channel system compared to systems in Subunits I and II (blue circles). Channel width increases down-system.

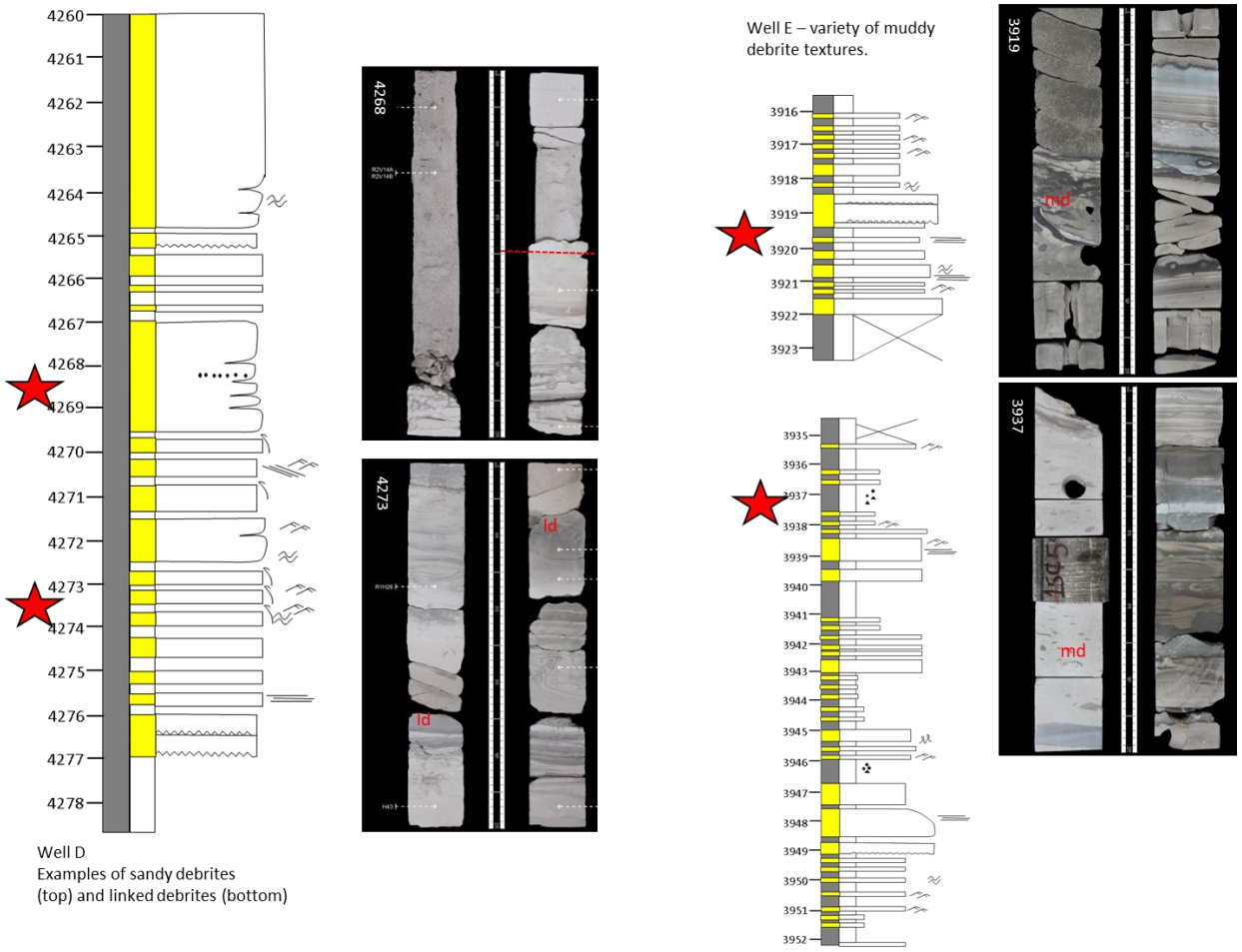

Figure 3.15: Core photographs showing common facies associations in subunit III. Logged sedimentary sections shown for reference. Red stars are location of photos. Wells D and E show typical facies away from channel systems and on the fringes of depositional lobes.

MIDDLE MIOCENE

In contrast to Subunits I-III of the Lower Miocene, the Middle Miocene succession exhibits a significant thickening into the basin, varying between 50-100 meters in the proximal wells A-D, and ~500 meters in well E & Fig. 3.4). The other major feature of this interval is the presence of a high-amplitude, sinuous, elongate feature on the RMS

amplitude map (Fig. 3.16). In seismic view (Fig. 3.17) this feature is highly erosive and significantly larger than the channel systems of the Lower Miocene. Widths vary between 5-10km, and erosive relief ranges from 250ms in the proximal region to 350ms further downdip. These observations are interpreted as a large, third (3^{rd}) order submarine channel system (after Mayall et al. 2006) compared to the broader, smaller-scale, lobe-capping channel complexes of the Lower Miocene. This feature (CMM) is observed to originate in the southeastern part of the dataset and runs northwest, before changing to a more north trending system, before changing to a north-eastern oriented feature Fig. 3.16). The channel complex appears to be narrowest (<5km) when it runs due north and increases in width when it trends northwest and northeast (>5km wide). The internal architecture of CMM shows a sub-vertical stacking of what appear to be km-scale, smaller individual channel systems contained in the master erosional surface, suggesting a long-lived, complex evolution of the channel belt. (Fig. 3.17)

This feature is shown on Well E in Fig. 3.4 and illustrates the location of a single 6- meter, poorly preserved core, that records a poorly-sorted, very coarse-grained sandstone (Fig. 3.16). Along the length of its profile, evidence is seen of differential compaction of the overlying stratigraphy, with a low-relief, mound-like morphology over CMM (Fig. 3.17). This is similar to other reported cases of differential compaction driven by sandstone lithologies (e.g. Heritier et al. 1980; Cherven and Fischer, 1992) and along with the core data from Well E, confirms the sandy nature of the channel complex. To the west of this feature are a series of smaller channels, similar in scale to the channels in the Lower Miocene, with a much straighter profile than CMM. These probably represent mud-filled or bypass channels of the upper slope, calibrated by Wells A-D. Most of the coarse-grained material is probably confined to CMM during this period. To the west of these

interpreted muddy channels is another larger-scaled, sinuous feature, interpreted as another third (3rd) order channel complex.

An additional feature observed on the seismic amplitude maps are a series of highly linear, north-south oriented artifacts that appear to run parallel to CMM. These are located on the eastern flank of the feature (central part of the study area, labelled in Fig. 3.16). In cross section, these features are wavy to shingled seismic reflections (Fig. 3.17, line 3, red circle), and their association with CMM suggest some type of overbank/levee complex. Vertical relief of the seismic reflections are up to 50ms, with wavelengths of 1.5km-3km. Superficially, these geometries are similar to the seismic reflection character near to the top of the seismic lines close to the modern seafloor (Fig. 3.18d). However, there are some notable differences; the modern features are not associated with any observed channel complexes, their morphology is east-west oriented (Fig. 3.18b) and they also appear to be more sinuous than the Middle Miocene features. In seismic cross section, these modern features are shown in Figs. 3.18c and 3.18d (depositional strike and dip), with the dip section showing a train of well-developed, seaward dipping accretion sets, with downslope asymmetry (after Cartigny et al. 2011). The internal bedforms exhibit a landward migration direction and are interpreted as turbidite current sedimentary waves or cyclic steps (Parker, 1996; Kostic, 2011; Covault et al. 2017a). The migration direction of the bedforms in the Middle Miocene are difficult to interpret, thus the term sedimentary wave bedforms are used to describe them.

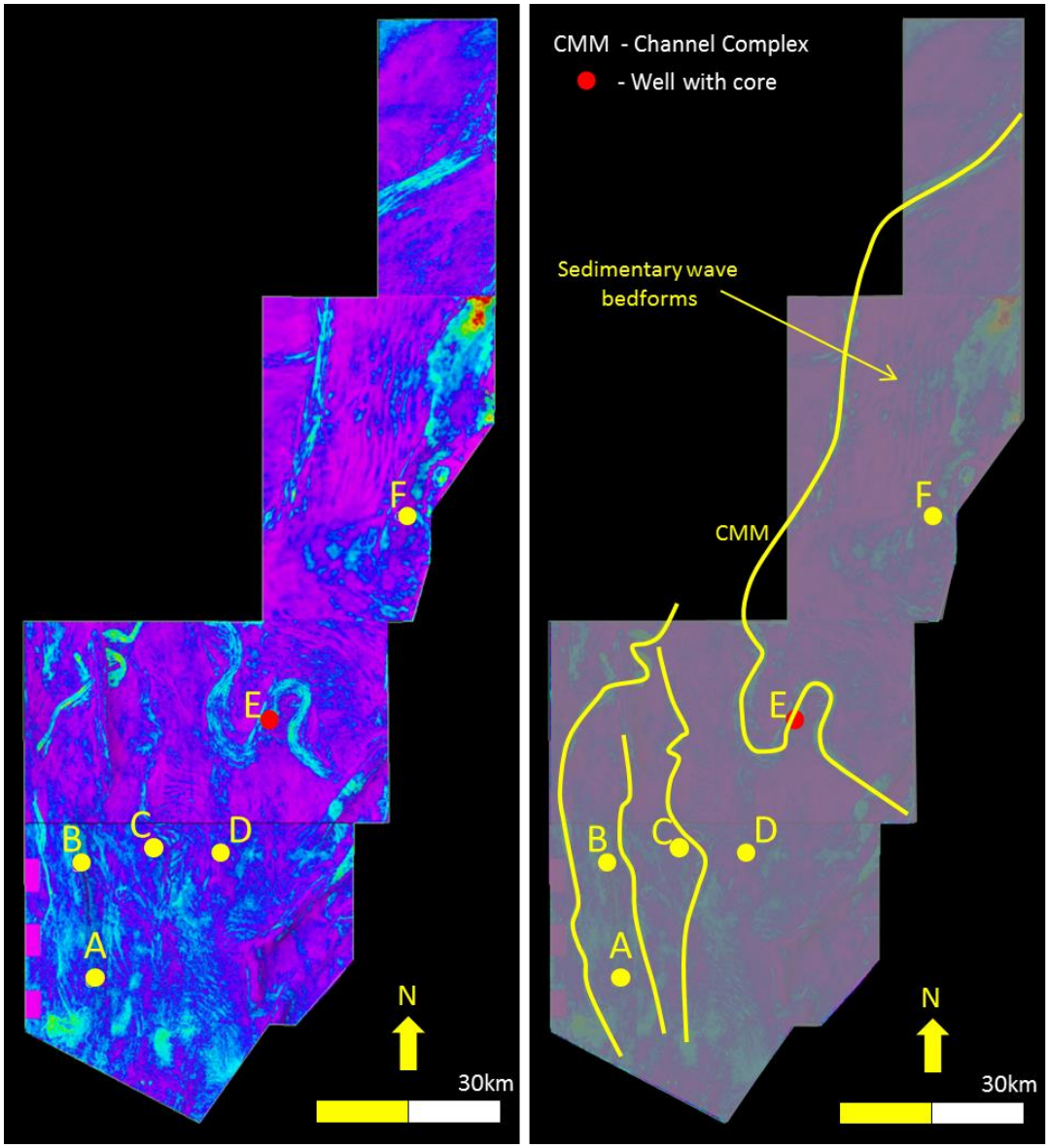

Figure 3.16: Amplitude (RMS) map for the Middle Miocene. Note high-amplitude sinuous feature CMM, interpreted as a 3rd order channel complex (after Mayall et al. 2006). Well E tests this feature and shows poorly sorted, very-coarse grained sandstones. Also note the parallel, linear features on the eastern flank of the channel complex, interpreted as sedimentary wave bedforms.

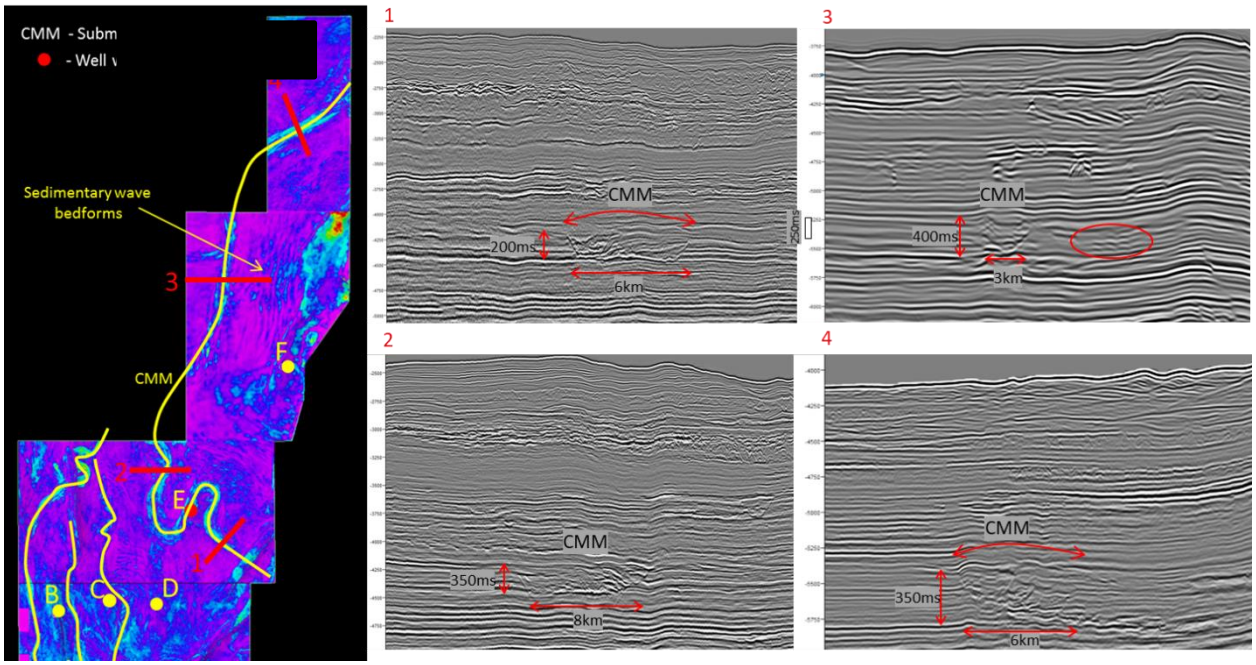

Figure 3.17: Profile of the Middle Miocene 3rd order channel complex. Lines 1-4 show the external and internal character of the erosive system. Note the scale of the system, differential compaction seen in Lines 1, and 4 (red arrows). Also note character of sedimentary wave bedforms in Line 3 (red circle).

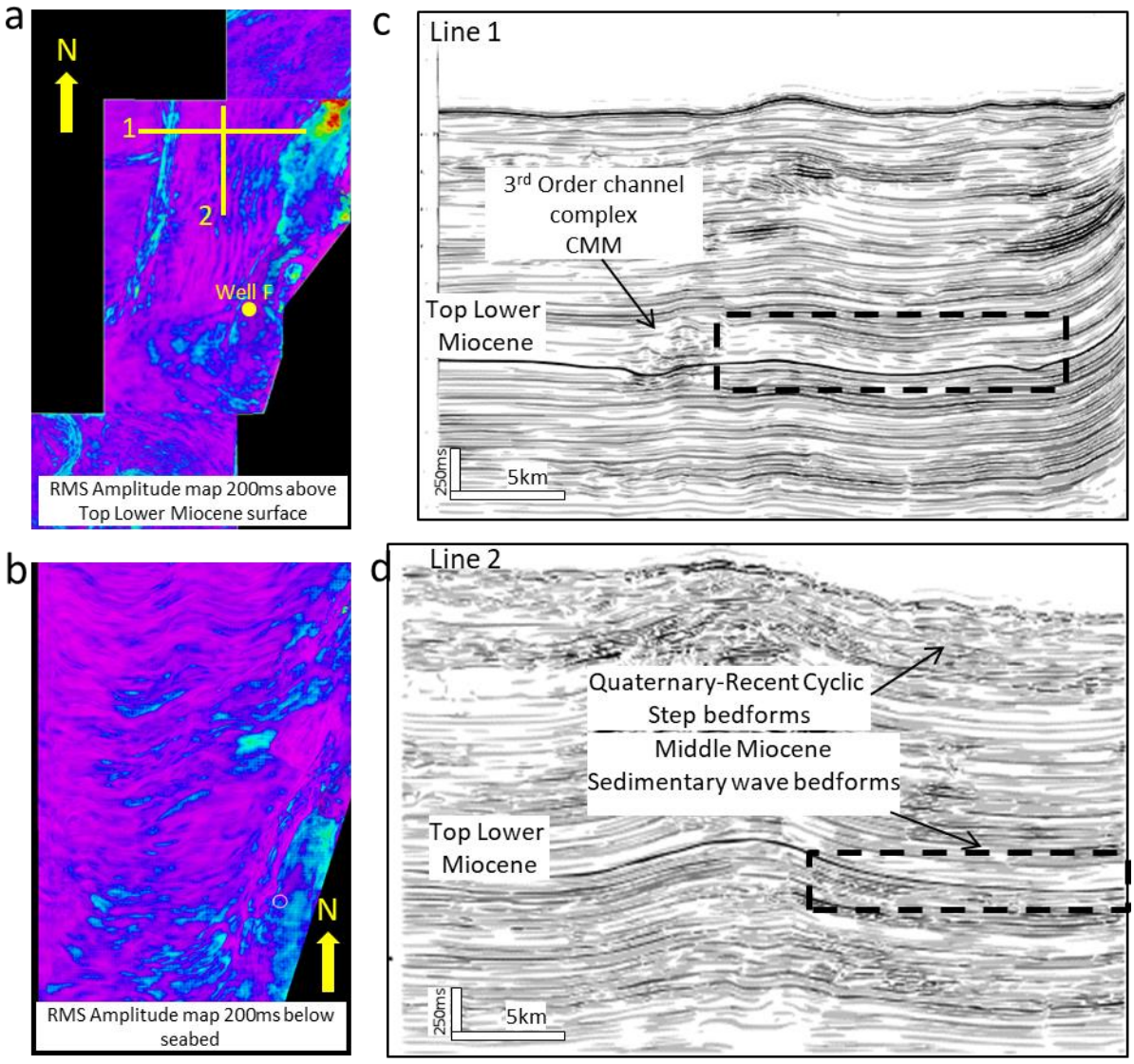

Figure 3.18: Line drawing of Sedimentary Wave Bedforms in the Deepwater Veracruz Basin. a- RMS amplitude map of Middle Miocene, showing morphology of these features in plan view, adjacent to the large channel complex (CMM), b – RMS amplitude map of near seabed deposits, showing similar sedimentary wave deposits (interpreted as cyclic steps), c and d – strike and dip line showing character of both Recent and Middle Miocene (black box) bedforms.

SLOPE TO BASIN FLOOR TRANSITION IN THE LOWER AND MIDDLE MIOCENE

The integration of seismic facies with lithology curves and sedimentary cores described above for the Lower Miocene suggests a basinal sandstone-prone, north-oriented, channelized fairway in the study area. This is consistent with the interpretation of Jennette et al. (2002) who proposed a series of submarine slope canyons updip to this study onshore Veracruz (Fig. 3.1) and postulated a fan system that extended into the offshore Gulf of Mexico. This study builds upon the previous work and extends the interpretation further into the southern GoM basin (Figure 3.19a). The Lower Miocene fairway is made up of 3 seismically mappable units that show a channelized system made up of relatively shallow (<50ms) and moderate (2-3km) sized channels with associated terminal and overbank facies. Fig. 3.20 shows a cross section of Wells A-E with the position of sedimentary cores within Subunits I-III. An interpretation of architectural elements, derived from the seismic attribute maps and core data is also given.

The cross section (Fig. 3.20) shows the vertical association of interpreted architectural elements, with terminal channel lobes being overrun by overbank channel splays and sandy channels (Wells A-C), suggesting a progradation of the deepwater system. The overlying Middle Miocene becomes very thin and mudstone-prone (<100m thick) in Wells A-D, which expands significantly and becomes more sandstone-prone in the distal wells E and F. This suggests a prograding slope in the region of wells A-D that transitions to a sandstone-prone, proximal channelized system further downdip. The development of CMM in the Middle Miocene supports this interpretation of a slope setting in the study area. Additionally, sedimentary wave bedforms have been described as occurring at the lower-slope to basin transition (Kostic, 2011; Covault et al. 2017a); their occurrence in the vicinity of Well F supports a lower slope setting for the Middle

Miocene in the study area. This new interpretation is superimposed onto the previous work by Jennette et al. (2002) and shown in Fig. 3.19b.

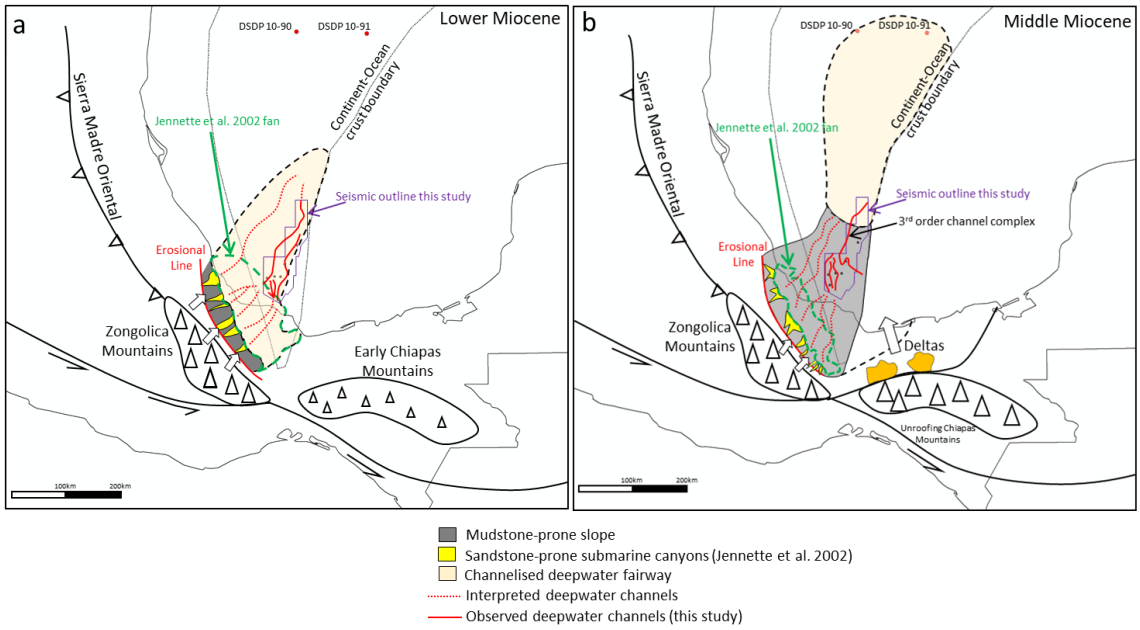

Figure 3.19: Summary of interpretation of Lower and Middle Miocene deepwater channelized fairway in the offshore Veracruz Basin. Extension of depositional systems shown in reference to previous work of Jennette et al. (2002) – green lines. Observed channel systems shown in solid RED line.

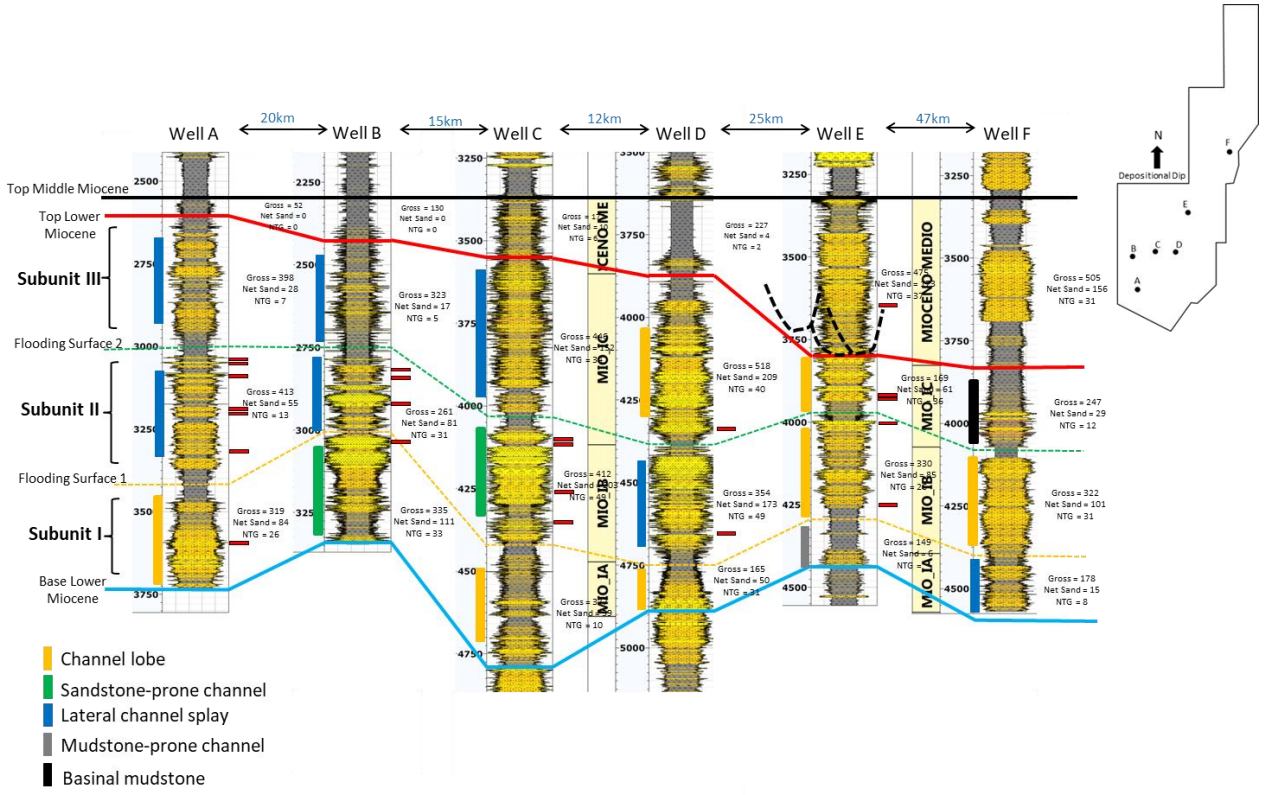

Figure 3.20: Interpreted architectural elements from core and seismic data for the Lower and Middle Miocene deposits in the deepwater Veracruz Basin. The Lower Miocene is interpreted as a sandstone-prone, basinal channelized fairway, with an overlying, channelized, prograding lower slope to proximal basin floor in the Middle Miocene.

A series of regional, summary paleogeographic maps for the three Subunits of the Lower Miocene and the overlying Middle Miocene depositional systems are shown in Fig. 3.21. These maps extend the basinal fans of Jenette et al. (2002) and Arreguín-López et al. (2011) further into the GoM basin and show the interaction of the active plate boundary to the southwest with basinal deposition. The progressive eastward migration of the deepwater depocenter is shown for the Miocene as well as the prograding slope and channel complexes of the Middle Miocene system.

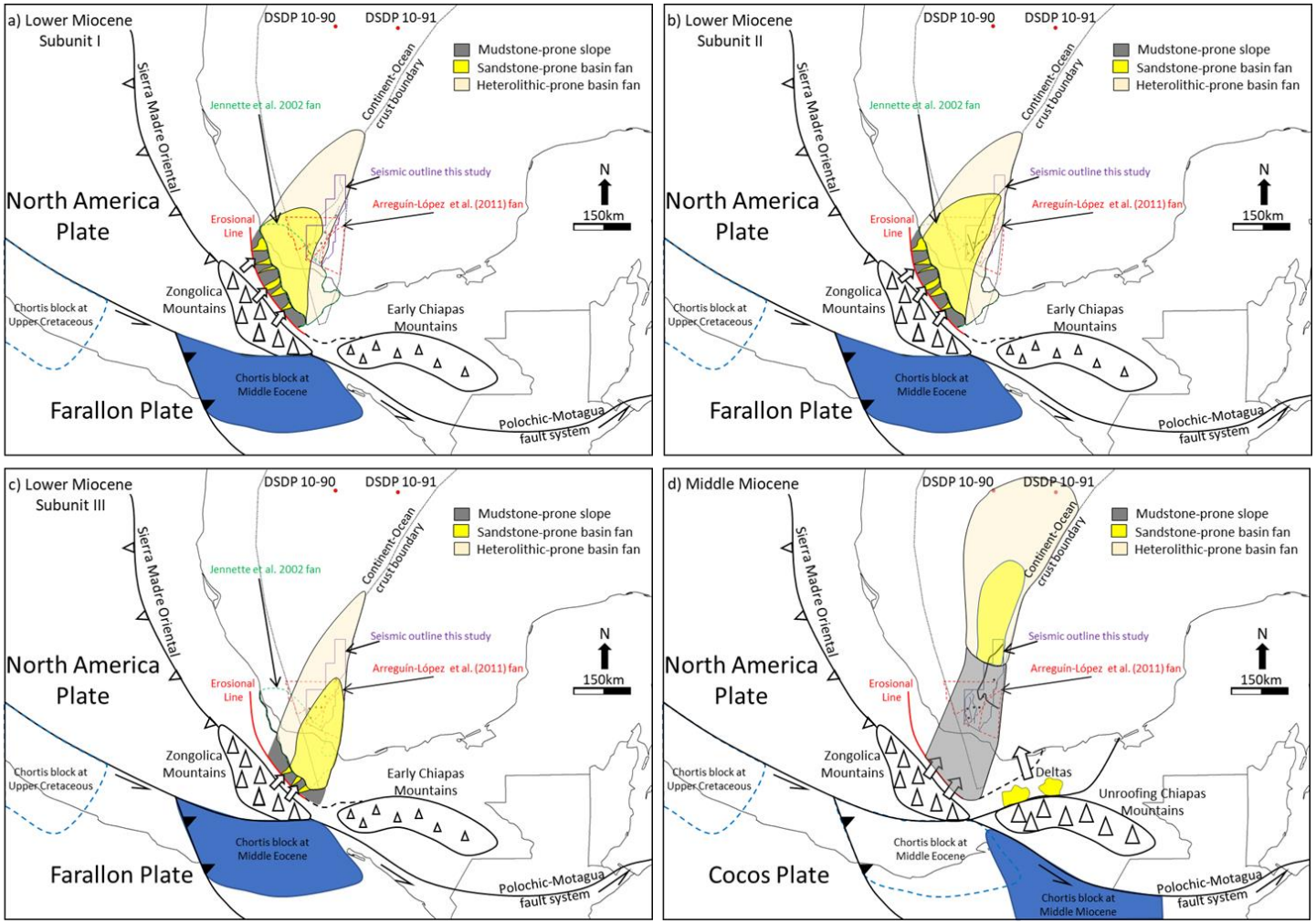

Fig. 3.21: Paleogeographic maps of the Lower Miocene (Subunits I-III) and the Middle Miocene. The structural complexity of the active plate margin is highlighted to the south of the study area. The location of the Chortis continental block is also shown throughout time. In Figures a-c, the main highlands are the Zongolica Mountains, while in the Middle Miocene the emergence of the Chiapas Mountains to the east provides an additional sedimentary source for basinal deposition. Note the eastward shifting depocenter in the basin due to this tectonic evolution in the hinterland. Basinal fans reported by Jennette et al. (2002) and Arreguín-López et al. (2011) are shown (green and red polygons). Compiled from: Meneses-Rocha (2001); Jennette et al. (2002); Moran-Zenteno et al. (2009); Arreguín-López et al. (2011); Witt et al. (2012);

DISCUSSION

i) Facies Associations and seismically defined architectural elements

For the Lower Miocene, interpreted channels, terminal lobes and overbank splays represent the main architectural elements of the channelized fairway in the basin (Figs. 3.7, 3.10 and 3.13). The presence of higher amounts of amalgamated, high density turbidites in the regions closer to channels that transition to increasing amounts of heterolithics, sandstone-prone, mudstone-prone and linked debrites in the extra-channel regions suggests a level of either proximal non-preservation of regionally extensive deposits or lateral/downdip facies transition away from the channels. This spatial organization is not dissimilar to other deepwater systems which report similar spatial facies ordering for sandstone and mudstone-prone debrites (Talling et al. 2012; Winter et al. 2018) and linked debrites (e.g. Haughton et al. 2003; Talling et al. 2004; Davis et al. 2009; Pyles and Jennette, 2009; Hodgson, 2009) on the lateral fringes and distal ends of lobes and fans. The presence of significant (>10% volume) debrites observed in the cores represents a continuation of the textural trend reported further updip in the onshore Veracruz Basin (Cruz-Helu, 1977; Jennette et al. 2002; Dutton et al. 2002). The active margin setting of the adjacent convergent plate boundary and associated fold belt provides a source of sediments for short-travelled, basinal deposition.

In the Middle Miocene, a large submarine channel complex (km-scale width and 100's of ms deep) is interpreted as the main erosive feature noted on the seismic data. The complex is made up of individual channels that exhibit sub-vertical stacking (Fig. 3.17). A series of linear seismic features that flank the eastern edge of CMM, interpreted as sedimentary wave bedforms, are noted (Fig. 3.18a). No wells test these seismic facies and their parallel association with the channel complex suggests an overbank levee complex. They are similar to overlying, near-surface, wavy seismic reflections, as well as

Neogene-aged, seismic features in the western Gulf of Mexico (Mexican Ridges), interpreted as contourite drift deposits (Snedden et al. 2012, 2017). As such, they probably represent bottom-current, reworked sediments that are not confined to the erosional feature. Alternatively, they may represent fine-grained, spillover waveforms, driven by turbidity currents, from the nearby CMM (e.g. Normark et al. 2002).

ii) Tectonic controls on deposition

For tectonically active margins with limited drainage areas like the Veracruz margin, quantitative source to sink data (e.g. Somme et al. 2009; Bouma, 2000) suggests an aereally limited shelf and slope runout. The Lower Miocene coarse-grained deposits described in this study lie >300km from their source terrane fold belts, representing a larger channelised fairway system than most analogous margins exhibit (Somme et al. 2009). Thinning rates in the basin show evidence for an elongate depocenter (lateral thinning rates >> distal rates), suggesting an inherited topographic seafloor. The Veracruz continental slope to the west and salt-basin province on attenuated continental crust to the east potentially provides this depositional trough into which Miocene sediments were focused (Figure 3.1 and 3.21). A measured downdip thinning rate of ~3m/km suggests the deepwater basin floor system likely extends a further 200km basinward of Well F before completely thinning out, giving a total depositional extent of ~500km for the Lower Miocene in this basinal trough. Possible factors for this large depositional extent include i) active and continued uplift of the highlands in the provenance regions, which provide a large volume of sediments for the nearby basin trough, ii) warm, humid Miocene climate (Covault et al. 2017b) which promote higher rates of weathering in the hinterland, iii) trough-like morphology of the receiving basin, which acts to funnel sediments further basinward, and iv) potential regional, northern tilt of the basin caused by flexural loading

of the crust by the western fold belts (Rodriguez et al. 2010) or dynamic crustal drawdown by the downgoing Farallon plate beneath the Gulf of Mexico (Hoggard et al. 2016). By comparison, the Middle Miocene exhibits thickening into the basin over the available datasets, which suggests progradation of the deepwater system and a more basinward extent of the channelised fairway. This is confirmed by Middle Miocene coarse-grained, conglomeratic sandstones are observed 500km further north at DSDP sites 90 and 91 (Leg 10) in the central Gulf of Mexico (Worzel et al. 1970). Covault et al. (2017b) describe the heavy mineral assemblage of these deposits as sourced from Chiapanecan terranes in southern onshore Mexico. These sediments are possibly partially sourced from the 3rd order channel complex (CMM), which is oriented to the DSDP wells at the northern seismic data edge, and represent far travelled sedimentary grains from the unroofing Chiapas mountains and reworked Lower Miocene sediments eroded on the continental margin.

The observed vertical transition from an interpreted basinal channelized fairway to a 3rd order channel-dominated slope system (Lower to Middle Miocene) is another possible sedimentary response to nearby tectonic activity. The end of the Lower Miocene in southern Mexico was linked with the onset of two (2) major tectonic episodes: the initiation of the main uplift phase of the Chiapas foldbelt in southern Mexico (Fig. 3.1), and the early uplift of the submarine Los Tuxtlas volcanic center just south of the deepwater basin. The Chiapas foldbelt was the result of the onset of the Chiapanecan Orogeny, a term used to describe the transition from Lower Tertiary-aged shortening from the subduction of the Pacific plate in the west (Pindell, 1994) to more complex plate tectonic interactions in the early Neogene. At the start of the Middle Miocene, rapid uplift of the Chiapas region over a very short period (13-11Ma, Mandujano-Velazquez and Keppie, 2009) resulted in wider uplift of the Campeche continental margin, evidenced by a regional Middle Miocene angular unconformity and series of folds in the nearshore regions (Gomez-Cabrera, 2003).

Fig. 3.22 shows evidence of this Lower to Middle Miocene uplift and subsequent erosion along parts of these contractional foldbelts, southeast of the study area, where the large channel complex (CMM) originates. The onset of these folds would also impose bathymetric relief that would confine sediment routing to intra-fold regions. It is this tectonic episode that is believed to provide the coarse-grained sediment and flow focus that initiates CMM that is seen on the seismic data and tested by Well E. Additionally, major thermal uplift of the Los Tuxtlas and Anegada volcanic complexes to the south of Wells A-D commenced in the Middle Miocene (Prost & Aranda, 2001, Jacobo et al. 1992), evidenced by another regional Middle Miocene unconformity in the onshore basin (Aranda-Garcia, 1999). This event would likely to have facilitated additional terrigenous sediment to be delivered to the deep basin from the south.

A progressive eastward shift in the depocenter can be observed throughout the Lower Miocene, with the highest sand percentages of Subunit 1 focussed near to Ch1a (Well B), which migrates eastward to Ch2b (Well C) for Subunit II and finally the high amplitude region just east of Well D for Subunit III (Fig. 3.20). This eastward shift could be due to compensational avulsion of the deepwater system, but the evolution also parallels the west to east uplift history in the hinterland. For much of the Paleocene – Lower Miocene, the Zongolica mountains to the southwest of the study area (Fig. 3.1) provided most of the sediment for the onshore and offshore Veracruz Basin. To the east of this was the incipient Chiapas Mountain range, which had topographic expression associated with Lower Tertiary convergence of the Cocos Plate (Mandujano-Velazquez and Keppie, 2009). The onset of significant Middle Miocene uplift of the Chiapas mountains, driven by possible interaction with the Chortis continental block to the south (Pindell et al. 2006; Ratschbacher et al. 2009), collision of the Tehuantepec Transform/Ridge with the Middle America Trench (Mandujano-Velazquez and Keppie, 2009) or combination of both, would

have facilitated onshore drainage reorganization and provided an additional, southern provenance region. In the deep basin, this new sediment source from the southeast would have resulted in a relative eastward shift of sedimentary depocenters (Fig. 3.20). This regional eastward shift in depocenters is also seen by the emergence of Upper Miocene to recent deltas (Grijalva and San Pedro), whose rivers originate in the foothills of the Chiapas foldbelt and flow northward into the southern Gulf of Mexico (Fig. 3.19b and 3.21).

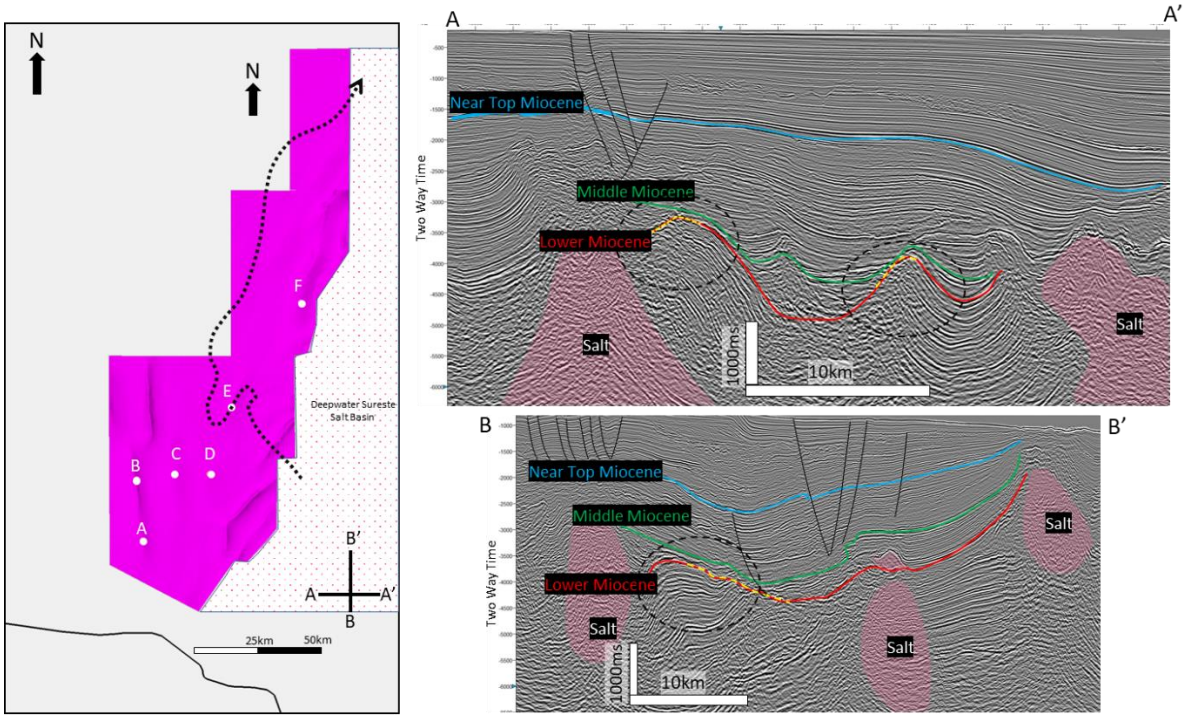

Figure 3.22: Proposed model for formation of Middle Miocene channel complex. Left – location of seismic lines relative to CMM, in proximal region. Right – seismic lines showing Lower to Middle Miocene-aged angular unconformity, associated with Chiapanecan Folding event. This compressional episode is driven by convergence to the west of the subducting Farallon plate and transpressional passage of the Chortis continental block south of this region. This relative uplift of the margin and significant sediment removal is proposed to play a key role in the formation of the submarine channel system.

iii) Comparison to other active and passive continental margins

Sedimentation in the deepwater Veracruz Basin exhibits features commonly associated with other active deepwater margins, including the presence of large channel-complexes, a tectonically-driven depositional focus and an immature textural fabric. The shape and extent of many of these depocenters are also controlled by tectonically modified basin floors. The California borderland fans occur in a series of closed and semi-closed, tectonically-defined, ponded basins (Normark et al. 2009b). Further north, sediments from the Columbia River, offshore Oregon, are deflected southward into an active oceanic trench formed by the interaction of the Pacific and North American plates, forming the morphologically elongate Astoria fan (Nelson et al. 1970). On many passive margins, thin-skinned deformation, driven by gravitational collapse of the shelf margin form deepwater foldbelts that influence sedimentation (Clark and Cartwright, 2009). Examples include the Perdido submarine foldbelt and Mississippi canyon area in the northern Gulf of Mexico (Pickering et al. 1986; Rowan et al. 2004), the Niger Delta margin (Deptuck et al., 2003; Adeogba et al., 2005), the Nile delta margin (Samuel et al. 2003) and Brunei (Demyttenaere et al., 2000). In these settings, relict bathymetry focusses sediments into discrete fairways, with changing gradients controlling the degree of channel incision and lateral accretion of levees, which ultimately control hydrocarbon reservoir distribution (Ferry et al. 2005; Gee and Gawthorpe, 2006). This may be analogous to the Middle Miocene in the offshore Veracruz Basin channel system, where early stage Catemaco folds might have been forming (Mandujano-Velazquez and Keppie, 2009).

Textural and compositional immaturity is another characteristic feature of active margins seen in the Miocene deposits offshore Veracruz. Deposits typically have elevated volcanic material because of adjacent island arcs along plate boundaries, e.g. the Aleutian,

Mariana and Toyoma fans (Shanmugam and Moiola, 1988) which are preserved by the relatively short sediment transport distances from source to sink. Fans near to active margins can be classified as sandstone-prone or mixed mudstone-sandstone (Reading and Richards, 1994). Net sandstone percentages in the Lower Miocene (up to 49% in Subunit II in wells C and D) are consistent with this classification. Similar fans are found in the canyon-fed California borderland region, e.g. the Recent La Jolla, Delgada and Navy fans (Normark, 1970; Piper and Normark, 1983; Carvajal et al. 2017). These fans typically display channel-levee systems and associated lobes, which are also noted on the Lower Miocene Veracruz fan in both seismic and core data. The size and shape of these fans are highly variable and depend on the sediment budget and basin geometry (Reading and Richards, 1994) as active tectonic forces usually modify basinal shape. This is in contrast to passive margin fans, which are typically fine-grained (Reading and Richards, 1994, Bouma, 2000) and made up of large inner fan canyons/fan valleys that transition downdip to highly meandering channel systems with very well-developed levees that dissipate into heretolithic terminal lobes. The scale of these fans can be many 100's of km in length and are typically elongate in nature on the passive basin floor. Ancient examples of mixed mudstone-sandstone fans include the Kongsford fan (Shanmugam and Moiola, 1988) and the Marnoso Arenacea (Talling et al. 2004). The latter exhibits well developed lobe deposits, which exhibit a spatially controlled facies association from high density turbidites in the proximal lobe to elevated debrites (stand-alone and linked varieties) toward the fringes and distal end of the system (Talling et al. 2004). This is similar to the facies associations noted on the Veracruz splays and lobes.

A key similarity of the deepwater Veracruz system to passive deepwater margins is the scale of the basinal deepwater system; passive margins frequently host very large fan systems (e.g. the Amazon, Mississippi, Indus, Bengal fans), with runout distances

>1000km (Barnes and Normark, 1985). Although bordered by an active plate boundary setting and a significantly smaller drainage basin, the basinal channelized fairway extent for the Veracruz system far exceed fan sizes of typical active, sand-rich systems (10's to few 100's km, Somme et al. 2009) and approach 500km for the Middle Miocene, because of the laterally restricted nature of the basin and presence of large channel complexes.

SUMMARY

Integration of seismic, well-log and core data reveal a channelized basin to slope fairway for the Lower and Middle Miocene in the deepwater Veracruz Basin, southern Gulf of Mexico. Sediments are delivered via a series of north northeast-trending channels and channel complexes, with associated overbank and terminal facies.

Sedimentary cores calibrate five (5) seismically defined sub-environments of the slope system: sandy and muddy channels, interchannel regions, overbank splays and terminal lobes. Sandstone content in channels are directly linked to the location of the depocenter: higher amplitude, longer channels tend to be sandier than lower amplitude systems, short-run systems. When sandstone-prone, channels are dominated by high density turbidites, with minor associations of slump-disturbed bedding. Sandstone development in the interchannel and overbank deposits appears to be a function of distance from the channel; proximal overbank settings typically have higher net to gross deposits. There also appears to be an increase in heterolithic and debrite deposits (linked, sandy and muddy) farther away from axial channels. The terminal deposits at the ends of individual channels show a similar facies development of increasing heterolithics and debrites on the margins of the depositional element. Muddy debrites are also most common in terminal channel deposits. A single 6m, Middle Miocene core exhibits a very coarse-grained, poorly

sorted sandstone that calibrates the sedimentary fill of a large 3rd order channel system. The extra-channel region is characterized by an uncalibrated, interpreted sedimentary wave-field. These linear bedforms are probably the result of turbidity current driven channel spillover and are superficially similar to overlying Quaternary to Recent cyclic-step deposits.

The channelised Lower Miocene interval in the basin can be subdivided into 3 Subunits, based on mappable mudstone markers. These Subunits show a progressive eastward migration of the coarse-grained depocenter, in an overall elongate sedimentary system that extends for ~500km in the basin. This transitions to a channel-complex-dominated Middle Miocene, which shows significant basinward thickening. In this context, the Lower to Middle Miocene is interpreted as a prograding basin to slope complex in the study area, where coarse-grained Middle Miocene deposits are observed 500km further basinward at DSDP well sites. For both Miocene intervals, a direct correlation between sandiness and gross interval thickness exists: thicker units tend to be sandier.

As a dual active-passive continental margin, the deepwater deposits exhibit features associated with both end-member margin types. Deposits are texturally immature, with angular grains, high lithic content and poor sorting with significant debrite deposition in the basin. Long-lived Tertiary tectonic forces in the hinterland of the Veracruz area result in high mountain regions adjacent to the deep basin. Coupled with warm and humid climates (Covault et al. 2017b), this provides a proximal source for large volumes of eroded material, available for marine deposition in a deepwater, north-facing trough. A large, tectonically-driven channel complex is observed in the basin, similar to many other active margin settings. Together with the nearby, large sediment supply and basin morphology, this channel system may be responsible for the anomalously long runout distances (~

500km) of the deepwater system in the basin, which is similar to the scale to large, fine-grained submarine fans on passive margin settings.

Chapter 5: Conclusions

The main conclusions of each chapter are described in detail in previous sections. The following provides a brief summary of the main thematic findings of this research.

New insights into the Los Molles Formation at La Jardinera and the Miocene offshore Veracruz Basin

This research has provided new descriptions for previously little-described geographic regions. The fans of the Los Molles Formation in the La Jardinera region have not been previously described as individual genetic units, from which insight into depositional processes and products across separate depositional systems can be documented. Despite recent exploration successes, the depositional systems of the Miocene deposits in the Veracruz Basin have similarly not been documented in detail. This study provides the first, basin-scale description of the fan extents and its internal architecture.

Local tectonic influence on basin sedimentation

The influence of tectonic forces on deepwater sedimentation has been investigated previously, however most of this focus has been on compression structures (deepwater fold belts) and their control on sediment routing systems (reviewed in Kneller et al. 2011; Mann and Escalona, 2011; Chapter 2 this Dissertation). The Los Molles Formation outcrops in the La Jardinera region show evidence for deposition on an irregular basin floor, caused by basinal extension and rift-controlled irregular bathymetric expression. Fans are highly confined to structural troughs, with evidence for significant stratigraphic onlap/truncation (>10m/km thinning rates and reduction in bed number). The internal facies association is

similar to other reported associations in sandstone-prone fans, with an increase in debritic facies to the lateral fan margin and downdip positions.

COARSE-GRAINED SEDIMENTATION IN FINE-GRAINED SOURCE ROCKS

The Los Molles Formation provides a unique opportunity to describe coarse-grained sandstones in a proven, fine-grained source rock. The Los Molles sandstone-prone fan exhibits many features similar to small, coarse-grained sandstone-prone fans on active tectonic margins: areally restricted nature, a coupled decrease in net sand and gross thickness out to the margins and downdip, prevalence of high density turbidites (structureless and horizontally laminated beds), texturally immature sands, absence of well-developed channels and dominance of depositional lobes. However, the fine-grained background sedimentation provides argillaceous material that promotes flow transformation and common formation of debritic facies, particularly observed on the lateral fan margin and distal fringe. This description should be combined with similar studies on the Los Molles slope system and the updip Lajas Formation, to investigate depositional linkages and possible controlling factors on sedimentation observed in the basin. These basin floor fan models should be compared to existing depositional systems in similar deep source rocks in the subsurface and in regions where it is not drilled, may provide a new reservoir play concept.

COUPLED REGIONAL AND LOCAL TECTONIC INFLUENCE ON DEEPWATER SEDIMENTATION

The Miocene deposits offshore Veracruz are an example of deepwater deposition influenced by both regional basin-scale and intra-basin tectonic processes. Although

possessing a relatively small drainage basin, onshore southern Mexico is characterized by high mountainous regions formed by a nearby convergent plate boundary. Denudation of this landscape provides the condition for high sediment influx into the basin, resulting in larger fans than commonly found in tectonically active margins. Within the basin, regional west-east compression has created a physiographic trough, confirmed by lateral (east-west) thinning rates, >6m/km, that focus sediment 100's of km to the northern Gulf of Mexico. Far-field tectonic deformations have also caused uplift of the margin and generation of submarine canyons, which have accentuated the long run-out distances of these coarse-grained fans. Facies associations of Miocene deposits are similar to the Jurassic Los Molles Formation in Neuquén Basin, with proximal areas dominated by high-density turbidites, which transition to heterolithics and debrites on the margins and downdip fringe. Future work in the region should investigate alternative sources for sediment input to confirm the source-to-sink model for elevated fan runout distances.

Bibliography

Adeogba, A.A., McHargue, T.R., Graham, S.A., 2005. Transient fan architecture and depositional controls from near surface 3-D seismic data, Niger Delta continental slope. AAPG Bulletin 85, 627–643.

Allen, P. A., Allen, J. R., 1990. Basin Analysis: Principles and Applications. Blackwell Scientific Publications, Inc., Cambridge, MA.

Allen, P.A., 2008b. Time scales of tectonic landscapes and their sediment routing systems, in: Gallagher, K., Jones, S.J., Wainwright, J., (Eds.), Landscape Evolution: Denudation, Climate and Tectonics Over Different Time and Space Scales. Geological Society of London Special Publication 296, 7-28.

Amy, L.A., Peachey, S.A., Gardiner, A.A., Talling, P.J., 2009. Prediction of hydrocarbon recovery from turbidite sandstones with linked-debrite facies: Numerical flow-simulation studies. Marine and Petroleum Geology 26, 10, 2032-2043.

Aranda-García, M., 1999. Evolution of Neogene contractional growth structures, southern Gulf of Mexico: Master's Thesis (Unpublished), Department of Geological Sciences, The University of Texas at Austin, USA.

Arreguín-López, M.A., Reyna-Martínez, G., Sánchez-Hernández, H., Escamilla-Herrera, A., Gutiérrez-Araiza, A., 2011. Tertiary Turbidite Systems in the Southwestern Gulf of Mexico. Gulf Coast Association of Geological Societies Transactions 61, 45–53.

Barnes, N. E., Normark, W. R., 1985. Diagnostic parameters for comparing modern submarine fans and ancient turbidite systems, in: Bouma, A.H., Normark, W.R., Barnes, N.E., (Eds.), Submarine Fans and Related Turbidite Systems. Springer-Verlag, New York, 13–14.

Best, J. Bridge, J., 1992. The morphology and dynamics of low amplitude bedwaves upon upper stage plane beds and the preservation of planar laminae. Sedimentology 39, 737– 752.

Best, J. Bridge, J., 1992. The morphology and dynamics of low amplitude bedwaves upon upper stage plane beds and the preservation of planar laminae. Sedimentology 39, 737– 752.

Boggs, S., 2006. Principles of Sedimentology and Stratigraphy (4th ed): Pearson Prentice Hall, Upper Saddle River, NJ. pp. 662.

Bouma, A.H., 1962. Sedimentology of Some Flysch Deposits, A graphic Approach to Facies Interpretation. Elsevier, Amsterdam, 168.

Bouma, A.H. (Ed.), 1983/1984. COMFAN. Geo-Marine Letters, pp. 53e224, 3, Nos. 2, 312/13/2005, 4.

Bouma, A. H., W. R. Normark, Barnes, N.E., 1985a, COMFAN: needs and initial results, in: Bouma, A.H., Normark, W.R., Barnes, N.E. (Eds.), Submarine fans and related turbidite systems: New York, Springer-Verlag, 7–11.

Bouma, A.H., 2000. Coarse-grained and fine-grained turbidite systems as end member models: applicability and dangers. Marine and Petroleum Geology 17, 137-143.

Brownfield M.E., Charpentier R.R., 2006. Geology and total petroleum systems of the West-Central Coastal Province (7203), West Africa: U.S. Geological Survey Bulletin 2207. 52pp.

Burgess, P. M., Flint, S., Johnson, S., 2000. Sequence stratigraphic interpretation of turbiditic strata: An example from Jurassic strata of the Neuquén basin, Argentina. Geological Society of America Bulletin 112, 11, 1650-1666.

Carbone, C., 1988. Sismoestratigrafía del Grupo Cuyo inferior en la cuenca neuquina: Boletin de Informaciones Petroleras, Tercera Epoca 16, 67-87.

Cartigny, M.J., Postma, G., van den Berg, J.H., Mastbergen, D.R., 2011. A comparative study of sediment waves and cyclic steps based on geometries, internal structures and numerical modeling. Marine Geology 280, 1, 40–56.

Carvajal, C.R., Steel, R.J., 2006. Thick turbidite successions from supply-dominated shelves during sea-level highstand. Geology 34, 665-668.

Carvajal, C., Steel, R., Petter, A., 2009. Sediment supply: The main driver of shelf-margin growth. Earth-Science Reviews 96, 4, 221-248.

Carvajal, C., Paull, C.K., Caress, D.W., Fildani, A., Lundsten, E., Anderson, K., Maier, K.L., McGann, M., Gwiazda, R., Herguera, J.C., 2017. Unraveling the Channel–Lobe Transition Zone With High-Resolution AUV Bathymetry: Navy Fan, Offshore Baja California, Mexico. Journal of Sedimentary Research 87, 10, 1049–1059.

Chandra, K., Rajus, D.S.N., Mishra, P.K., 1993. Sea level changes, anoxic conditions, organic matter enrichment and petroleum source rock potential of the Cretaceous sequences of the Cauvery Basin, India. Source rocks in a Sequence Stratigraphic Framework. American Associations of Petroleum Geologists Studies in Geology 37, 131-146.

Cherven, V.B., Fisher, P.J., 1992. Non-tectonic structures caused by drape and differential compaction over lenticular sand bodies, southern Sacramento Basin, in: Cherven, V.B., Edmondson, W.F., (Eds.), Structural Geology of the Sacramento Basin. Annual Meeting Pacific Section AAPG, Sacramento, California, April 27–May 2, 1992. The Pacific Section, American Association of Petroleum Geologists, Bakersfield, California, USA.

Clark, I.R., Cartwright, J.A., 2009. Interactions between submarine channel systems and deformation in deepwater fold belts: Examples from the Levant Basin, Eastern Mediterranean Sea. Marine and Petroleum Geology 26, 1465–1482.

Covault, J.A., Normark, W.R., Romans, B.W., Graham, S.A., 2007. Highstand fans in the California borderland; the overlooked deep-water depositional systems. Geology 35, 783–786.

Covault, J.A., Romans, B.W., Graham, S.A., 2009. Outcrop expression of a continental-margin-scale shelf- edge delta from the Cretaceous Magallanes Basin, Chile. Journal of Sedimentary Research 79, 523–539.

Covault, J.A., Graham, S.A., 2010. Submarine fans at all sea-level stands: tectono-morphologic and climatic controls on terrigenous sediment delivery to the deep sea. Geology 38, 939-942.

Covault, J.A., Kostic, S., Paull, C.K., Sylvester, Z., Fildani, A., 2017a. Cyclic steps and related supercritical bedforms: Building blocks of deep-water depositional systems, western North America. Marine Geology 393, 4-20.

Covault, J.A., Stockli, D.F., Fildani, A., Sharman, G., Snedden, J.W., 2017b. Small Rivers and Big Fans: New Geochronologic Constraints From the Miocene-Pliocene Deep-Water Mexican Continental Margin. AAPG Annual Convention and Exhibition, Houston, Texas, April 2-5, 2017.

Cruz-Helu, P., Verdugo, V.R., Barcenas, P.R., 1977. Origin and distribution of Tertiary conglomerates, Veracruz Basin, Mexico. AAPG Bulletin 61, 2, 207–226.

Dailly, P., Henderson, T., Hudgens, E., Kanschat, K., Lowry, P., 2013. Exploration for Cretaceous stratigraphic traps in the Gulf of Guinea, West Africa and the discovery of the Jubilee Field: a play opening discovery in the Tano Basin, Offshore Ghana. Geological Society of London Special Publications 369, 235-248.

Davis, C., Haughton, P., McCaffrey, W., Scott, E., Hogg, N., Kitching, D., 2009. Character and distribution of hybrid sediment gravity flow deposits from the outer Forties Fan, Paleocene Central North Sea. UKCS. Marine and Petroleum Geology 26,1919–1939.

De'Ath, N. G., Schuyleman, S.F., 1981. The geology of the Magnus oilfield, in: Illing, L.V., Hobson, G.D. (Eds.), Petroleum geology of the continental shelf of north-west Europe. London, Heyden, 342–351.

Demyttenaere, R., Tromp, J.P., Ibrahim, A., Alliman-Ward. T., 2000. Brunei deepwater exploration: from sea floor images and shallow seismic analogues to depositional models in a slope turbidite setting. In: Gulf Coast Section SEPM Foundation 20th Annual Research Conference Deep-Water Reservoirs of the World December 3–6, 2000, 304-317.

Deptuck, M.E., Steffens, G.S., Barton, M., Pirmez, C., 2003. Architecture and evolution of upper fan channel belts on the Niger Delta slope and in the Arabian Sea. Marine and Petroleum Geology 20, 649–676.

Dickinson, W.R., 1974. Plate Tectonics and Sedimentation. Tectonics and sedimentation: SEPM Special Publication 22, 1-27.

Dixon, J.F., Steel, RJ., Olariu, C., 2012. Shelf-edge delta regime as a predictor of deep-water deposition. Journal of Sedimentary Research 86, 681-687.

Donovan, A.D., 2003. Depositional topography and sequence development, in: Roberts,

H.H., Rosen, N.C., Fillon, R.H., Anderson, J.B. (Eds.), Shelf Margin Deltas and Linked Downslope Petroleum Systems, Gulf Coast Section, SEPM Foundation, 23rd Annual Research Conference, 493–522.

Dore, G., Robbins, J., 2005. The Buzzard Field. Geological Society, London, Petroleum Geology Conference series 6, 241-252.

Dott Jr., R.H., 1963. Dynamics of subaqueous gravity depositional processes. AAPG Bulletin 47, 104-128.

Dutton, S. P., Jennette, D.C., Ambrose, W.A., Martinez, M., 2002. Petrography and reservoir quality of Tertiary deep-water sandstones in the Veracruz Basin, Mexico. Gulf Coast Association of Geological Societies Transactions 52, 229–240.

Ferry, J.N., Mulder, T., Parize, O., Raillard, S., 2005. Concept of equilibrium profile in deep water turbidite systems: effects of local physiographic changes on the nature of sedimentary processes and the geometries of deposits, in: Hodgson, D.M., Flint, S.S., (Eds.), Submarine Slope Systems: Processes and Products. Geological Society Special Publication 244, 181–193. London.

Fisher, W.L., McGowen, J.H., 1967. Depositional Systems in the Wilcox Group of Texas and Their Relationship to Occurrence of Oil and Gas. Gulf Coast Association of Geological Societies Transactions 17 105-125.

Galloway, W.E., Ganey-Curry, P.E., Li, X., Buffler, R.T., 2000, Cenozoic depositional history of the Gulf of Mexico basin: AAPG Bulletin 84, 1743–1774.

Galloway, W.E., Whiteaker, T.L., Ganey-Curry, P.E., 2011. History of Cenozoic North American drainage basin evolution, sediment yield, and accumulation in the Gulf of Mexico basin. Geosphere 7, 4, 938-973.

Gardner, M.H., Borer, J.M., Melick, J.J., Mavilla, N., Dechesne, M., Wagerle, R.N., 2003. Stratigraphic process-response model for submarine channels and related features from studies of Permian Brushy Canyon outcrops, West Texas. Marine and Petroleum Geology 20, 6–8, 757-787.

Gee, M.J.R., Gawthorpe, R.L., 2006. Submarine channels controlled by salt tectonics: examples from 3D seismic data offshore Angola. Marine and Petroleum Geology 23, 443–458.

Gómez Omil, R.G., Schmithalter, J., Cangini, A., Albariño, Corsi, A., 2002. El Grupo Cuyo en la Dorsal de Huincul: consideraciones estratigráficas, tectónicas y petroleras, Cuenca Neuquina. 5º Congreso de Exploración y Desarrollo de Hidrocarburos, Actas en CDROM, Mar del Plata.

Gomez-Cabrera, P.T., 2003. Stratigraphic and Structural Analysis of the Neogene Sediments of the Offshore Portion of the Salina del Istmo Basin, Southeastern Mexico. PhD Dissertation (Unpublished), Department of Geological Sciences, The University of Texas at Austin, USA.

Granjeon, D., Joseph, P., 1999. Concepts and applications of a 3-D multiple lithology, diffusive model in stratigraphic modeling, in: Harbaugh, J.W., Lynn Watney, W., Rankey, E.C., Slingerland, R., Goldstein, R.H., Franseen, E.K., (Eds.), Numerical experiments in stratigraphy: recent advances in stratigraphic and sedimentologic computer simulations. Society of Sedimentary Geology Special Publication 62, 197–210.

Gulisano, C.A., Gutierrez Pleimling, A.R., Digregorio, R.E., 1984b. Esquema estratigrafico de la secuencia Jurasica del oeaste de la provincia del Neuquén, Buenos Aires, IX8 Congreso Geologico Argentina, Secretaria de Minera de la Nacion, Direccion Nacional Servico Geologico Publicacion, v. I, 236–259.

Gulisano, C.A., Minniti, S.M., Rossi, G.C., Villar, H.J., 2001. The Agrio Petroleum System: hydrocarbon contribution and key elements. Neuquén Basin, Argentina. New Technologies and New Play Concepts in Latin America. AAPG 2001 Hedberg Research Conference, Mendoza, 114-115.

Gutierrez Paredes, H. C., Martinez Medrano, M., Sessarego, H.L., 2009. Provenance for the middle and upper Miocene sandstones of the Veracruz Basin, Mexico, in: Bartolini, C., Roman Ramos, J.R., (Eds.), Petroleum systems in the southern Gulf of Mexico: AAPG Memoir 90, p. 397– 407.

Haner, B. E., 1971. Morphology and sediments of Redondo submarine fan, southern California. Geological Society of America Bulletin 82, 2413–2432.

Harms, J. C., Southard, J. B., Walker, R. G., 1982. Structures and sequences in clastic rocks: Society of Economic Paleontologists and Mineralogists Short Course 9, Calgary, 249 p.

Haughton, P. D. W., Barker, S. P., McCaffrey, W. D., 2003. 'Linked' debrites in sand-rich turbidite systems - origin and significance. Sedimentology 50, 459-482.

Hay, W.W., Behensky Jr, J.F., 1981. The Northern Gulf of Mexico as an Anomalous Passive Margin. Gulf Coast Association of Geological Societies Transactions 31, 309-313.

Heritier, F.E., Lossel, P., Wathne, E., 1980. Frigg Field - Large Submarine-Fan Trap in Lower Eocene Rocks of the Viking Graben, North Sea, in: Halbouty, M.T., (Ed.), Giant Oil and Gas Fields of the Decade 1968-1978. AAPG Memoir 30, 59-79.

Hinterwimmer, G. A., Jauregui, J. M., 1984. Análisis de facies de los depósitos de turbiditas de la Formación Los Molles en el sondeo Barda Colorada Este, Provincia del Neuquén: Noveno Congreso Geológico Argentino, San Carlos de Bariloche 5, 124–135.

Hodgson, D.M., Flint, S.S., Hodgetts, D., Drinkwater, N., Johannessen, E.P., Luthi, S.M., 2006. Stratigraphic Evolution of Fine-Grained Submarine Fan Systems, Tanqua Depocenter, Karoo Basin, South Africa. Journal of Sedimentary Research 76, 20-40.

Hodgson, D. M., 2009. Distribution and origin of hybrid beds in sand-rich submarine fans of the Tanqua depocentre, Karoo Basin, South Africa. Marine and Petroleum Geology 26, 10, 1940-1956.

Hoggard, M.J., White, N., Al-Attar, D., 2016. Global dynamic topography observations reveal limited influence of large-scale mantle flow. Nature Geoscience 9, 456-465.

Howell, J. A., Schwarz, E., Spalletti, L. A., Veiga, G. D., 2005. The Neuquén basin: an overview. Geological Society of London Special Publications 252, 1, 1-14.

Hubbard, S.M., Fildani, A., Romans, B.W., Covault, J.A., McHargue, T.R., 2010. High-relief clinoform development: insights from outcrop, Magallanes Basin, Chile. Journal of Sedimentary Research 80, 357-375.

Hudec, M.R., Norton, I.O., Jackson, M.P.A., Peel, F.J., 2013. Jurassic evolution of the Gulf of Mexico salt basin. AAPG Bulletin 97, 10, 1683–1710.

Jacobo Albarabn., J., Garduño, M., Innocenti, F., Pasquare, M.G., Tonarini, S., 1992. Datos sobre el vulcanismo neogénico-reciente del complejo volcánico de Los Tuxtlas, Edo. de Veracruz, México: Evolución petrológica y geovulcanológica: 11.o Convención Geológica Nacional, Veracruz, Libro de Resúmenes, p. 97-98.

Jennette, D., Wawrzyniec, T., Fouad, K., Dunlap, D.B., Meneses-Rocha, J., Grimaldo, F., Munoz, R., Barrera, D., Williams-Rojas, C.T., Escamilla-Herrera, A., 2002. Traps and turbidite reservoir characteristics from a complex and evolving tectonic setting, Veracruz Basin, southeastern Mexico. AAPG Bulletin 87, 10, 1599-1622.

Johannessen, E.P., Steel, R.J., 2005. Shelf-margin clinoforms and prediction of deepwater sands. Basin Research 15, 521-550.

Johnson, A.M., 1970. Physical processes in geology. San Francisco: Freeman-Cooper

Kane, I. A., Ponten, A. S. M., 2012. Submarine transitional flow deposits in the Paleogene Gulf of Mexico. Geology, 40, 12, 1119–1122.

Katz, B.J., 1995. Petroleum Source Rocks: An Introductory Overview, in: Petroleum Source Rocks, Springer-Verlag.

Katz, B. J., Mello, M.R., 2000. Petroleum systems of South Atlantic Marginal basins—an overview, in: Mello, M.R., Katz, B.J., (Eds.), Petroleum systems of South Atlantic margins. AAPG Memoir 73, 1–13.

Katz, B.J., 2012. Petroleum Source Rocks. Springer Science and Business Media.

Klemme, H.D., Ulmishek, G.F., 1991. Effective Petroleum Source Rocks of the World: Stratigraphic Distribution and Controlling Depositional Factors (1). AAPG Bulletin 75, 12, 1809-1851.

Kneller, B., Martinsen, O.J., McCaffrey, B., 2009. External Controls on Deep-Water Depositional Systems. SEPM Special Publication 92. 402pp. Tulsa, OK, USA.

Koo, W.M., Olariu, C., Steel, R.J., Olariu, M.I., Carvajal, C.R., Kim, W., 2016. Coupling Between Shelf-Edge Architecture and Submarine-Fan Growth Style in A Supply-Dominated Margin. Journal of Sedimentary Research 86, 613-628.

Kostic, S., 2011. Modeling of submarine cyclic steps: controls on their formation, migration and architecture. Geosphere 7, 2, 294–304.

Levell, B., Argent, J., Dore, A.G., Fraser, S., 2011. Passive Margins: overview. Geological Society, London, Petroleum Geology Conference series, 7, 823-830.

Link, M.H., Welton, J.E., 1982. Sedimentology and reservoir potential of Matilija Sandstone: an Eocene sand-rich deep-sea fan and shallow marine complex, California. AAPG Bulletin 66, 1514–1534.

Liro, L. M., Dawson, W.C., 2000. Reservoir systems of selected basins of the South Atlantic, in: Mello, M.R., Katz, B.J., (Eds.), Petroleum systems of South Atlantic margins. AAPG Memoir 73, 77–92.

Lowe, D.R., 1975. Water escape structures in coarse-grained sediments. Sedimentology 22, 2, 157-204.

Lowe, D.R., 1982. Sediment gravity flows: II. Depositional models with special reference to the deposits of high-density turbidity currents. Journal of Sedimentary Petrology 52, 279-297.

Lowe, D.R., 1988. Suspended-load fallout rate as an independent variable in the analysis of current structures. Sedimentology 35, 765-776.

Major, J.J., Iverson, R.M., 1999. Debris-flow deposition — effects of pore-fluid pressure and friction concentrated at flow margins. Geological Society of America Bulletin 111, 1424-1434.

Mandujano-Velazquez, J.J., Keppie, J.D., 2009. Middle Miocene Chiapas fold and thrust belt of Mexico: a result of collision of the Tehuantepec Transform/Ridge with the Middle America. Geological Society of London Special Publication 327, 1, 55–69.

Mann, P., Escalona, A., 2011. Introduction to the special issue of Marine and Petroleum Geology: Tectonics, basinal framework, and petroleum systems of eastern Venezuela, the Leeward Antilles, Trinidad and Tobago, and offshore areas. Marine and Petroleum Geology 28, 1, 4-7.

Martinez, M. A., Pramparo, M. B., Quattrocchio, M. E., and Zavala, C., 2008. Depositional environments and hydrocarbon potential of the Middle Jurassic Los Molles Formation, Neuquén Basin, Argentina: palynofacies and organic geochemical data. Revista Geologica de Chile 35, 2, 279-305.

Martinez-Medrano, M., Vazquez-Benitez, R., Valdivieso-Ramos, V.M., Arreguin-Lopez, M.A., Rivera-Cruz, S., 2006. Upper Miocene-Pliocene Plays and their Economical Importance in the Tertiary Veracruz Basin, Mexico. Gulf Coast Association of Geological Societies Transactions 56, 575.

Mattern, F., 2005. Ancient sand-rich submarine fans, depositional systems, models, identification, and analysis. Earth-Science Reviews 70, 167-202.

Mayall, M., Jones, E., Casey, M., 2006. Turbidite channel reservoirs—Key elements in facies prediction and effective development. Marine and Petroleum Geology 23, 821-841.

McGovney, J. E., Radovich, B.J., 1985. Seismic stratigraphy and facies of the Frigg fan complex, in: Berg, O.R., Woolverton, D.G., (Eds.), Seismic stratigraphy II, an integrated approach. AAPG Memoir 39, 139–156.

McKenzie, D., 1978. Some remarks on the development of sedimentary basins. Earth and Planetary Science Letters 40, 1, 25-32.

Meneses-Rocha, J. J., 2001. Tectonic evolution of the Ixtapa graben, anexample of a strike-slip basin in southeastern Mexico: Implications for regional petroleum systems, in: Bartolini, C., Buffler, R.T., Cantú-Chapa, A., (Eds.), The western Gulf of Mexico Basin: Tectonics, sedimentary basins, and petroleum systems: AAPG Memoir 75, 183-216.

Mohriak, W.U., Mello, M.R., Bassetto, M., Vieira, I.S., Koutsoukos, E.A., 2000. Crustal Architecture, Sedimentation, and Petroleum Systems in the Sergipe-Alagoas Basin, Northeastern Brazil, in: Mello, M.R., Katz, B.J., (Eds.), Petroleum Systems of South Atlantic Margins. AAPG Memoir 73, 273–300.

Moran-Zenteno, D., Keppie, D.J., Martiny, B., González-Torres, E., 2009. Reassessment of the Paleogene Position of the Chortis Block Relative to Southern Mexico: Hierarchical Ranking of Data and Features, Revista Mexicana De Ciencias Geologicas 26, 177–188.

Mutti, E., Ricci Lucchi, F., 1972. Turbidites of the northern Apennines, introduction to facies analysis (English translation by T.H. Nilsen, 1978). International Geology Review 20, 125-166.

Mutti, E., 1979. Turbidites et cones sous-marins profonds: 3me Cycle Romand Sciences de la Terre, Friourg, Sedimentation detritique 355-419.

Mutti, E., Normark, W.R., 1987. Comparing examples of modern and ancient turbidite systems, problems and concepts. In: Leggett, J.K., Zuffa, G.G. (Eds.), Marine Clastic Sedimentology, Concepts and Case Studies. London. Graham and Trotman, London, 1-37.

Nelson, C.H., Carlson, P.R., Byrne, J.V., Alpha, T.R., 1970. Development of the Astoria Canyon-Fan physiography and comparison with similar systems. Marine Geology 8, 3-4, 259-291.

Nelson, C.H., Nilsen, T.H., 1984. Modern and Ancient Deep-sea Fan Sedimentation. SEPM Short Course 14, 404pp.

Normark, W. R., 1970. Growth patterns of deep sea fans. AAPG Bulletin 54, 2170–2195.

Normark, W.R., 1978. Fan Valleys, Channels, and Depositional Lobes on Modern Submarine Fans: Characters for Recognition of Sandy Turbidite Environments. AAPG Bulletin 62, 6, 912-931.

Normark, W.R., Piper, D.J.W., Posamentier, H., Pirmez, C., Migeon, S., 2002. Variability in form and growth of sediment waves on turbidite channel levees. Marine Geology 192, 1–3, 23-58.

Normark, W.R., Piper, D.J.W., Romans, B.W., Covault, J.A., Dartnell, P., Sliter, R.W., 2009b. Submarine canyon and fan systems of the California continental borderland, in: Lee, H.J., Normark, W.R., (Eds.), Earth science in the urban ocean; the southern California continental borderland. Geological Society of America Special Paper 454, 141–168.

Olariu, C., Steel, R.J., 2009. Influence of point-source sediment-supply on modern shelf-slope morphology: implications for interpretation of ancient shelf margins. Basin Research 21, 484-501.

Olariu, C., Vann, N., Tudor, E.P., Winter, R., Shin, M., Steel, R., Dykstra, M., 2015. Shelf Edge to Slope to Basin-Floor Clinoforms and Turbidite Variability of the Southernmost Neuquén Basin Infill: Jurassic Los Molles Formation, Argentina. Abstract. American Association of Petroleum Geologists Annual Convention and Exhibition, Denver, Colorado.

Paim, P. S. G., Silveira, A., Lavina, E., Faccini, U., Leanza, H., Teixeira de Oliveira, J. M. M., D'avila, R., 2008. High resolution stratigraphy and gravity flow deposits in the Los Molles Formation (Cuyo Group - Jurassic) at La Jardinera Region, Neuquén Basin. Revista de la Asociacion Geologica Argentina 63, 728-753.

Paim, P. S. G., E. L. C. Lavina, U. F. Faccini, A. S. da Silveira, H. Leanza, D'Avila, R., 2011. Fluvial-derived turbidites in the Los Molles Formation (Jurassic of the Neuquén Basin): Initiation, transport, and deposition, in: Slatt, M., Zavala, C.,

(Eds.), Sediment transfer from shelf to deep water—Revisiting the delivery system. American Association of Petroleum Geologists Studies in Geology 61, 95–116.

Parker, G., 1996. Some speculations on the relation between channel morphology and channel-scale flow structures: Proceedings, Coherent Flow in Open Channels, John Wiley and Sons.

Pickering, K.T., Coleman, J., Cremer, M., Droz, L., Kohl, B., Normark, W., O'Connell, S., Stow, D., Meyer-Wright, A., 1986. A high sinuosity, laterally migrating submarine fan channel–levee-overbank: results from DSDP Leg 96 on the Mississippi Fan, Gulf of Mexico. Marine and Petroleum Geology 3, 3–18.

Pindell, J.L., 1985. Alleghenian reconstruction and the subsequent evolution of the Gulf of Mexico, Bahamas and Proto-Caribbean Sea. Tectonics, 4,1-39.

Pindell J.L., Erikson J.P., 1994. The Mesozoic Passive Margin of Northern South America, in: Salfity J.A. (Ed.), Cretaceous Tectonics of the Andes. Earth Evolution Sciences. Vieweg+Teubner Verlag, Wiesbaden.

Pindell, J., Kennan, L., Stanek, K.P., Maresch, W.V., Draper, G., 2006. Foundations of Gulf of Mexico and Caribbean evolution: Eight controversies resolved, Geologica Acta 4, 303–341.

Pindell, J. L., Kennan, L., 2009. Tectonic evolution of the Gulf of Mexico, Caribbean and northern South America in the mantle reference frame: An update, in: James, K.H., Lorente, M.A., Pindell, J.L., (Eds.), The Origin and Evolution of the Caribbean Plate. Geological Society Special Publication 328, 1-55.

Piper, D. J. W., Normark, W.R., 1983. Turbidite depositional patterns and flow characteristics, Navy submarine fan, California borderland. Sedimentology 30, 681–694.

Poyatos-Moré, M., Jones, G.D., Brunt, R.L., Hodgson, D.M., Wild, R.J., Flint, A.S., 2016. Mud-dominated basin-margin progradation: processes and implications. Journal of Sedimentary Research 86, 863-878.

Prélat, A., Hodgson, D. M., Flint, S.S., 2009. Evolution, architecture and hierarchy of distributary deep-water deposits: a high-resolution outcrop investigation from the Permian Karoo Basin, South Africa. Sedimentology 56, 7, 2132-2154.

Prost, G., Aranda, M., 2001. Tectonics and hydrocarbon systems of the Veracruz Basin, Mexico, in: Bartolini, C., Buffler, R.T., Cantú-Chapa, A., (Eds.), The western Gulf of Mexico Basin: Tectonics, sedimentary basins, and petroleum systems. AAPG Memoir 75, 271-291.

Pyles, D.R., Jennette, D.C., 2009. Geometry and architectural associations of co-genetic debrite–turbidite beds in basin-margin strata, Carboniferous Ross Sandstone (Ireland): Applications to reservoirs located on the margins of structurally confined submarine fans. Marine and Petroleum Geology 26, 10, 1974-1996.

Radovich, B.J., Moon, J., Connors, C.D., Bird, D.E., 2007. Insights into structure and stratigraphy of the northern Gulf of Mexico from 2D pre-stack depth migration imaging of mega-regional onshore to deep water, long-offset seismic data. Gulf Coast Association of Geological Societies Transactions 57, 633–637.

Ramos, V.A., 1988. The tectonics of the Central Andes; 30 to 33 S Latitude. In: Clark, S.P., Burchfiel, B.C., Suppe, J., (Eds.), Processes in Continental Lithospheric Deformation. Geological Society America Special Paper 218, 31–54.

Ratschbacher, L., Franz, L., Min, M., Bachmann, R., U. Martens, Stanek, K, Stübner, K., Nelson, B.K., Herrmann, U., Weber, B., López-Martínez, M., Jonckheere, R., Sperner, B., Tichomirowa, M., Mcwilliams, M.O., Gordon, M., Meschede, M., Bock, P., 2009. The North American-Caribbean Plate boundary in Mexico-Guatemala-Honduras. Geological Society, London, Special Publications 328, 219-293.

Reading, H.G., Richards, M., 1994. Turbidite systems in deep-water basin margins classified by grain size and feeder system: AAPG Bulletin 78, 792-822.

Rodriguez, A. B., Mann, P., Galloway, W.E., 2010. Effects of Laramide foreland basin tectonics on structure, subsidence, and hydrocarbons of the Mexican sector of the Gulf of Mexico. American Association of Petroleum Geologists Search and Discovery Article 90104.

Romans, B.W., Castelltort, S., Covault, J.A., Fildani, A., Walsh, J.P., 2016. Environmental signal propagation in sedimentary systems across timescales. Earth-Science Reviews 153, 7-29.

Roure, F., Alzaga-Ruiz, H., Callot, J.P., Ferket, H., Granjeon, D., Gonzalez-Mercado, G.E., Guilhaumou, N., Lopez, M., Mougin, P., Ortuno-Arzate, S., Séranne, M., 2009. Long lasting interactions between tectonic loading, unroofing, post-rift thermal subsidence and sedimentary transfers along the western margin of the Gulf of Mexico: Some insights from integrated quantitative studies. Tectonophysics 475, 1, 169-189.

Rossi, V.M., Steel, R.J., 2016. The role of tidal, wave and river currents in the evolution of mixed-energy deltas: example from the Lajas Formation (Argentina). Sedimentology 63, 824-864.

Rowan, M.G., Peel, F.J., Vendeville, B.C., 2004. Gravity-driven fold belts on passive margins, in: McClay, K.R., (Ed.), Thrust Tectonics and Hydrocarbon Systems. AAPG Memoir 82, 157–182.

Ryan, M.C., Helland-Hansen, W., Johannessen, E.P., Steel, R.J., 2009. Erosional vs. accretionary shelf margins: the influence of margin type on deepwater sedimentation: an example from the Porcupine Basin, offshore western Ireland. Basin Research 21, 5, 676-703.

Samuel, A., Kneller, B., Raslan, S., Sharp, A., Parsons, C., 2003. Prolific deep-marine slope channels of the Nile Delta, Egypt. AAPG Bulletin 87, 4, 541-560.

Sandwell, D.T., Muller, R.D., Smith, W.H.F., Garcia, E., Francis, R., 2014. New global marine gravity model from CryoSat-2 andJason-1 reveals buried tectonic structure. Science 346, 6205, 65-67.

Santra, M., Steel, R.J., Olariu, C., Sweet, M.L., 2013. Stages of sedimentary prism development on a convergent margin — Eocene Tyee Forearc Basin, Coast Range, Oregon, USA. Global and Planetary Change 103, 207-231.

Scott, R.M., Tillman, R.W., 1981. Stevens Sandstone (Miocene), San Joaquin Basin, California, in: Siemers, C.T., Tillman, R.W., Williamson, C.R. (Eds.), Deep-water Clastic Sediments. Society of Economic Paleontologists Mineral Core Workshop 2, 116–248.

Seelke, C.R., Ratner, M., Villareal, M.A., Brown, P., 2015. Mexico's Oil and Gas Sector: Background, Reform Efforts, and Implications for the United States. Congressional Research Service, CRS Report, 26p.

Shanmugam, G., Moiola, R.J., 1988. Submarine fans, Characteristics, models, classification, and reservoir potential. Earth-Science Reviews 24, 383-428.

Shanmugam, G., Bloch, R.B., Mitchell, S.M., Beamish, G.W.J., Hodgkinson, R.J., Damuth, J.E., Straume, T., Syvertsen, S.E., Shields, K.E., 1995. Basin-floor fans in the North Sea, sequence stratigraphic models vs. sedimentary facies. AAPG Bulletin 79, 477-512.

Shanmugam, G., 1996. High-density turbidity currents, are they sandy debris flows? Journal of Sedimentary Research 66, 2-10.

Shin, M., 2014. Architecture of coarse grained (conglomeratic) deep water lobes at the base of a sandstone dominated fan, Jurassic Los Molles Formation, Neuquén Basin, Argentina. Master's Thesis (unpublished) Department of Geological Science, The University of Texas at Austin, USA.

Snedden, J.W., Galloway, W.E., Whiteaker, T.L., Ganey-Curry, P.E., 2012. Eastward shift of deepwater fan axes during the Miocene in the Gulf of Mexico: Possible causes and models. Gulf Coast Association of Geological Societies 1, 131-144.

Snedden, J.W., Decker, J., Arce, E., Bate, D., 2017. Diversity of Large-Scale, Deepwater Bed Forms in Mexico Offshore Areas: Neogene to Modern. AAPG Annual Conference and Exhibition, Houston Texas.

Somme, T.O., Helland-Hansen, W., Martinsen, O.J., Thurmond, J.B., 2009. Relationships between morphological and sedimentological parameters in source- to-sink systems: a basis for predicting semi-quantitative characteristics in subsurface systems. Basin Research 21, 361 387.

Sømme, O. T., Jackson, C.A.L., Vaksdal, M., 2013. Source to- sink analysis of ancient sedimentary systems using a subsurface case study from the More-Trondelag area of southern Norway: Part 1-depositional setting and fan evolution. Basin Research 25, 489–511.

Stanley, D. J., 1980. The Saint-Antonin conglomerate in the Maritime Alps: a model for coarse sedimentation on a submarine slope. Smithsonian Contributions to the Marine Sciences 5.

Steel, R., Olsen, T., 2002. Clinoforms, clinoform trajectories and deepwater sands, in: Armentrout, J.M., Rosen, N.C., (Eds.), Sequence stratigraphic models for exploration and production: Evolving methodology, emerging models and applications histories. Gulf Coast Section SEPM Proceedings, 22nd Annual Research Conference, 367–380.

Steel, R., Olariu, C., Rossi, V. M., De Almeida F. Jr., Steel, E., Gan, Y., Jung, E., 2017. Mid-Jurassic Shelf-Margin Growth in Neuquén Basin: Coarse-Grained, River-Tide Interaction at the Shelf Edge. Abstract. American Association of Petroleum Geologists Annual Convention & Exhibition, Houston, Texas.

Steel, E., Buttles, J., Simms, A., Mohrig, D., Meiburg, E., 2017. The role of buoyancy reversal in turbidite deposition and submarine fan geometry. Geology 45, 1, 35-38.

Stow, D.A.V., Johannson, M., 2000. Deep-water massive sands: nature, origin and hydrocarbon implications. Marine and Petroleum Geology 17, 145–174.

Surlyk, F., 1987. Slope and Deep Shelf Gully Sandstones, Upper Jurassic, East Greenland. AAPG Bulletin 71, 4, 464-475.

Syvitski, J.P.M., Peckham, S.D., Hilberman, R., Mulder, T., 2003. Predicting the terrestrial flux of sediment to the global ocean: a planetary perspective. Sedimentary Geology 162, 5-24.

Syvitski, J., Milliman, J., 2007. Geology, Geography, and Humans Battle for Dominance over the Delivery of Fluvial Sediment to the Coastal Ocean. The Journal of Geology 115, 1, 1-19.

Talling, P. J., Amy, L. A., Wynn, R. B., Peakall, J., & Robinson, M., 2004. Beds comprising debrite sandwiched within cogenetic turbidite: origin and widespread occurrence in distal depositional environments. Sedimentology 51,1, 163-194.

Talling, P.J., Masson, D.G., Sumner, E.J. and Malgesini, G., 2012. Subaqueous sediment density flows: Depositional processes and deposit types. Sedimentology 59, 1937-2003.

Thompson, D.L., Stilwell, J.D., Hall, M., 2015. Lacustrine carbonate reservoirs from Early Cretaceous rift lakes of Western Gondwana: Pre-Salt coquinas of Brazil and West Africa, Gondwana Research 28, 1, 26-51.

Tillman, R.W., Ali, S.A., 1982. Deep Water Canyons, Fans, and Facies, Models for Stratigraphic Trap Exploration. American Association of Petroleum Geologists Reprint Series No. 26, 596.

Timbrell, G., 1993. Sandstone architecture of the Balder Formation depositional system, UK Quadrant 9 and adjacent areas, in: Parker, J.R. (Eds.), Petroleum geology of northwest Europe. Proceedings of the 4th Congress, The Geological Society of London, 107–121.

Tudor, E. P., 2014. Facies variability in deep water channel-to-love transition zone: Jurassic Los Molles Formation, Neuquén Basin Argentina. Master's Thesis (unpublished) Department of Geological Science, The University of Texas at Austin, USA.

US EIA, 2013 Report: https://www.eia.gov/analysis/studies/worldshalegas/pdf/fullreport.pdf

Vann, N. K., 2013. Slope to basin floor evolution of channels to lobes, Jurassic Los Molles Formation, Neuquén Basin, Argentina. Master's Thesis (unpublished) Department of Geological Science, The University of Texas at Austin, USA.

Van der Werff, W., Johnson, S., 2003. High resolution stratigraphic analysis of a turbidite system, Tanqua Karoo Basin, South Africa. Marine and Petroleum Geology 20, 45–69.

Van Wagoner, J. C., Posamentier, H.W., Mitchum, R. M., Vail, P. R., Sarg, J. F., Loutit, T. S., Hardenbol, J., 1988. An overview of sequence stratigraphy and key definitions, in: Wilgus, C. K., Hastings, B. S., Kendall, C. G. St. C., Posamentier, H.W., Ross, C. A., Van Wagoner, J. C., (Eds.), Sea Level Changes – An Integrated Approach SEPM Special Publication 42, 39–45.Weimer, P., 1989. Sequence stratigraphy of the Mississippi Fan (Plio-Pleistocene) Gulf of Mexico. Geo-Marine Letters 9, 4, 185-272.

Vergani, G. D., Tankard, A. J., Belotti, H. J., Welsink, H. J., 1995. Tectonic evolution and paleogeography of the Neuquén Basin, Argentina. AAPG Memoir 62, 383-402.

Verzi, H., Raggio, M.F., Suarez, M., 2005. Volume interpretation of a turbidite system, Los Molles Formation, Neuquén Basin, Argentina, in: Soubies, D., Arteaga, M., Fantín, F., (Eds.), La Sísmica de Reflexión, más allá de la Imagen Estructural. 5° Congreso de Exploración y Desarrollo de Hidrocarburos, Actas: 219-226, Mar del Plata.

Weimer, P., 1989. Sequence stratigraphy of the Mississippi Fan (Plio-Pleistocene) Gulf of Mexico. Geo-Marine Letters 9, 4, 185-272.

Wen, Z., Xu, H., Wang, Z., He, Z., Song, C., Chen, Xi., Wang, Y., 2015. Classification and hydrocarbon distribution of passive continental margin basins. Petroleum Exploration and Development 43, 5, 740-750.

Whyatt, M., Bowen, J.M., Rhodes, D.N.,1991. Nelson-successful application of a development geoseismic model in North Sea exploration. First Break 9, 265–280.

Wignall, P.B., Maynard, J.R., 1993. The sequence stratigraphy of transgressive black shales. American Association of Petroleum Geologists Studies in Geology 37, 35-47.

Wild, R., Flint, S.S., Hodgson, D.M., 2009. Stratigraphic evolution of the upper slope and shelf edge in the Karoo Basin, South Africa. Basin Research 21, 5, 502-527

Williamson, C.R., Hill, D.R., 1981. Submarine-fan deposition of the Upper Cretaceous Winters Sandstone, Union Island gas field, Sacramento Valley, California, in: Siemers, C.T., Tillman, C.T., Williamson, R.W. (Eds.), Deep-water Clastic Sediments. Society Economic Paleontologists Mineral Core Workshop, San Francisco 2, 78– 115.

Winker, C.D., Buffler, R.T., 1988. Paleogeographic Evolution of Early Deep-Water Gulf of Mexico and Margins, Jurassic to Middle Cretaceous (Comanchean). AAPG Bulletin 72, 3, 318-346.

Winter, R.R., Steel, R.J., Olariu, C., Shin, M., 2018. Architectural and internal textural trends of a small, coarse-grained deepwater fan system, Jurassic Los Molles Formation, Neuquén Basin, Argentina. PhD Dissertation (Unpublished), Department of Geological Sciences, The University of Texas at Austin, USA.

Witt, C., Brichau, S., Carter, A., 2012. New constraints on the origin of the Sierra Madre de Chiapas (south Mexico) from sediment provenance and apatite thermochronometry. Tectonics 31, 1-15.

Worzel, J.L., Bryant, W., Beall, A.O. Jr., Capo, R., Dickinson, K., Foreman, H.P., Laury, R., McNeely, B.W., Smith, L.A., 1970. Site 90, in: Worzel, J.L., Bryant, W.R. (Eds.), Initial Reports of the Deep-Sea Drilling Project, 10, 89-115. U.S. Govt. Printing Office Washington, D.C 737–748.

Zarra, L., 2007. Chronostratigraphic framework for the Wilcox Formation (upper Paleocene-Lower Eocene) in the deep-water Gulf of Mexico: Biostratigraphy, sequences, and depositional systems, in: Kennen, L., Pindell, J., Rosen, N.C., (Eds.), The Paleogene of the Gulf of Mexico and Caribbean basins: Processes, events, and petroleum systems: Gulf Coast Section SEPM 27th Annual GCSSEPM Foundation Bob F. Perkins Research Conference Proceedings,81–145.

Zavala, C., 1993. Estratigrafía y análisis de facies de la Formación Lajas (Jurásico medio) en el sector sur occidental de la Cuenca Neuquina, Provincia del Neuquén, República Argentina. Tesis Doctoral, Departamento de Geología, Universidad Nacional del Sur (unpublished), 260 p, Bahía Blanca.

Zavala, C., Gamero, H., Arcuri, M., 2006. Lofting rhythmites: A diagnostic feature for recognition of hyperpycnal deposits. Geological Society of America Abstracts with Programs 38, 7, 541.